

✓  
043  
BAS  
LOW FREQUENCY PLASMA WAVES IN A MAGNETIC FIELD : 13080  
INSTABILITIES, TURBULENT DIFFUSION AND SPECTRA ✓

by

Aparna Basu  
Physical Research Laboratory  
Ahmedabad, India.

A THESIS  
SUBMITTED TO  
GUJARAT UNIVERSITY  
FOR THE DEGREE OF  
DOCTOR OF PHILOSOPHY

043



B13080

*dedicated to*

*my parents*

*SUKUMAR and HIMANI CHAUDHURI*

*and to*

*my parents-in-law*

*PABITRA KUMAR and NILIMA BASU*



CERTIFICATE

*I hereby declare that the work  
presented in this thesis is original and has not  
formed the basis for the award of any degree or  
diploma by any University or Institution.*

*Aparna Basu*  
(APARNA BASU)  
AUTHOR

*Certified by:*

*Attas.*  
A. C. DAS

APRIL 3, 1984

## ACKNOWLEDGEMENTS

*It is impossible to thank individually all the people - teachers, friends and colleagues - who have moulded my understanding of the subject over the years. I am deeply conscious of their contribution, and warmly thank all those, who, through books, lectures, discussions and other indirect ways, have influenced this work.*

*I shall always remain indebted to Professor A.C. Das for consenting to supervise the study towards this thesis. I deeply appreciate not only his able guidance and his kind consideration, but also the considerable freedom he has generously given me during the course of this study. I have learned a great deal due to my association with him. I thank him for carefully reading the manuscript and suggesting important changes.*

*I am very grateful to Dr. A.S. Sharma for introducing me to the problem of the ion-acoustic spectrum. I thank him for many hours of fruitful discussions and help with many initial problems, and for the use of his computer programs in Chapter 6.*

*I sincerely thank Dr. V.B. Sheorey for enlightening me on Chebyshev Polynomials, and for his kind and painstaking assistance with the calculations in Chapter 4.*

*Several discussions with Prof. A. Sen and Prof. S.M. Mahajan have been of considerable help in clearing the concepts underlying turbulence theory. I gratefully acknowledge their contribution.*

*I thank all the members of the Theory Group, with whom I have been continually associated over the last several years, for providing a very congenial atmosphere for research.*

*I must also thank all my friends in PRL who have helped unfailingly in keeping morale and spirits high. It is a pleasure to thank Dr. M. Mohan who has helped me over many initial hurdles.*

*I thank the Physical Research Laboratory for financial support and the use of the facilities in the Laboratory. I must mention, in particular, the prompt, helpful and friendly atmosphere in the library. In all technical matters relating to the thesis, I have received full co-operation from all concerned. I thank Mr. S.C. Bhavsar, Mr. J.G. Vora, Mr. N.F. Khoja and Mrs. Bhatt for*

*the diagrams, Mr. V.T. Viswanathan for his excellent typing, and Babubhai for the neat cyclostyling.*

*It is impossible to state the innumerable ways in which my family members have contributed to this venture. My parents have given the initial inspiration and support for the work. My husband Dipankar has provided continued encouragement, and support on a day to day basis. My sister Mitali has been invaluable in many different ways. The entire checking and collating of the thesis was done by her. Were it not for their joint efforts, this task would never have been concluded.*

*Special thanks go to my little son, Upal, who has not only cheerfully put up with many hours of my absence from home, but also provided positive encouragement in many ways.*



## CONTENTS

### PART I : ELECTROMAGNETIC INSTA- BILITIES IN SPACE PLASMA

	<i>Introduction</i>	1
CHAPTER 1	ENHANCED SCINTILLATIONS ASSOCIATED WITH HIGH SPEED STREAMS IN THE SOLAR WIND	4
	<i>Introduction</i>	5
	<i>Dispersion Relation</i>	8
	<i>Summary</i>	15
	<i>References</i>	17
CHAPTER 2	FIELD ALIGNED PARTICLE STREAMING AND GEOMAGNETIC MICROPULSATIONS	19
2.1	<i>Introduction</i>	20
2.2	<i>Dispersion Relation</i>	21
2.3	<i>Stability Criterion &amp; Growth Rate</i>	25
2.4	<i>Micropulsations</i>	29
	<i>References</i>	31
CHAPTER 3	ENHANCED SCINTILLATIONS ASSOCIATED WITH HIGH SPEED STREAMS IN THE SOLAR WIND	34
	<i>Introduction</i>	35
	<i>Dispersion Relation</i>	38
	<i>Summary</i>	40
	<i>References</i>	41

PART II : WAVE PARTICLE EFFECTS  
IN TURBULENT PLASMA

	<i>Introduction</i>	32
CHAPTER 3	PARTICLE DIFFUSION IN A TURBULENT BACKGROUND	36
	3.1 <i>Electrostatic Fluctuations</i> ( $\omega \ll \Omega_i$ )	37
	3.1.a. <i>Turbulent Diffusion D across B</i>	42
	3.1.b. <i>Velocity Space Diffusion D</i>	44
	3.2 <i>Electrostatic Fluctuations</i> ( $\omega \gg \Omega_i$ )	48
	3.2.a. <i>Integration over the Perturbed Orbit</i>	53
	3.2.b. <i>Diffusion Coefficient in the Quasilinear Limit</i>	55
	3.2.c. <i>Spatial Diffusion in Electrostatic Turbulence ( <math>\omega \sim \Omega_i</math> )</i>	57
	3.3 <i>Electromagnetic Fluctuations</i> ( $\omega \ll \Omega_i$ )	60
	<i>References</i>	64
CHAPTER 4	CALCULATIONS OF THE PERTURBED ORBIT	65
	4.1 <i>The Perturbed Orbit as a Convolu- tion Integral</i>	67

4.2	Limiting values of the Perturbed Orbit	70
4.2.a.	Strong Spatial Diffusion, $K_{\perp}^2 D_{\perp} \gg 3 (K_{\parallel}^2 D_{\parallel})^{1/3}$	70
4.2.b.	Strong Velocity Space Diffusion, $(K_{\parallel}^2 D_{\parallel})^{1/3} \gg 1/3 K_{\perp}^2 D_{\perp}$	73
4.3	Numerical Integration of the Perturbed Orbit	76
4.4	Self-Consistent Values of the Diffusion Co-efficient	79
	References	83

CHAPTER 5	NONLINEAR DISPERSION RELATION	84
5.1	Dielectric Function in a Turbulent Plasma	86
5.2	Ion-Acoustic Waves in a Magnetic Field	90
5.3	Effect of Velocity Space Diffusion	98
5.3.a.	Ion Diffusion	99
5.3.b.	Electron Diffusion	102
5.4	Non-Linear Ion-Cyclotron Dispersion Relation	102
	References	105

CHAPTER 6	SPECTRUM OF TURBULENT ION ACOUSTIC WAVES	106
-----------	---	-----

6.1	<i>Ion Acoustic Spectrum</i>	108
6.2	<i>Superposition Principle of Dressed Particles</i>	109
6.3	<i>Calculation of the Spectrum</i>	110
6.4	<i>Numerical Results</i>	115
6.5	<i>Comparison with Observed Spectra and Simulations</i>	116
6.6	<i>Comparison with Theoretical Spectra</i>	118
6.7	<i>Conclusions</i>	119
	<i>References</i>	120

CHAPTER 7	FLUCTUATION SPECTRUM OF HIGHER FREQUENCY ELECTROSTATIC AND ELECTROMAGNETIC TURBULENCE	122
-----------	---	-----

7.1	<i>Electrostatic Fluctuations</i>	122
7.2	<i>Spectrum of Electromagnetic Fluctuations</i>	129
	<i>References</i>	132
	<i>NUMERICAL RESULTS</i>	115
	<i>SUMMARY AND CONCLUSIONS</i>	133

APPENDIX I: Properties of the Lommel Function	138
--	-----



PART I : ELECTROMAGNETIC INSTABILITIES  
IN SPACE PLASMA

## INTRODUCTION

The linear theory of plasma waves is now well understood, and many naturally occurring and laboratory plasma phenomena have been satisfactorily explained on this basis. The linear theory is valid if fluctuations about the macroscopic fields are small, but breaks down near a wave particle resonance or in the presence of suprathermal fluctuations. The effect of finite fluctuations, wave particle resonances, the saturation of instabilities, and the onset of turbulence can be described only in terms of a non linear theory. There are several existing theories of plasma turbulence, but they still need to be verified by detailed comparison with experiments.

For the present we shall be concerned only with low frequency waves ( $\omega \ll \Omega_i$  to  $\omega \sim \Omega_i$ ), excited by particle streaming along the external magnetic field, both in the linear and turbulent regimes. Certain low frequency modes are commonly observed in laboratory and space plasmas. It is necessary to understand their generation mechanism, identify the method of saturation, and study the characteristics of the turbulent state which may be formed through the nonlinear interactions. These are the points that we shall consider in this thesis.

The thesis is divided into two independent parts dealing with the linear and turbulent regimes respectively. Part I consists of two chapters where we attempt to explain certain space phenomena arising from electromagnetic waves, using linear instability theory.

In Chapter 1 we consider the generation of magnetosonic waves by high speed solar wind streams. These waves can explain the increase in interplanetary scintillation observed at the leading edges of the fast streams. A stabilizing mechanism operates by which the instability is turned off with the advance of the stream.

In Chapter 2 we consider the thermally anisotropic plasma in the magnetosphere with particle streaming along the earth's magnetic field. It is well known that temperature anisotropy leads to low frequency instabilities like the "firehose" and "mirror" instabilities in high plasmas. In a homogeneous plasma, the mirror instability has a vanishing real frequency, but finite growth rate. The presence of the stream introduces a real frequency for the mirror instability, which sets up oscillations in the magnetic field at the same frequency. This model suggests an explanation for geomagnetic micropulsations triggered by ~~substorm~~ particles.

In Part II, we turn to the study of non-linear effects in turbulent plasmas. These could be due to



wave-particle or wave-wave interactions, (i.e. mode coupling), of which we shall consider only wave-particle effects. Of the existing theories of plasma turbulence, the self-consistent statistical theories appear to be the most promising. Our main goal here is two fold:

- (i) to extend the framework of the above theories to include higher frequency electrostatic waves and electromagnetic waves, and
- (ii) to calculate the electric field fluctuation spectrum explicitly, and compare it with the several existing measurements of turbulent spectra to gauge the predictive ability of the self-consistent formulation.

The nature and scope of our study of plasma turbulence will be described in the introduction to Part II.



## CHAPTER I

### ENHANCED SCINTILLATIONS ASSOCIATED WITH HIGH SPEED STREAMS IN THE SOLAR WIND

*Abstract: The long wavelength ( $\lambda > \rho_i$  ion-gyro radius) density inhomogeneities in the solar wind that raise the stellar radio scintillation index during the onset of a high-velocity stream, may be generated by a low-frequency compressional electromagnetic mode such as the magnetosonic (MS) wave. Our investigation shows that obliquely propagating MS waves are driven unstable by the*

double-peaked proton distributions observed in the solar wind. We propose this as a reason for the correlation of high speed streams with enhanced scintillation. The stability at 1 AU of the observed nonequilibrium, double-peaked particle distributions emerges as a natural consequence of the suggested mechanism.

### INTRODUCTION

It had been observed as far back as 1972 (Houminer and Hewish, 1972) that long-lived (3-4 days) strong scintillation of radio sources was directly related to high speed solar wind streams (700-800 km/s). The sectors of enhanced scintillation preceded the fast streams by about 2.5 days. These sectors were found to be regions of increased density (Belcher and Davis, 1971), and the ad hoc assumption that electron density fluctuations are proportional to density was employed to explain the increased scintillations.

We can reasonably assume that the enhanced scintillations are due to a compressional plasma mode that produces 'microscale' ( $\sim 100$  km) density fluctuations in the solar wind near the sun and across the line of sight to the radio source. Of the low-frequency hydromagnetic modes the Alfvén wave, although commonly observed in the solar wind, is not efficient in producing density fluctuations in the linear regime (Wu and Huba, 1975). In situ

observations indicate that while trains of pure Alfvén waves are seen within fast and slow streams as well as in the trailing edges of fast streams, there is at least 10% magneto acoustic noise at the leading edges of fast streams (Barnes, 1978; Lichenstein and Sonett, 1980).

The wave mode must be supported by a source of free energy in the system. Some energy sources, discussed earlier by several investigators, are particle temperature anisotropy and heat flux from the base of the corona, which do not relate specifically to fast streams. Belcher and Davis (1971) qualitatively discuss the interaction (collision) of fast and slow streams, but there is no evidence of spirally aligned shock fronts within 1 AU.

For the solar wind the wave modes invoked have been the ion-acoustic (Forslund, 1970), seen to be associated with bursts of electrostatic turbulence in the quiescent solar wind (Gurnett and Frank, 1978), the magnetosonic, and ion cyclotron waves. The ion-cyclotron mode gives rise to a narrow band of frequencies around  $\Omega_i$  and is invoked to explain the enhancement of the power spectra near  $\mathcal{P}_i$  (Neugebauer et al., 1978). The scale of irregularities generated by ion acoustic waves ranges from the Debye length  $\lambda_D$  ( $\sim$  km) to  $\mathcal{P}_i$  ( $\sim$  50 km), whereas the magnetosonic wave irregularities are larger than  $\mathcal{P}_i$ , which is the relevant scale for radio-

scintillation at Megahertz frequencies. The enhanced magnetic field fluctuations during the onset of a fast stream also point to an electromagnetic mode.

In connection with fast streams, the 'beam' instability appears to be the most natural choice. The proton velocity distributions observed at 1 AU in high speed streams are indeed double peaked with relative velocity  $\sim 64$  km/s and beam densities varying from  $\sim 0.1$  at the onset to  $\sim 0.3$  during a fast stream (e.g., Abraham-Shrauner and Feldman, 1977). Such distributions may have the required free energy to sustain the waves, but careful note must be taken of the fact that the distributions observed at 1 AU are necessarily stable on a time scale of several days.

The ambient solar wind velocity ( $\sim 400$  km/s) is less than the fast stream velocity ( $\sim 700$ -800 km/s) by more than 300 km/s. Yet in the distributions observed at 1 AU the relative velocity between the peaks is only  $\sim 64$  km/s. We infer that at least a part of the streaming energy has gone toward excitation of plasma instabilities ultimately resulting in the double peaked distributions with reduced relative velocity as observed at 1 AU. If magnetoacoustic waves are built up by this mechanism, they can provide density bunching on the scale length responsible for scintillation. We investigate therefore the



stability of obliquely propagating magnetoacoustic waves in the presence of double peaked proton distributions with arbitrary relative velocity using the Vlasov theory.

Montgomery et al. (1976) have numerically analyzed the interaction of hydromagnetic waves with double ion streams over a wide range of parameters such as  $\beta$ , the drift velocity  $V$ , and temperature anisotropy. However, they do not discuss the resonant instability of oblique MS waves.

### DISPERSION RELATION

The basic equations used for deriving the dispersion relation for low-frequency ( $\omega < \Omega_i$  ion-gyrofrequency) hydromagnetic modes are the Maxwell and Vlasov equations. For a  $z$ -directed magnetic field and propagation vector  $\vec{k}$  lying in the  $xz$  plane,

$\vec{k} = (k_x, 0, k_z)$  or  $(k \sin \theta, 0, k \cos \theta)$ , the dielectric constant  $\vec{\epsilon}$  is a tensor (see, e.g., Hasegawa, 1975). In the absence of currents some of the elements of  $\vec{\epsilon}$  vanish, and the dispersion relation decouples to

$$\left( \epsilon_{yy} - \frac{c^2 k^2}{\omega^2} \right) \epsilon_{zz} + \epsilon_{yz}^2 = 0 \quad (1)$$

and further to

$$\epsilon_{yy} - \frac{c^2 k^2}{\omega^2} = 0 \quad (2)$$

in the limit of large conductivity when  $\epsilon_{zz}$  is large.

$$\epsilon_{yy} = \sum_j \frac{\omega_{pj}^2}{\Omega_j^2} \left[ \left\langle \left( 1 - \frac{k_{||} v_{||j}}{\omega} \right)^2 \right\rangle - \frac{k_{||}^2}{2\omega^2} \langle v_{||j}^2 \rangle \right. \\ \left. - \frac{k_{\perp}^2}{\omega^2} \langle v_{\perp j}^2 \rangle + \frac{k_{\perp}^2}{4\omega^2} \langle v_{\perp j}^4 \rangle I_j \right] \quad (3)$$

where

$$I_j = \int_{-\infty}^{\infty} dv_{||} \int_0^{\infty} 2\pi v_{\perp} dv_{\perp} \frac{\frac{\partial f_j(v_{\perp}, v_{||})}{\partial v_{||}}}{\left( v_{||} - \frac{\omega}{k_{||}} \right)} \quad (4)$$

and

$$\langle v_j^n \rangle = \int_{-\infty}^{\infty} dv_{||} \int_0^{\infty} 2\pi v_{\perp} dv_{\perp} v_j^n f_j(v_{\perp}, v_{||}) \quad (5)$$

$\omega_{pj}$ ,  $\Omega_j$ , and  $f_j$  are the plasma and cyclotron frequencies and distribution function of the particle species  $j$ .

The initial normalized proton distribution function is taken to be a double Maxwellian in the center of mass frame of the protons:

$$f_i = \frac{(n_i/n)}{\left(\frac{2\pi T_e}{m_i}\right)^{3/2}} \exp \left\{ - \frac{(v_{||} - v_B)^2 + v_{\perp}^2}{\left(\frac{2 T_e}{m_i}\right)} \right\} \\ + \frac{(n_M/n)}{\left(\frac{2\pi T_M}{m_i}\right)^{3/2}} \exp \left\{ - \frac{(v_{||} + v_M)^2 + v_{\perp}^2}{\left(\frac{2 T_M}{m_i}\right)} \right\}$$

(6)

in which the high velocity beam protons with temperature  $T_B$  drift away from the sun with speed  $V_B$  while the main protons at temperature  $T_M$  drift slowly back toward the sun at a speed  $V_M$ .

The electron distribution is also observed to be double-peaked (Feldman et al., 1973) but since we find that the electron contribution to the required dispersion relation is  $O(m_e/m_i)$  of the proton contribution, we shall not deal with the details of the electron distribution here. It is simply assumed to be a Maxwellian drifting at the center of mass velocity of the protons, with a temperature  $\sim 10^5$  °K.

We assume that pressure anisotropy is not important for MS modes following Kennel and Wong (1967), who derive a general particle instability criterion which shows that while anisotropy drives ion-cyclotron waves unstable, beam instabilities are more important for magnetosonic waves.

The dispersion relation obtained for obliquely propagating low-frequency waves in the center of mass frame of the wind is

$$\left(\frac{\omega}{k}\right)^2 = V_A^2 + \frac{\left(k_\perp^2 - \frac{k_\parallel^2}{2}\right)}{k^2} V_S^2 - \frac{k_\parallel^2}{k^2} V^2 \frac{n_B n_M}{n^2} - \frac{k_\perp^2}{k^2} \sqrt{2} \mathcal{Z}^0 \quad (7)$$

$$\mathcal{Z}^0 = \frac{2T_e}{m_i} \frac{2T_e}{m_e} W\left(\frac{\omega/k_\parallel}{\sqrt{2T_e/m_e}}\right) + \frac{n_B}{n} \left(\frac{2T_B}{m_i}\right)^2 W\left(\frac{\omega/k_\parallel - V_B}{\sqrt{2T_B/m_i}}\right) + \frac{n_M}{n} \left(\frac{2T_M}{m_i}\right)^2 W\left(\frac{\omega/k_\parallel - V_M}{\sqrt{2T_M/m_i}}\right) \quad (8)$$

where  $V_A = B/\sqrt{4\pi\varphi}$  is the Alfvén velocity,  
 $V_S = \sqrt{(T_e + \gamma T_i)/\varphi}$  is the sound velocity and

$$W(z) = \frac{1}{\sqrt{2\pi}} \int_{-\infty}^{\infty} \frac{x}{x-z} e^{-x^2/2} dx \quad (9)$$

The phase velocity of the wave is

$$V_p^2 = V_A^2 + \left(\sin^2\theta - \frac{\cos^2\theta}{2}\right) V_S^2 - \cos^2\theta V^2 \frac{n_B n_M}{n} \quad (10)$$



in terms of the relative velocity  $V = V_B + V_M$ . In the absence of streaming, and  $k$  perpendicular to  $B$ , (10) reduces to the familiar magnetosonic velocity.

In the direction of  $B$  for a high plasma ( $\beta = nKT/(B^2/8\pi)$ ) we would obtain a pure acoustic wave provided the full equation (2) was taken (e.g., Spitzer, 1962, p. 67) or a modified Alfvén wave if  $\beta < 1$ .

The  $W$  function can be expanded when  $|z| < 1$  as

$$W(z) = i\sqrt{\frac{\pi}{z}} \exp\left(-\frac{z^2}{z}\right) + 1 - z^2 + \dots \quad (11)$$

$$W\left(\frac{\omega/k_{\parallel} - v_B}{\sqrt{2T_E/m_i}}\right) = i\sqrt{\frac{\pi}{2}} \left(\frac{\omega/k_{\parallel} - v_B}{\sqrt{2T_E/m_i}}\right) \exp\left[-\frac{(\omega/k_{\parallel} - v_B)^2}{4T_E/m_i}\right] \quad (12a)$$

$$\left| \frac{\omega/k_{\parallel} - v_B}{\sqrt{2T_E/m_i}} \right| < 1 \quad (12b)$$

From (12a) and (12b) we obtain the lower and upper limits of the range of frequencies that grow in the forward direction:

$$V_B > \left( \frac{\omega}{k_{||}} \right)_+ > V_E - \sqrt{\frac{2T_E}{m_i}}$$

(13a)

Similarly, for backward propagating waves,

$$V_M > \left| \left( \frac{\omega}{k_{||}} \right)_- \right| > V_M - \sqrt{\frac{2T_M}{m_i}}$$

(13b)

The growth rates of the waves are

$$\gamma_f = \frac{n_B}{n} \frac{\sqrt{\pi}}{2} \frac{k_{\perp}^2}{\omega} \left( \frac{2T_E}{m_i} \right)^{3/2} \left( \frac{\omega}{k_{||}} - V_B \right)$$

$$\exp \left\{ - \frac{\left( \frac{\omega}{k_{||}} - V_B \right)^2}{4T_E/m_i} \right\}$$

(14)

$$\gamma_b = \frac{n_M}{n} \frac{\sqrt{\pi}}{2} \frac{k_{\perp}^2}{\omega} \left( \frac{2T_M}{m_i} \right)^{3/2} \left( \frac{\omega}{k_{||}} + V_M \right)$$

$$\exp \left\{ - \frac{\left( \frac{\omega}{k_{||}} + V_M \right)^2}{4T_M/m_i} \right\}$$

(15)

The threshold conditions (13) rewritten in terms of the relative velocity  $V$  ( $V = (n/n_B) V_M = (n/n_M) V_B$ ) are

$$\left(1 - \frac{n_B}{n}\right) v > \left(\frac{\omega}{k_{\parallel}}\right)_f$$

(16)

and

$$\left|\left(\frac{\omega}{k_{\parallel}}\right)_b\right| < \frac{n_B v}{n}$$

(17)

Comparison of (14) to (17) shows that at the onset of the fast particles the forward wave grows, the rate increasing with the number of beam protons. As the fast stream advances, the increase in  $n_B$  may reverse the threshold condition (16) and arrest the growth of the forward wave. The backward wave begins to grow only after there are a sufficient number of beam protons to satisfy the threshold condition (17), but the growth rate, being proportional to  $n_M$ , decreases with the advance of the high-velocity stream. This means that the maximum density fluctuations are generated at the leading edge of the high-speed stream followed by a quenching of the instability with the advance of the stream. Since the instability is not self-limited by nonlinear amplitude growth but is quenched by an externally changing proton distribution function, we may safely assume that the use of linear theory is adequate under the circumstances. The electron Landau damping represented by the first term in (8) is effective for large propagation angles.

An interesting consequence of the beam instability is that energy is drained from the fast particles (e.g., Spitzer, 1962, p. 89) as long as there exists a wave with phase velocity less than the beam velocity. As the particles slow down by beam retardation, they may cross the threshold velocity of the slowest wave. After this, the particles cannot lose energy to any wave and are prevented from reaching equilibrium in the collisionless solar wind. Qualitatively, we expect therefore to see nonequilibrium particle distribution functions with peaks separated by a velocity of the order of the MS mode ( $V_{\text{obs}} = 64 \text{ km/s}$ ) at 1 AU. To study the exact change in the nature of the distribution function as a result of interaction with the waves requires a nonlinear calculation.

#### SUMMARY

The enhancement of stellar radio-scintillation during the onset of high-speed streams is due to density fluctuations on a scale  $\sim 100 \text{ km}$ . In this range the MS mode is the most efficient in producing density fluctuations. The onset of a fast stream creates appropriate conditions for the ion-resonant beam instability of obliquely propagating MS waves. At a fixed observer the instability is initiated by the fast stream



and quenched with the advance of the stream. The double-humped proton distribution function continues to act as a source of energy to the waves until the streaming velocity falls below the threshold for exciting the slowest ( $\sim V_A$  or  $V_S$ ) wave. We expect therefore to see enhanced scintillation along the leading edges of high speed streams and non-equilibrium ion distribution functions with  $V \sim 50-60$  km/s at 1 AU. These facts are well borne out by observations.

REFERENCES

- Abraham-Shrauner, B., and W.C. Feldman, Nonlinear Alfvén waves in high-speed solar wind streams, *J. Geophys. Res.*, 82, 618, 1977.
- Barnes, A., Hydromagnetic waves and turbulence in the solar wind, in *Solar System Plasma Physics*, edited by C.F. Kennel, L.J. Lanzerotti, and E.N. Parker, North Holland, Amsterdam, 1978.
- Belcher, J.W., and L. Davis, Jr., Large amplitude Alfvén waves in the interplanetary medium 2, *J. Geophys. Res.*, 76, 3534, 1971.
- Feldman, W.C., J.R. Asbridge, S.J. Bame, and M.D. Montgomery, Double ion streams in the solar wind, *J. Geophys. Res.*, 78, 2017, 1973.
- Forslund, D.W., Instabilities associated with heat conduction in the solar wind and their consequences, *J. Geophys. Res.*, 75, 17, 1970.
- Gurnett, D.A., and L.A. Frank, Ion acoustic waves in the solar wind, *J. Geophys. Res.*, 83, 58-74, 1978.
- Hasegawa, A., *Plasma Instabilities and Nonlinear Effects*, p. 93, Springer-Verlag, New York, 1975.
- Houminer, Z., and A. Hewish, Long-lived sectors of enhanced density irregularities in the solar wind, *Planet. Space Sci.*, 20, 1703-1716, 1972.

- Kennel, C.F., and H.V. Wong, Resonant particle instabilities in a uniform magnetic field, *J. Plasma Phys.*, 1, 81-104, 1967.
- Lichenstein, B.R., and C.P. Sonett, Large amplitude Alfvénic variations in the solar wind, *Geophys. Res. Lett.*, 7, 189, 1980.
- Montgomery, M.D., S.P. Gary, W.C. Feldman, and D.W. Forslund, Electromagnetic instabilities driven by unequal proton beams in the solar wind, *J. Geophys. Res.*, 81, 2743, 1976.
- Neugebauer, M., C.S. Wu, and J.D. Huba, Plasma fluctuations in the solar wind and their consequences, *J. Geophys. Res.*, 83, 1027, 1978.
- Spitzer, L., Jr., *Physics of Fully Ionized Gases*, Interscience, New York, 1962.
- Wu, C.S., and J.D. Huba, Low frequency fluctuations in the solar wind, I, Theory, *Astrophys. J.*, 196, 847-857, 1975.

## CHAPTER 2

### FIELD ALIGNED PARTICLE STREAMING AND GEOMAGNETIC MICRO- PULSATIONS

Abstract: Particle streaming is invariably associated with certain types of micropulsations. These particles, released from the geomagnetic tail into the magnetosphere during substorms, may be a primary source for the onset of geomagnetic micropulsations. We suggest a mechanism by which particle streaming along the magnetic field in an otherwise stable, homogeneous plasma with anisotropic temperature, generates low frequency electromagnetic modes similar to the "mirror" instability. The plasma density and magnetic field undergo a periodic modulation at a frequency which is a function of the particle streaming velocity.



## 2.1. INTRODUCTION

Several distinct classes of micropulsations of the geomagnetic field have been studied by McPherron et al (1968). The micropulsations are often associated with impulsive electron and ion precipitations. The energetic particles probably enter from the tail during substorms and stream along the magnetic field in the magnetosphere. The streaming velocity can be of the order of the Alfvén speed. In general this speed is lower than the threshold velocity required for the generation of low frequency electrostatic or electromagnetic modes in a thermally isotropic plasma.

The early theories on the generation of micropulsations (Dungey 1955, Southwood 1974, Radoski 1967, Newton et al. 1978) considered the guided propagation of Alfvén waves in toroidal and transverse poloidal mode. Hasegawa (1975) explained micropulsations on the basis of the drift mirror instability. The mirror instability is excited in an anisotropic plasma with  $\beta_{\perp} > \beta_{\parallel}$  where  $\beta = \left( \frac{8\pi nT}{B^2} \right)^{1/2}$ . This mode neither propagates nor does it have a real frequency. When coupled to a gradient in the magnetic field, the mode has a low frequency which has been associated with Pc-5 micropulsations by Hasegawa. The role of particle streaming in the triggering of micropulsations has not been considered.

## 2.2. DISPERSION RELATION

We consider an idealized collisionless homogeneous plasma with anisotropic temperature and carrying a beam of particles along the magnetic field. The implicit assumption is that although we shall be considering low frequency, long wavelength phenomena, the scale is small as compared to the length of the magnetic field lines and the scale of variation of plasma density and temperature along them.

The low frequency electromagnetic waves that may be excited in a high  $\beta$  plasma are the Alfvén and magnetosonic waves. Of these, the Alfvén wave is not significantly affected by wave particle interactions. Moreover, since Alfvén waves are recognised to cause a rotation in the magnetic vector without change of magnitude, their influence on geomagnetic micropulsations must be limited.

The magnetosonic wave dispersion relation (Hasegawa 1975) when decoupled from the acoustic wave is

$$\frac{c^2 k^2}{\omega^2} - \epsilon_{yy} = 0$$

$$\epsilon_{yy} = \sum_j \frac{\omega_{pj}^2}{\Omega_j^2} \left[ \left\langle \left( 1 - \frac{k_{\parallel} v_{\parallel j}}{\omega} \right)^2 \right\rangle - \frac{k_{\parallel}^2 \langle v_{\parallel j}^2 \rangle}{2 \omega^2} \right. \\ \left. - \frac{k_{\perp}^2 \langle v_{\perp j}^2 \rangle}{\omega^2} + \frac{k_{\perp}^2 \langle v_{\perp j}^4 \rangle}{4 \omega^2} \right] I_j \quad (1)$$

where  $k_{\parallel}$  and  $k_{\perp}$  are the wave vector components parallel and perpendicular to the  $z$ -directed magnetic field,  $\omega_{pj}$  and  $\Omega_j$  are the plasma and gyrofrequency of the  $j^{\text{th}}$  species, and

$$\langle v_j^n \rangle = \int v_j^n f_{0j}(v) d^3v$$

$$\Gamma_j = \int \frac{f_0(v)}{(v_{\parallel} - \omega/k_{\parallel})^2} d^3v; \quad \text{Im } \omega > 0$$

Assuming a Maxwell distribution in the parallel direction for the ambient plasma, and a drifting Maxwellian for the stream, we obtain

$$\begin{aligned} \epsilon_{yy} = \sum_j \frac{\omega_{pj}^2}{\Omega_j^2} - \frac{c^2}{\omega^2} \left[ k_{\parallel}^2 \frac{\beta_{\perp j} - \beta_{\parallel j}}{2} \right. \\ \left. + k_{\perp}^2 \beta_{\perp j} \left( 1 + \frac{\beta_{\perp j}}{2\beta_{\parallel j}} Z' \left( \frac{\omega - k_{\parallel} v_j}{\sqrt{2} k_{\parallel} v_{Tj}} \right) \right) \right] \end{aligned}$$

where

$$\beta_{\perp j} = \frac{1}{2} \frac{m_j n \langle v_{\perp j}^2 \rangle}{B_0^2/2\mu_0} = \frac{2 \omega_{pj}^2}{\Omega_j^2} \frac{v_{Tj}^2}{c^2}$$

$$\beta_{\parallel j} = \frac{m_j n \langle v_{\parallel j}^2 \rangle}{B_0^2/2\mu_0} = \frac{2 \omega_{pj}^2}{\Omega_j^2} \frac{v_{Tj}^2}{c^2}$$

and  $V_j = 0$  for all particles except those streaming with velocity  $V_0$ .

As is evident from the fact that  $\omega_{pi}^2/\Omega_i^2$  for electrons is  $O(m_e/m_i)$  smaller than for protons, and as expected, for low frequency modes, the electrons hardly affect the dispersion relation except in Landau damping or growth. Assuming that the beam density is small, the dispersion relation becomes

$$\omega^2 = k^2 V_A^2 \left[ \left\{ 1 + \frac{\cos^2 \theta}{2} \left( \beta_{Li} - \beta_{Hi} \right) + \sin^2 \theta \left( \beta_{Li} - \frac{\beta_{Li}^2}{\beta_{Hi}} \right) \right\} \right.$$

$$\left. - i \sin^2 \theta \sqrt{\frac{\pi}{2}} \left\{ \frac{\omega}{k_{\parallel} V_{Hi}} \left( \frac{\beta_{Li}^2}{\beta_{Hi}} \right) + \frac{\beta_{Li}^2}{\beta_{Hi}} \frac{(\omega - k_{\parallel} V_0)}{k_{\parallel} V_B} \right\} \right]$$

(2)

where  $V_A = c \Omega_i / \omega_{pi}$  is the Alfvén velocity.

Furthermore, if the beam temperature is comparable to the ion temperature, the imaginary part of Eq. (1) reduces to

$$\text{Im} \omega^2 \approx \sqrt{\frac{\pi}{2}} \left\{ \frac{\omega}{k_{\parallel} V_{Hi}} \left( \frac{\beta_{Li}^2}{\beta_{Hi}} \right) - \frac{\beta_{Li}^2}{\beta_{Hi}} \frac{V_0}{V_{Hi}} \right\}$$

(3)

In the low frequency limit,  $\omega \ll k V_A$ , an anisotropic plasma is unstable even in the absence of a



beam. The instability, driven by the anisotropy, is obtained under two limiting conditions:

$$(i) \text{ If } 1 + \sum_j \frac{\beta_{Lj} - \beta_{Hj}}{2} < 0 \quad (5)$$

for large  $k_{\parallel}/k_{\perp}$  : i.e. almost parallel propagation

and (ii) If

$$1 + \sum_j \left( \beta_{Lj} \left( 1 - \frac{\beta_{Lj}}{\beta_{Hj}} \right) \right) < 0 \quad (6)$$

for large  $k_{\perp}/k_{\parallel}$  : i.e. almost perpendicular propagation.

These are the firehose and mirror instabilities. The conditions can be further simplified to

$$\beta_{Hj} > \beta_{Lj} + 2 \quad \text{for } k_{\parallel} \gg k_{\perp}$$

$$\beta_{Lj} > \beta_{Hj} \quad \text{for } k_{\perp} \gg k_{\parallel}$$

The plasma is stable if  $\beta_{Lj} < \beta_{Hj} < \beta_{Lj} + 2$ . The presence of a beam can render such a plasma unstable. The nature of the instability is similar to the mirror instability, but unlike the mirror instability where the frequency is purely imaginary, the instability excited by the beam has a complex frequency. In the next section we solve the dispersion Eq.(2) keeping in mind that the real part of the frequency may be small, or comparable to the imaginary part.

### 2.3. STABILITY CRITERION AND GROWTH RATE

The dispersion Eq. (2) is a quadratic in  $\omega$  of the type

$$\omega^2 + b\omega + c = 0$$

where

$$b = k^2 v_A^2 \left\{ i \frac{\sin^2 \theta}{k_{\parallel} v_{\text{th}}} \sqrt{\frac{\pi}{2}} \frac{\beta_{\perp i}^2}{\beta_{\text{th}}} \right\} \quad (7)$$

and

$$c = -k^2 v_A^2 \left[ \left\{ 1 + \frac{(\cos^2 \theta)}{2} (\beta_{\perp i} - \beta_{\text{th}}) + \Delta \sin^2 \theta \times \right. \right. \\ \left. \left. \left( \beta_{\perp i} - \frac{\beta_{\perp i}^2}{\beta_{\text{th}}} \right) \right\} + i \sin^2 \theta \sqrt{\frac{\pi}{2}} \frac{\beta_{\perp i}^2}{\beta_{\text{th}}} \right] \quad (8)$$

The complex frequency is

$$\omega = -\frac{b}{2} \pm \frac{1}{2} \sqrt{b^2 - 4c}$$

which can be expressed as

$$\omega = -id \left[ 1 \pm (K_r - iK_i)^{1/2} \right] \quad (9)$$

where

$$d = \frac{k v_A}{2} \left( \frac{k v_A}{k_{\parallel} v_{\parallel i}} \sin^2 \theta \sqrt{\frac{\pi}{2}} \frac{\beta_{\perp i}^2}{\beta_{\parallel i}} \right) \quad (10)$$

$$K_r = \left| - \left\{ \frac{1 + (\cos^2 \theta (\beta_{\perp i} - \beta_{\parallel i}))}{(d^2 / k^2 v_A^2)} + \frac{\sin^2 \theta (\beta_{\perp i} - \frac{\beta_{\perp i}^2}{\beta_{\parallel i}})}{d^2 / k^2 v_A^2} \right\} \right| \quad (11)$$

$$K_i = \sin^2 \theta \sqrt{\frac{\pi}{2}} \left( \frac{\beta_{\perp B}^2}{\beta_{\parallel B}} \right) \left( \frac{v_o}{v_{\parallel B}} \right) / \left( d^2 / k^2 v_A^2 \right) \quad (12)$$

For growing modes,

$$\omega = -id \left[ 1 - r^{1/2} e^{i\psi/2} \right] \quad (13)$$

where

$$r = \left[ K_r^2 + K_i^2 \right]^{1/2}, \quad \tan \psi = \frac{K_i}{K_r} \quad (14)$$

The instability threshold is defined by  $r^{1/2} \cos \psi/2 > 1$  which gives  $K_i^2 > 4(1 - Kr)$

From (13) we get,

$$\left( \frac{V_0}{V_{th}} \right)^2 \geq \frac{k^2 V_A^2}{k_{||}^2 V_{th}^2} \left( \frac{\beta_{Li}^2 / \beta_{ni}}{\beta_{Li}^2 / \beta_{nB}} \right) \left\{ 1 + \cos^2 \theta (\beta_{Li} - \beta_{ni}) + \sin^2 \theta \left( \beta_{Li} - \frac{\beta_{Li}^2}{\beta_{ni}} \right) \right\} \quad (15)$$

which defines the threshold value of the streaming velocity.

Eqn. (15) shows that depending on the degree of thermal anisotropy, even a low streaming velocity is sufficient to excite an instability. The streaming velocity does not have to exceed the phase velocity of the wave in order to trigger the instability.

The above situation is interesting because even when neither the beam nor the anisotropy is sufficient to drive an instability, in conjunction they can trigger a low frequency instability.

The wave frequency is given by

$$\omega_k = k V_A \left\{ 1 + \frac{\cos^2 \theta}{2} (\beta_{Li} - \beta_{ni}) + \sin^2 \theta \left( \beta_{Li} - \frac{\beta_{Li}^2}{\beta_{ni}} \right) \right\} \quad (16)$$

The growth rate is

$$\omega_i = d \left[ r^{1/2} (\cos \psi/2 - 1) \right]$$

where  $\omega_g = d r^{1/2} \sin \psi/2$

Therefore,

$$\frac{\omega_A}{d} \left( \frac{\omega_i}{d} + 1 \right) = r \sin^2 \psi/2 \cos \psi/2 = \frac{K_i}{2}$$

This gives

$$\begin{aligned} \omega_i &= \frac{d^2}{\omega_A^2} \frac{K_i^2}{2} - d \\ &= \frac{K_{VA}^2}{2} \sqrt{\frac{\pi}{2}} \sin^2 \theta \left[ \frac{\frac{\beta_{LB}^2}{\beta_{UB}} \frac{V_L}{V_{UB}}}{\omega_{Te}} - \frac{\frac{\beta_{Li}^2}{\beta_{Hi}}}{K_{Hi} V_i} \right] \quad (17) \end{aligned}$$

To have large growth we need

$$\cos \psi/2 > r^{-1/2}$$

(At  $\psi = 0$ ,  $\omega_{Te}$  vanishes). Under these conditions we have  $K_i \ll K_r$  which gives

$$\omega_{Te}^2 = d^2 r \sin^2 \psi/2 \approx \frac{d^2}{4} \frac{K_i^2}{K_r}$$

and



$$\omega_r \approx \frac{k V_A}{2} \sin^2 \theta \sqrt{\frac{\pi}{2}} \left( \frac{\beta_{\perp B}}{\beta_{ne}} \right) \left( \frac{v_s}{V_{ne}} \right) /$$

$$\left[ \frac{1}{4} \left( \frac{k^2 V_A^2}{k_{\parallel} V_{ni}^2} \right) \sin^4 \theta \frac{\pi}{2} \left( \frac{\beta_{\perp i}^2}{\beta_{ni}} \right) - \right.$$

$$\left. \left\{ 1 + \cos^2 \theta \left( \beta_{\perp i} - \beta_{ni} \right) + \sin^2 \theta \left( \beta_{\perp i} - \frac{\beta_{\perp i}^2}{\beta_{ni}} \right) \right\} \right]$$

(18)

The mode has an oscillation frequency that depends on the streaming velocity. At  $\theta = 0$ , the growth rate vanishes, and at  $\theta = \pi/2$  the threshold streaming velocity tends to infinity. The oblique modes are therefore most favoured.

Both electron and proton streaming can excite these waves but the threshold velocity is lower and the growth rates higher in the case of protons.

#### 2.4. MICROPULSATIONS

The above analysis shows that even small fluxes of particles flowing at low velocity along the field lines in the anisotropic magnetospheric plasma can excite electromagnetic waves. Thus the role of the substorm particles associated with geomagnetic micropulsations must be

carefully considered. Unlike the usual mirror instability which is purely growing and cannot modulate the geomagnetic field, the magnetic field fluctuations of these waves when excited will modulate the geomagnetic field at a frequency which is a function of the streaming velocity.

The density fluctuations induced will be out of phase with the magnetic field fluctuations by a factor of  $\pi$ . This and the associated existence of proton fluxes (134 keV) have been observed (Brown et al 1968). The mechanism suggested here may act along with the drift mirror instability suggested by Hasegawa, or by itself for a smaller degree of anisotropy when the mirror instability is not operative. Detailed correlation measurements of micropulsations and associated particle fluxes, their flow velocity and energy, and the background plasma anisotropy are required before the validity of the theory can be established.

REFERENCES

- Brown W.L., Cahill L.J., Davis L.R., McIlwain C.E.,  
 Roberts C.S., *J. Geophys. Res.* (1968)  
73, 153.
- Dungey, J.W. (1955), *Electrodynamics of the Outer  
 Atmosphere, Report of Conference on the  
 Physics of the Ionosphere, Physical  
 Society, London.*
- Hasegawa, A. (1969), *Drift Mirror Instability in the  
 Magnetosphere, Phys. Fluids* 12, 2642.
- McPherron, R.L., G.K. Parks, F.V. Coroniti and S.H. Ward  
 (1968) *J. Geophys. Res.* 73, 1967.
- Newton R.S., D.J. Southwood and W.J. Hughes (1978)  
*Planet. Space Sci.* 26, 202.
- Radoski H.R. (1967) *Highly Asymmetric MHD Resonances,  
 the guided poloidal mode, J. Geophys. Res.*  
72, 4026.
- Southwood D.J. (1974), *Planet. Space Sci.* 27, 483.

*PART II : WAVE PARTICLE EFFECTS IN  
TURBULENT PLASMA*

## INTRODUCTION

The linearised Vlasov theory used in Part I offers a precise description of a quiescent plasma. For a turbulent plasma, the theory suffers from serious limitations. Firstly, the linearization procedure becomes invalid with the growth of fields that, lead to the onset of turbulence. Secondly, the description in terms of smoothed or averaged quantities cannot take into account the effects of particle discreteness, correlations, and fluctuations that characterize the turbulent plasma.

Let us briefly examine here the assumptions used in the Vlasov description, and where they break down. Due to Debye screening, a charged particle is assumed to move in a potential due to the smoothed, averaged fields of all the other particles. The trajectory of the particle is then completely determined by the initial conditions on the invariant surfaces on which it is constrained to move. It is evident that even in a quiescent plasma, over distances comparable to the Debye distance, the particle is subject to random fluctuations about these smoothed fields. For turbulent plasmas this is true over distances much larger than  $k\lambda_d$ . These random perturbations in the potential result in the breaking of the invariant surfaces, leading to Kolmogorov-Arnold-Moser diffusion about them.



Consequently, instead of the sharply defined trajectory, a number of trajectories are now possible for different realizations of the microscopic turbulent fields. A statistical average over the fluctuations leads to an average diffused trajectory. This forms the basis of the Perturbed Orbit Theory of Dupree and Weinstock which we shall be using. It is a Renormalized Propagator Theory, which correctly takes into account the coherent part of the contribution of all the other particles to the test particle trajectory or propagator. In this manner, correlations are taken into account, without explicitly including collisional effects.

As in the linear theory, a consistent description of the turbulent plasma has been built up in terms of the perturbed orbit. In particular, the dielectric response is altered. Turbulent diffusion was shown to broaden the wave-particle resonance, which stabilizes the growth of the fluctuations.

In an alternative approach to Vlasov theory, based on the Klimontovich description in which all particle discreteness effects are included, it was shown by Cook and Taylor (1973) that the altered dielectric response in a turbulent plasma can self-consistently quench the growth of the fluctuations. The fluctuations then exist in a dynamically stable or "stationary" state.

Further, using a superposition principle of dressed particles applicable to the turbulent state, Cook and Taylor obtained a formal expression for the spectrum of fluctuations of the background turbulence. This was not done in the original theory of Dupree and Weinstock, which was in this sense incomplete.

We reexamine in this part, some of the aspects of the turbulence theories, with a view towards extending their region of applicability. The wave autocorrelation time is assumed to be short compared to the particle trapping time, so that the wave particle interaction is diffusive. In addition to spatial diffusion, velocity space diffusion coefficients are obtained in a magnetic field, both with and without the guiding centre approximation. The effect of low frequency turbulent electromagnetic waves on the diffusion coefficient is also obtained (Chapter 3).

In Chapter 3, the coupling between the components of the guiding-centre diffusion coefficients in the perturbed orbit had been neglected. In Chapter 4, we numerically evaluate the complete perturbed orbit, and use an iteration scheme to obtain self-consistent values of the diffusion coefficient,

The influence of orbit perturbation on the plasma dielectric function is examined in Chapter 5. The nonlinear dispersion relation for ion acoustic waves is solved. In particular, we find that velocity space diffusion does not contribute to resonance broadening.

The test particle diffusion discussed above is not observable in the absence of gradients. One of the important observables of the turbulent plasma is the fluctuation spectrum. In Chapter 6, we use the superposition principle of dressed particles to calculate, analytically, the ion acoustic spectrum in a magnetic field. This is compared to theoretical and experimental spectra, and computer simulations.

In Chapter 7, we obtain the spectrum of higher frequency ( $\omega \sim \Omega_i$ ) electrostatic turbulence, and low frequency electromagnetic turbulence in a magnetic field. The results and conclusions are summarised in the last section.

### CHAPTER 3

#### PARTICLE DIFFUSION IN A TURBULENT BACKGROUND

In this Chapter we present a statistical approach<sup>(1)</sup> to deal with particle motion in a turbulent plasma with a suprathermal level of fluctuations. It begins with calculating the mean diffused trajectory or 'perturbed orbit', which is identical to the characteristic function of the random walk executed by the particle in the turbulent background. The diffusion coefficients of the **particles** are defined in terms of the perturbed orbit, which is in turn a function of the diffusion. The formulation is therefore self-consistent.

In the following section we rederive the spatial diffusion coefficient (Dupree<sup>(1)</sup> - Weinstock<sup>(2)</sup>) in the guiding centre approximation. We then obtain the velocity space diffusion coefficient, by neglecting the coupling terms in the perturbed orbit. In Sections 2 and 3 we extend the formalism to the case of higher frequency ( $\omega \sim \Omega_i$ ) electrostatic waves, and to electromagnetic waves.

### 3.1. ELECTROSTATIC FLUCTUATIONS ( $\omega \ll \Omega_i$ )

In the absence of fluctuations in the electric field  $\vec{E}$ , the  $(\vec{E} \times \vec{B})$  velocity  $v_\perp$  of the guiding centre is an invariant of the motion. The particle moves on surfaces of constant  $v_\perp$  in phase space. The acceleration parallel to  $B$  is also constant. Small fluctuations in the Hamiltonian of the particles, arising from the background turbulence, break the invariant surfaces in accordance with the KAM theory<sup>(3)</sup>, which allows for the diffusion of particles in a certain region about the invariant surface.

The components of the diffusion tensor are the spatial diffusion  $D_\perp = \int \langle v_\perp(\tau) v_\perp(\tau+t) \rangle dt$  across the magnetic field  $B_0$ , the velocity space diffusion  $D_\parallel = \int \langle \dot{v}_\parallel(\tau) \dot{v}_\parallel(\tau+t) \rangle dt$  in the direction of  $B_0$ , and a cross diffusion term  $D_{\perp\parallel} = \int \langle v_\perp(\tau) \dot{v}_\parallel(\tau+t) \rangle dt$ . In general, the three diffusion processes proceed on



different time scales, the shortest time scale defining the dominant diffusion process.

The evaluation of the time correlation requires the knowledge of the exact particle propagator. In the Dupree-Weinstock theory, this is replaced by a statistically averaged propagator or perturbed orbit

. In terms of this, the diffusion coefficient is

$$\begin{aligned}\vec{D} &= \int dt \langle \vec{X}(\tau) \vec{X}'(\tau+t) \rangle \\ &= \sum_k \int_0^\infty dt \langle |\vec{X}_k \vec{X}_k'| e^{ik \cdot \Delta R(t)} \rangle e^{i\omega t} \quad (3.1.1)\end{aligned}$$

where  $\Delta R(t) = R(\tau+t) - R(\tau)$  is a section of the particle orbit, and is independent of  $\tau$  under stationary conditions. The correlations between Fourier components at different wave number (the incoherent contribution) have been neglected.

Replacing  $\vec{X}, \vec{X}'$  in Eq.(3.1.1) by  $\vec{v}_\perp = c \vec{E}_\perp / B_0$  and  $\vec{v}_\parallel = e E_\parallel / m$ , we obtain the components of  $\vec{D}$ .

$$\begin{aligned}
D_{\perp} &= \frac{3e^2}{m^2} \sum_k \langle |E_{1k}|^2 \rangle \int_0^\infty dt \langle e^{-ik \cdot \Delta R(t)} \rangle e^{i\omega t} + \\
D_{\parallel} &= \frac{ce}{mB} \sum_k \langle |E_{1k} E_{\parallel k}| \rangle \int_0^\infty dt \langle e^{-ik \cdot \Delta R(t)} \rangle e^{i\omega t} \\
D_{\perp} &= \frac{c^2}{2B^2} \sum_k \langle |E_{1k}|^2 \rangle \int_0^\infty dt \langle e^{-ik \cdot \Delta R(t)} \rangle e^{i\omega t} \quad (3.1.2)
\end{aligned}$$

where it has been assumed that the electric field fluctuations and the orbit function  $\exp[i\omega t - ik \cdot \Delta R(t)]$  are uncorrelated, so that the ensemble average over their product may be written as the product

$$\langle |E_K|^2 \rangle \langle \exp[i\omega t - ik \cdot \Delta R(t)] \rangle \quad \text{of the averages.}$$

This assumption, made in several places, is not explicitly stated hereafter.  $\langle |E_K|^2 \rangle$  represents the electric field fluctuation spectrum of the turbulent fluctuations which is undetermined.

---

\* The factor 3 has been introduced to keep the perturbed orbit in the same form as that used by Dupree and Weinstock.

Note:  $D_{\perp}$  represents velocity space diffusion;  $D_{\parallel}$  spatial diffusion; and  $D$ , diffusion in mixed velocity and configuration space.

The perturbed orbit is the characteristic function  $\langle \exp [ik \cdot \Delta R(t)] \rangle$  of the step size  $\Delta R(t)$  of the random walk executed by the diffusing particle. The characteristic function can, in general, be expanded in terms of the cumulants of the distribution of the variable  $\Delta R$ , as

$$\ln \langle \exp [-ik \cdot \Delta R(t)] \rangle = \sum_{n=0}^{\infty} \frac{K_n}{n!} (ik)^n \quad (3.1.3)$$

The cumulants  $K_n$  can be written in terms of the moments of  $\Delta R$  (e.g.  $K_0 = 0$ ,  $K_1 = \langle \Delta R(t) \rangle$ ,  $K_2 = \langle [\Delta R(t)]^2 \rangle - \langle [\Delta R(t)] \rangle^2$  etc.)

Retaining cumulants upto second order only, the perturbed orbit for guiding centre diffusion is<sup>(2)</sup>

$$\begin{aligned} \langle \exp [-ik \cdot \Delta R(t)] \rangle &= \exp \left[ \langle -ik \cdot \Delta R(t) \rangle \right. \\ &\quad \left. + \frac{1}{2} \langle [-ik \cdot \Delta R(t)]^2 \rangle \right. \\ &\quad \left. - \langle -ik \cdot \Delta R(t) \rangle^2 \right] \quad (3.1.4) \end{aligned}$$

$$= \exp \left[ -k_{||} v_{||} t - k_{\perp}^2 D_{\perp} t - k_{\perp} k_{||} D_{||} t^2 - k_{||}^2 D_{||} t^3 \right]$$

The higher order cumulants vanish identically when the distribution is Gaussian.

Substituting Eq. (3.1.4) in Eq. (3.1.2) we get a set of coupled equations for the diffusion coefficients,

$$\begin{aligned} D_{\parallel} &= \frac{3e^2}{m^2} \sum_k \langle |E_{\parallel k}|^2 \rangle I \\ D_{\perp\parallel} &= \frac{ce}{mB} \sum_k \langle |E_{\perp k} E_{\parallel k}| \rangle I \\ D_{\perp} &= \frac{e^2}{2B^2} \sum_k \langle |E_{\perp k}|^2 \rangle I \end{aligned} \quad (3.1.5)$$

where

$$I = \int_0^{\infty} dt \exp \left[ i(\omega - k_{\parallel} v_{\parallel} t) - k_{\perp}^2 D_{\perp} t - k_{\perp} k_{\parallel} D_{\perp\parallel} t^2 - \frac{1}{3} k_{\parallel}^2 D_{\parallel} t^3 \right] \quad (3.1.6)$$

It follows that the evaluation of any of the components of  $D$  requires a knowledge of all the other components unless some of them can be regarded as dominant and the others neglected. We examine below the relative importance of each term in the orbit function Eq. (3.1.6).

The diffusion coefficients for the  $j^{\text{th}}$  species satisfy an ordering relation

$$\eta_{\perp j} t : \eta_{\perp\parallel j} t^2 : \eta_{\parallel j} t^3 = \tan^4 \theta : \tan^2 \theta \Omega_j t : \Omega_j^2 t^2 \quad (3.1.7)$$

where  $t$  is some large multiple of the correlation time of the waves ( $\eta_{\perp} = k_{\perp} D_{\perp} k_{\perp}$ ,  $\eta_{\perp\parallel} = k_{\perp} D_{\perp\parallel} k_{\parallel}$ ,  $\eta_{\parallel} = k_{\parallel} D_{\parallel} k_{\parallel}$ ). At  $t \sim \Omega_i^{-1}$ , the ratio is

$$\eta_{\perp j} t : \eta_{\perp\parallel j} t^2 : \eta_{\parallel j} t^3 = \tan^4 \theta : \tan^2 \theta \frac{\Omega_j}{\Omega_i} : \left(\frac{\Omega_j}{\Omega_i}\right)^2$$

For electrons, therefore, the effect of parallel diffusion dominates for almost all propagation angles since  $\Omega_e / \Omega_i \sim (m_e/m_i)^{-1}$ . For ions, parallel diffusion dominates for propagation angles less than  $45^\circ$  on either side of B. For larger angles perpendicular diffusion is dominant on this time scale. After a sufficiently long time, velocity diffusion will ultimately dominate over the others.

Each diffusion coefficient is now calculated approximately, in the region in which it is dominant. The cross diffusion  $D_{\perp\parallel}$  cannot be calculated in this limit. The complete orbit integral is treated in Chapter 2.

### 3.1.a) Turbulent Diffusion $D_{\perp}$ across B

Neglecting the coupling terms in the orbit integral, the spatial diffusion is



$$\begin{aligned}
 D_{\perp} &= \frac{c^2}{2B^2} \sum_k \langle |E_{1k}|^2 \rangle \int_0^{\infty} dt \exp \left[ i(\omega - k_{\parallel} v_{\parallel})t - k_{\perp}^2 D_{\perp} t \right] \\
 &= \frac{c^2}{2B^2} \sum_k \frac{k_{\perp}^2}{k^2} \langle |E_{1k}|^2 \rangle \frac{k_{\perp}^2 D_{\perp}}{(\omega - k_{\parallel} v_{\parallel})^2 + k_{\perp}^4 D_{\perp}^2} \quad (3.1.8)
 \end{aligned}$$

In the limit of  $D \rightarrow 0$  there are no orbit perturbation effects and Eq. (3.1.8) reduces to the quasilinear diffusion

$$D_{\text{quasilinear}} = \frac{\pi c^2}{2B^2} \sum_k \langle |E_{1k}|^2 \rangle \delta(\omega - k_{\parallel} v_{\parallel}) \quad (3.1.9)$$

which is classical ( $\sim 1/B^2$ ), and strongly peaked at the resonant velocity.

In the limit of strong diffusion

$k_{\perp}^2 D_{\perp} \gg |\omega - k_{\parallel} v_{\parallel}|$ , when orbit perturbation effects are most important,

$$D_{\perp}(v_{\parallel}) = c \Phi / \sqrt{2} B \quad (3.1.10)$$

where  $\Phi = \left( \sum_k \langle |E_{1k}|^2 \rangle \right)^{1/2}$  is the turbulent potential. The diffusion is Bohm like ( $\sim 1/B$ ), and in contrast to

quasilinear diffusion, is independent of the particle velocity. In other words, the presence of orbit diffusion broadens the sharp quasilinear resonance (Eq. 3.1.8) and completely smears it out for high levels of turbulence.

If  $V_{Te} \gg \omega/k > V_{Ti}$ , it follows from Eq. (3.1.8) that the condition for strong diffusion will be satisfied for the bulk of the electron distribution if

$\Phi_e > \sqrt{2} B k_{\perp} v_{Te} / k_{\perp}^2 c$ , and for the bulk of the ion distribution if  $\Phi_i > \sqrt{2} B k_{\perp} v_{Ti} / k_{\perp}^2 c$ .

This means that for spatial diffusion, ion orbit perturbation effects are important at much lower levels of electric fluctuation than electron orbit perturbation effects, even though the diffusion coefficient  $D_{\perp}$  is the same for both species.

### 3.1.b) Velocity Space Diffusion $D$

The parallel velocity space diffusion coefficient is

$$\dot{\Phi}_{\parallel} = \frac{3e^2}{m^2} \int_0^{\infty} dt \sum_k \frac{k_{\parallel}^2}{k^2} \langle |E_k|^2 \rangle \exp \left[ i(\omega - k_{\parallel} v_{\parallel})t - \frac{1}{3} k_{\parallel}^2 \dot{\Phi}_{\parallel} t^3 \right] \quad (3.1.11)$$

if coupling between the components of the diffusion tensor is neglected.

The time integration of Eq. (3.1.11) gives

$$\delta_{||} = \frac{3e^2}{m^2} \sum_k \frac{k_{||}^2}{k^2} \langle |E_k|^2 \rangle \frac{\pi}{(k_{||}^2 \mathcal{D}_{||}/3)^{1/2}} \text{Ei}_3 \left[ -\frac{i(\omega - k_{||}v_{||})}{3(k_{||}^2 \mathcal{D}_{||}/3)^{1/2}} \right] \quad (3.1.12)$$

where  $\text{Ei}_3(x) = \int_0^\infty \exp[-t^3 - 3\alpha t] dt$  is Hardy's generalization of the Airy integral<sup>(4)</sup>.

Resonant particles with  $v_{||} \approx \omega/k_{||}$ , contribute to the real part of  $\mathcal{D}_{||}$ , and exchange energy irreversibly with the waves. The imaginary part of  $\mathcal{D}_{||}$  arises from reversible energy exchange with the waves, which does not give rise to real diffusion. The imaginary part of  $\mathcal{D}_{||}$  is therefore neglected. It can be seen from the properties of the  $\text{Ei}_3$  function that non-resonant particles contribute mainly to the imaginary part of  $\mathcal{D}_{||}$ , which means that there is no diffusion associated with them.

For particles close to resonance,

$\frac{1}{3} (\omega - k_{||}v_{||}) / (k_{||}^2 \mathcal{D}_{||})^{1/2} < 1$ ,  $\text{Ei}_3(x)$  can be expanded<sup>(4)</sup> in powers of  $x$  to give

$$\delta_{||} = \frac{e^2}{m^2} \sum_k \frac{k_{||}^2}{k^2} \langle |E_k|^2 \rangle \frac{2\pi}{\sqrt{3} \Gamma(4/3) (k_{||}^2 \mathcal{D}_{||}/3)^{1/2}} \times \left[ 1 - \frac{(\omega - k_{||}v_{||})^2}{(k_{||}^2 \mathcal{D}_{||}/3)^{2/3}} \frac{1}{2\Gamma(4/3)} + \dots \right] \quad (3.1.13)$$

For particles very close to resonance,  $D_{||}$  becomes independent of the particle velocity. Assuming that the wave spectrum is peaked at  $k = k_T$ , we may write for these particles,

$$D_{||} \approx 2.76 k_{||T} u_T^3 \quad (3.1.14)$$

where  $u_T$  is a measure of the turbulent velocity,

$$u_T = \left[ (e^2/m^2) \sum_k \langle |\Phi_k|^2 \rangle \right]^{1/4}.$$

Substituting the zero order value of  $D_{||}$  given by Eq. (3.1.14) in Eq. (3.1.13) we get

$$D_{||}(v_{||}) = 2.76 k_{||T}^3 u_T^3 \left[ 1 - 0.2 (v_{pT} - v_{||})^2 / u_T^2 \right]^{3/4} \quad (3.1.15)$$

where  $v_{pT}$  is the wave phase velocity at  $k = k_T$ , and  $|v_{pT} - v_{||}| \ll u_T$ .

The diffusion coefficient is a function of the particle velocity except for particles very close to resonance or for very high values of  $D$ , when the resonant nature of the diffusion is completely smeared out.

The scaling of the nonlinear diffusion given by Eq. (3.1.14) is different from quasilinear diffusion which scales as  $k_{||T}^2 u_T^4$ .

We conclude from this section that:

- (i) the smaller mass of the electron causes it to diffuse more rapidly in velocity space than the ions
- (ii) spatial diffusion of electrons is negligible except at large angles to  $B$ .
- (iii) the larger spread in the electron thermal velocity requires a level of turbulence higher by a factor  $(m_i/m_e)^{1/2}$  for bulk diffusion of electrons
- (iv) on short time scales, spatial diffusion of ions is more important than velocity space diffusion
- (v) the resonant character of the diffusion is smeared out at high turbulence levels. This feature is of particular importance in the calculation of the spectrum (Chapter 6).
- (vi) the scaling laws are different for non-linear and quasilinear diffusion.

$$\mathcal{D}_{\text{nonlinear}} \sim k_T u_T^3 \quad ; \quad \mathcal{D}_{\text{quasilinear}} \sim k_T^2 u_T^4$$

$$D_{\text{nonlinear}} \sim \frac{\Phi}{B} \quad ; \quad D_{\text{quasilinear}} \sim \frac{\Phi^2}{B^2}$$

### 3.2. ELECTROSTATIC FLUCTUATIONS ( $\omega \sim \Omega_L$ )

Till now we have considered only low frequency fluctuations and guiding centre diffusion. We now consider the motion of charged particles in a turbulent background where the wave frequency is higher and the guiding centre approximation breaks down.

In a Cartesian frame, the helical motion of the particles is given by

$$\begin{aligned}\dot{V}_{x,y} &= \frac{e}{m} \bar{E}_{x,y} \pm \Omega_L V_{y,x} \\ \dot{V}_z &= \frac{e}{m} \bar{E}_z\end{aligned}\quad (3.2.1)$$

In a rotating reference frame with  $V_{\pm} = V_x + iV_y = V_{\perp} e^{i\theta}$  the motion in  $(x,y)$  is decoupled, to give the equations of motion

$$\left( \frac{d}{dt} \pm i\Omega \right) V_{\pm} = \frac{e}{m} \bar{E}_{\pm} \quad (3.2.2)$$

$$\frac{d}{dt} V_z = \frac{e}{m} \bar{E}_z \quad (3.2.3)$$

Fluctuations in the electric field cause the particles to diffuse in velocity space. The diffusion coefficient  $\bar{D}$  is given by the correlations  $\int \langle \vec{V} \vec{V}^* \rangle dt$ . In obtaining the correlations, the gyro motion due to the



magnetic field alone must be separated out. This is given by the solutions  $e^{\pm i\Omega t}$  of the homogeneous part of Eq. (3.2.2).

Let the solution of Eq. (3.2.2) be

$\underline{V}_{\pm} = \underline{V}_{\pm}(t) e^{\mp i\Omega t}$ . Substituting in (3.2.2) we get

$$\dot{\underline{V}}_{\pm} = \frac{e}{m} \underline{E}_{\pm} e^{\pm i\Omega t} \quad (3.2.4)$$

$$\underline{V}_{\pm} = \frac{e}{m} \underline{E}_{\pm}$$

This gives the acceleration of the particles due to the fields  $\underline{E}_{\pm}$  along the gyro path of the particle in the field  $B_0$ . By taking the correlation of the acceleration  $\dot{\underline{V}}$ , we obtain the diffusion tensor,

$$\underline{D} = \begin{pmatrix} D_{++} & D_{+-} & D_{+z} \\ D_{-+} & D_{--} & D_{-z} \\ D_{z+} & D_{z-} & D_{zz} \end{pmatrix} \quad (3.2.5)$$

where  $D_{ab} = \int_0^{\infty} dt \langle \dot{\underline{V}}_a(t) \dot{\underline{V}}_b^*(t+t) \rangle$ , and is independent of  $t$  under stationary conditions. Neglecting the incoherent contribution (arising from correlations between different Fourier modes), we have

$$\begin{aligned}
 \chi_{ab} &= \frac{e^2}{m^2} \int_0^\infty dt \int_{-\infty}^\infty d\omega \sum_{\mathbf{k}} \left\langle \dot{\mathbf{v}}_{a, \mathbf{k}, \omega} \dot{\mathbf{v}}_{b, \mathbf{k}, \omega}^* e^{i\omega t - i\mathbf{k} \cdot \Delta \mathbf{R}(t)} \right\rangle \\
 &= \frac{e^2}{m^2} \int_0^\infty dt \int d\omega \sum_{\mathbf{k}} \left\langle \dot{\mathbf{v}}_{a, \mathbf{k}, \omega} \dot{\mathbf{v}}_{b, \mathbf{k}, \omega} \right\rangle \left\langle e^{i\omega t - i\mathbf{k} \cdot \Delta \mathbf{R}(t)} \right\rangle
 \end{aligned}
 \tag{3.2.6}$$

The expansion of the perturbed orbit in a magnetic field  $B_0$ , retaining cumulants upto second order is

$$\begin{aligned}
 \left\langle \exp[-i\mathbf{k} \cdot \Delta \mathbf{R}(t)] \right\rangle &= \exp \left[ -\frac{1}{2} \sum_{+,-} i \mathbf{k}_\pm \cdot \Delta \mathbf{R}_\pm^0(t) \right. \\
 &\quad \left. - i \mathbf{k}_\pm \cdot \Delta \mathbf{R}_\pm^0(t) - \frac{1}{6} \mathbf{k} \cdot \ddot{\mathbf{R}} \cdot \mathbf{k} t^3 \right]
 \end{aligned}
 \tag{3.2.7}$$

where  $\mathbf{k}_\pm = \mathbf{k}_\perp e^{\pm i\phi}$ , and  $\Delta \mathbf{R}^0(t)$  is the unperturbed trajectory.

Substituting for  $\Delta \mathbf{R}_\pm^0$ , we get

$$\begin{aligned}
 \left\langle \exp[-i\mathbf{k} \cdot \Delta \mathbf{R}(t)] \right\rangle &= \exp \left[ \frac{i k_\perp v_\perp}{2\Omega} \sum_{+,-} \left\{ e^{\pm i\phi \mp i(\Omega t + \psi)} \right. \right. \\
 &\quad \left. \left. - e^{\pm i\phi \mp i\psi} \right\} - i k_z v_z t - \frac{1}{6} \mathbf{k} \cdot \ddot{\mathbf{R}} \cdot \mathbf{k} t^3 \right]
 \end{aligned}$$

$$= \exp \left[ \frac{i \vec{k} \cdot \vec{v}_1}{\Omega} \left\{ \cos(\Omega t + \psi + \phi) - \cos(\psi - \phi) \right\} \right. \\ \left. - i \vec{k}_1 \cdot \vec{v}_1 t - \frac{\vec{k} \cdot \vec{\omega} \cdot \vec{k}}{\Omega} t^3 \right]$$

(3.2.8)

Using the expansion,  $\exp [i x \sin x] = \sum_{n=-\infty}^{\infty} J_n(x) e^{i n x}$   
and averaging over the initial phase  $\psi$  we get

$$\langle \exp[-i \vec{k} \cdot \Delta \vec{R}(t)] \rangle = \sum_{n=-\infty}^{\infty} \sum_{m=-\infty}^{\infty} J_n \left( \frac{\vec{k}_1 \cdot \vec{v}_1}{\Omega} \right) J_m \left( \frac{\vec{k}_1 \cdot \vec{v}_1}{\Omega} \right) \times$$

$$\exp \left[ -i (\vec{k}_1 \cdot \vec{v}_1 + n \Omega) t - \frac{\vec{k} \cdot \vec{\omega} \cdot \vec{k}}{\Omega} t^3 \right] e^{i(n-m)t} \delta_{m,n}$$

(3.2.9)

The characteristic function given by Eq.(3.2.9) is substituted in Eq.(3.2.6) and averaged over  $\phi$  to obtain the components of the diffusion tensor  $\vec{D}$ . The off-diagonal elements contain  $\phi$  dependent terms which vanish on averaging over the phase  $\phi$ . In the  $(+, z)$  representation,  $\vec{D}$  is diagonal and is given by

$$\begin{pmatrix} \vec{D}_{++} \\ \vec{D}_{--} \\ \vec{D}_{zz} \end{pmatrix} = \frac{e^2}{m^2} \int dt \int d\omega \sum_k \sum_{n=-\infty}^{\infty} \frac{1}{k^2} \begin{pmatrix} k_L^2 J_{n-1}^2\left(\frac{k_L v_L}{\Omega}\right) \\ k_J^2 J_{n+1}^2\left(\frac{k_L v_L}{\Omega}\right) \\ k_{||}^2 J_n^2\left(\frac{k_L v_L}{\Omega}\right) \end{pmatrix} \times$$

$$\langle |E_{k,\omega}|^2 \rangle \exp \left[ i(\omega - k_{||} v_L - n\Omega)t - \vec{k} \cdot \vec{\hat{D}} \cdot \vec{k} t^{\frac{1}{2}} \right]$$

(3.2.10)

where

$$\begin{aligned} \vec{k} \cdot \vec{\hat{D}} \cdot \vec{k} &= k_x \hat{D}_{xx} k_x + k_y \hat{D}_{yy} k_y + k_z \hat{D}_{zz} k_z \\ &\quad + k_x \hat{D}_{xy} k_y + k_y \hat{D}_{yx} k_x \end{aligned}$$

$$= \frac{1}{4} \left[ k_+^* \hat{D}_{++} k_+ + k_-^* \hat{D}_{--} k_- \right] + k_z \hat{D}_{zz} k_z \quad (3.2.11)$$

The equations (3.2.10), are a set of coupled self consistent equations for  $\vec{\hat{D}}$ , which we have obtained by taking the diffusive spread of the unperturbed trajectory due to the turbulent fluctuations into account. In the next section we integrate

over the perturbed orbit, and obtain the components of  $\vec{D}$  by neglecting the coupling terms in the orbit as before.

### 3.2.a) Integration over the Perturbed Orbit

The time integration of Eq. (3.2.10) gives

$$\vec{D} = \frac{e^2}{m^2} \int d\omega \sum_k \sum_{n=-\infty}^{\infty} \frac{1}{k^2} \begin{pmatrix} k_{\perp}^2 & J_{n-1}^2 \\ k_{\perp}^2 & J_{n+1}^2 \\ k_{\parallel}^2 & J_n^2 \end{pmatrix} \langle |E_{k,\omega}|^2 \rangle$$

$$\frac{\pi}{(\vec{k} \cdot \vec{D} \cdot \vec{k})^{1/3}} Ei_3 \left[ -\frac{i(\omega - k_{\parallel} v_{\parallel} - n\Omega)}{3(\vec{k} \cdot \vec{D} \cdot \vec{k})^{1/3}} \right] \quad (3.2.12)$$

where  $Ei_3(\alpha)$  is the generalized Airy Hardy function<sup>(4)</sup> and the argument of the Bessel function has been suppressed. For particles close to resonance, or for strong diffusion when  $\alpha \ll 1$ ,  $Ei_3(\alpha)$  can be expanded to give

$$Ei_3 \left[ -\frac{i(\omega - k_{\parallel} v_{\parallel} - n\Omega)}{3(\vec{k} \cdot \vec{D} \cdot \vec{k})^{1/3}} \right] = \frac{2}{3\sqrt{3}\Gamma(4/3)} \left[ 1 - \frac{(\omega - k_{\parallel} v_{\parallel} - n\Omega)^2}{2\Gamma(1/3)(\vec{k} \cdot \vec{D} \cdot \vec{k})^{2/3}} \right]$$

(3.2.13)

In the limit of very strong diffusion when  $3(k \cdot D \cdot k)^{1/3} \gg |\omega - k_{||} v_{||}|$  for all the particles,  $Ei_3(\infty) = 2/3\sqrt{3} \Gamma(2/3)$ , and is independent of the particle velocity. The resonant nature of the diffusion is smeared out in the limit of very strong fluctuations. In this limit we obtain the components of the diffusion coefficient by neglecting the coupling terms. Defining  $D_{\perp} = (D_{++} + D_{--})/4$ , we have

$$\left(\frac{D_{\perp}}{m^2}\right)^{4/3} = \frac{2\pi}{3^{3/2} \Gamma(4/3)} \frac{e^2}{m^2} \int d\omega \sum_k \sum_n \frac{k_{\perp}^{4/3}}{4k^2} \left( J_{n-1}^2 + J_{n+1}^2 \right) \langle |E_{k,\omega}|^2 \rangle$$

$$\left(\frac{D_{||}}{m^2}\right)^{4/3} = \frac{2\pi}{3^{3/2} \Gamma(2/3)} \frac{e^2}{m^2} \int d\omega \sum_k \sum_n \frac{k_{||}^{4/3}}{k} J_n^2 \langle |E_{k,\omega}|^2 \rangle$$

(3.2.14)

Not all the harmonics  $n$  in the summation need be considered. The higher harmonics which do not satisfy the condition  $|\omega - k_{||} v_{||} - n\Omega| \ll 3(\vec{k} \cdot \vec{A} \cdot \vec{k})^{1/3}$  will not contribute to the diffusion. Since  $\sum_{n=-\infty}^{\infty} J_n^2 = 1$ , Eq. (3.2.14) can be simplified to give

$$D_{\perp} \propto \left( \frac{e^2}{m^2} \sum_k k_{\perp}^{4/3} \Phi_k^2 \right)^{3/4}$$

$$D_{||} \propto \left( \frac{e^2}{m^2} \sum_k k_{||}^{4/3} \Phi_k^2 \right)^{3/4}$$

(3.2.15)



If we further assume the energy to be peaked around  $k = k_T$ , so that  $\sum_k k_L^{4/3} E_k^2 = k_T^{4/3} \sum_k \Phi_k^2 = k_T^{4/3} \Phi$ , and take  $u_T = (e\Phi/m)^{1/2}$  to be a measure of the turbulent velocity of the particle, we may write

$$D_{\perp \parallel} \propto \left(\frac{e}{m}\right)^{3/2} k_{T \perp \parallel} u_T^3 \quad (3.2.16)$$

with different constants of proportionality along and across  $B_0$ .

### 3.2.b) Diffusion Coefficient in the Quasilinear Limit

For low values of the electric field fluctuations, we should be able to recover the quasilinear diffusion coefficient by neglecting the orbit perturbation in Eq. (3.2.10).

$$\begin{pmatrix} D_{\perp} \\ D_{\parallel} \end{pmatrix}_{\text{quasilinear}} = \frac{2\pi e^2}{m^2} \int d\omega \sum_k \sum_n \frac{\langle |E_{k,n}|^2 \rangle}{k^2} \left( \frac{k_{\perp}^2 (J_{n-1}^2 + J_{n+1}^2)}{k_{\parallel}^2 J_n^2} \right) \times \delta(\omega - k_{\parallel} v_{\parallel} - n\Omega)$$

$$= \frac{2\pi e^2}{m^2} \sum_k \sum_n \frac{\langle |E_{k, k, v_n + n\Omega}|^2 \rangle}{k^2} \begin{pmatrix} \frac{k_\perp^2}{4} (J_{n-1}^2 + J_{n+1}^2) \\ k_n^2 J_n^2 \end{pmatrix}$$

(3.2.17)

The expression for  $\mathcal{D}$  in Eq. (3.2.17) differs from the diffusion coefficient obtained by Ichimaru<sup>(5)</sup> using Fokker-Planck theory, which is diagonal in the Cartesian frame of reference with  $\mathcal{D}_{xx} = \mathcal{D}_{yy} = \mathcal{D}_\perp$ . In Eq. (3.2.17),  $\mathcal{D}$  is diagonal in the rotating system  $(+, -, z)$  with  $\mathcal{D}_\perp = (\mathcal{D}_{++} + \mathcal{D}_{--})/4 = (\mathcal{D}_{xx} + \mathcal{D}_{yy})/2$ . The off diagonal elements of  $\mathcal{D}$  in the Cartesian frame contain terms of the type  $J_n J_{n-1}$  and  $J_n J_{n+1}$ . The quasilinear diffusion coefficient is the lowest order approximation of the nonlinear diffusion coefficient we have obtained (Eq. (3.2.12)).

It is important to note that the scaling of the quasilinear diffusion, which we write approximately as

$$D_{\text{quasilinear}} \sim \left(\frac{E}{m\omega}\right)^2 k_\perp^2 \omega^4$$

(3.2.18)

is quite different from the scaling of the nonlinear diffusion

$$D \sim \left(\frac{e}{m}\right)^{3/2} k_T u_T^3$$

(3.2.19)

This feature should be of considerable importance in problems of plasma confinement, since the scaling of particle and energy transport determine the confinement time of the plasma.

### 3.2.c) Spatial Diffusion in Electrostatic Turbulence

( $\omega \sim \Omega_i$ )

To obtain the spatial diffusion coefficient  $D_s$ , we consider the correlation of particle velocities along the perturbed orbit. From Eq. (3.2.4)

$$\begin{aligned} \Delta \tilde{v}_{k\pm}(\tau) &= v_{k\pm}(\tau) - v_{k\pm}(0) \\ &= \frac{e}{m} \int_0^\tau dt E_{k\pm} e^{\pm i\Omega t} \\ &= \frac{e}{m} \int_0^\tau dt \int_{-\infty}^{\infty} d\omega E_{k,\omega\pm} e^{-i\omega t \pm i\Omega t} \\ &= \frac{ie}{m} \int_{-\infty}^{\infty} d\omega \frac{E_{k,\omega\pm}}{(\omega \mp \Omega)} e^{i(\omega \mp \Omega)\tau} \end{aligned}$$

20)

The spatial diffusion is  $\vec{D} = \int_{-\infty}^{\infty} dt \langle \Delta \vec{v}(t) \Delta \vec{v}(t+t) \rangle$

As in the case of velocity space diffusion, the off-diagonal components of  $\vec{D}$  vanish on averaging over the phase  $\phi$ , so that  $\vec{D}$  is diagonal. Incorporating spatial diffusion in the orbit term, we obtain,

$$\begin{pmatrix} D_{++} \\ D_{--} \\ D_{||} \end{pmatrix} = \frac{e^2}{m^2} \int_0^\infty dt \int_{-\infty}^\infty d\omega \sum_k \sum_n \begin{pmatrix} \frac{k_\perp^2 J_{n-1}^2}{(\omega - \Omega)^2} \\ \frac{k_\perp^2 J_{n+1}^2}{(\omega + \Omega)^2} \\ \frac{k_{||}^2 J_n^2}{\omega^2} \end{pmatrix}$$

$$\frac{\langle |E_{k,\omega}|^2 \rangle}{k^2} \exp \left[ i(\omega - k_{||}v_{||} - n\Omega)t - \vec{k} \cdot \vec{D} \cdot \vec{k}t \right] \quad (3.2.21)$$

Only in the low frequency limit,  $\omega \ll \Omega$ , when  $D_{++}$  and  $D_{--}$  become independent of  $\omega$ , do they represent true spatial diffusion. Combining them to give  $D_\perp = (D_{++} + D_{--})/4$  and integrating over  $t$ , we have

$$D_{\perp} = \frac{c^2}{2B^2} \int_{-\infty}^{\infty} d\omega \sum_k \sum_n k_{\perp}^2 \left( J_{n-1}^2 + J_{n+1}^2 \right) \left\langle \frac{|E_{k,n}|^2}{k^2} \right\rangle$$

$$\times \frac{k_{\perp}^4 D_{\perp}}{(10 - k_{\parallel} v_{th} - n\Omega)^2 + k_{\perp}^4 D_{\perp}^2}$$

(3.2.22)

where the coupling term in the orbit has been neglected.

From Eq.(3.2.22) in the limit of small and large  $D_{\perp}$ , we recover the quasilinear diffusion coefficients.

$$D_{\perp \text{ quasilinear}} = \frac{\pi c^2}{B^2} \sum_k \sum_n \left\langle |E_{\perp}(\vec{k}, k_{\parallel} v_{th} - n\Omega)|^2 \right\rangle \left( J_{n-1}^2 + J_{n+1}^2 \right) \quad (3.2.23)$$

which agrees with Matsuda<sup>(6)</sup>, and

$$D_{\perp} = c\Phi / \sqrt{2} B$$

which scales like Bohm diffusion and agrees with the guiding centre diffusion obtained in Section 3.1.

### 3.3. ELECTROMAGNETIC FLUCTUATIONS<sup>+</sup> ( $\omega \ll \Omega_i$ )

In this section we consider the motion of the guiding centre of a test particle in a background of electromagnetic turbulence and an external magnetic field. Following Schmidt<sup>(7)</sup>, the equations of motion are

$$\left(\frac{d\vec{w}}{dt}\right)_{||} = \frac{e}{m} E_{||} - \frac{\mu_m}{mB} \left[ (\vec{B} \cdot \vec{\nabla}) \vec{B} \right]_{||} \quad (3.3.1)$$

$$\begin{aligned} \vec{w}_{\perp} = & \vec{w}_E + \frac{\mu_m}{eB^3} \left[ \vec{B} \times \frac{\nabla B^2}{2} \right] \\ & + \frac{m}{eB^2} \left[ \vec{B} \times \vec{w}_0 \right] \end{aligned} \quad (3.3.2)$$

where  $\vec{w}$  = velocity of the guiding centre,  $\vec{w}_E = \frac{\vec{E} \times \vec{B}}{B^2}$ , the electric drift,  $\vec{w}_0 = \vec{w}_E + \vec{w}$ , the zeroth order guiding centre motion, and  $\mu_m = \frac{1}{2} \frac{e^2 R^2 B}{m}$  is the magnetic moment of the particle.

---

<sup>+</sup> MKS units have been used in this section.



The two low frequency electromagnetic modes supported by a plasma in an external magnetic field are the Alfvén and magnetosonic waves. We now examine whether orbit perturbation effects are significant for these modes. As seen in Section 3.1, the perturbed orbit terms are of the form  $\exp[-k \cdot D \cdot k \cdot t^n]$ . In the case of pure Alfvén waves, the guiding centre motion is in a direction perpendicular to  $k$ . (Fig. 3.1). The diffusion coefficient, therefore, has no components in the direction of  $k$ . Consequently, the perturbed orbit contribution  $k \cdot D \cdot k$  vanishes for purely transverse Alfvén waves.

In the magnetosonic wave geometry, the wave vector  $\vec{k}$  is largely in the plane perpendicular to  $B_0$ , with  $k_\perp \gg k_\parallel$ . The magnetic perturbation  $B_1$  is almost in the direction of  $B_0$ , and  $E_1$  is perpendicular to  $B_1$  as shown in Fig. 3.2. It is assumed that  $B_1$  is much less than the static field  $B_0$ .

From Eqs. (3.3.1), we have

$$W_\parallel = \frac{e}{m} E_\parallel - \frac{\mu_m}{mB} \left[ (\vec{B}_0 + \vec{B}_1) \cdot \frac{\partial B_1}{\partial z} \right]$$

where  $W_\parallel$  is the velocity parallel to the total field  $B$ . Retaining only terms linear in the turbulent field quantities we have

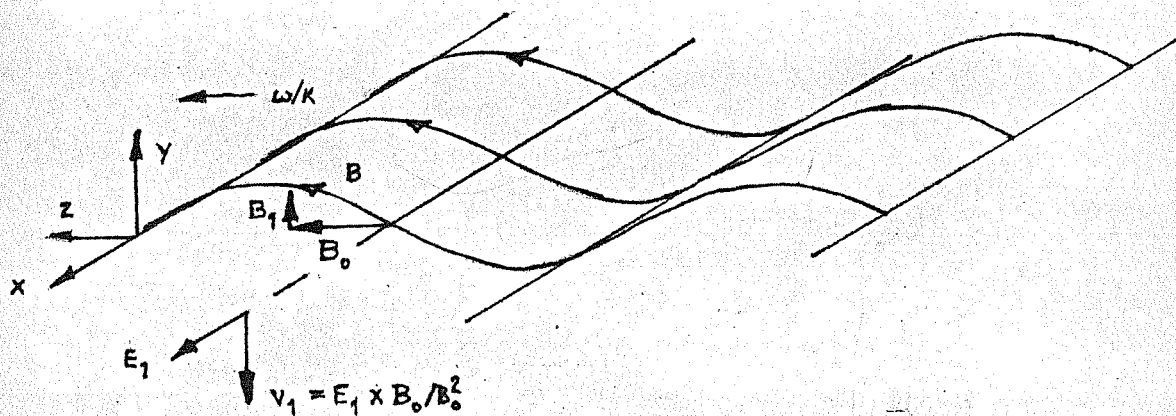
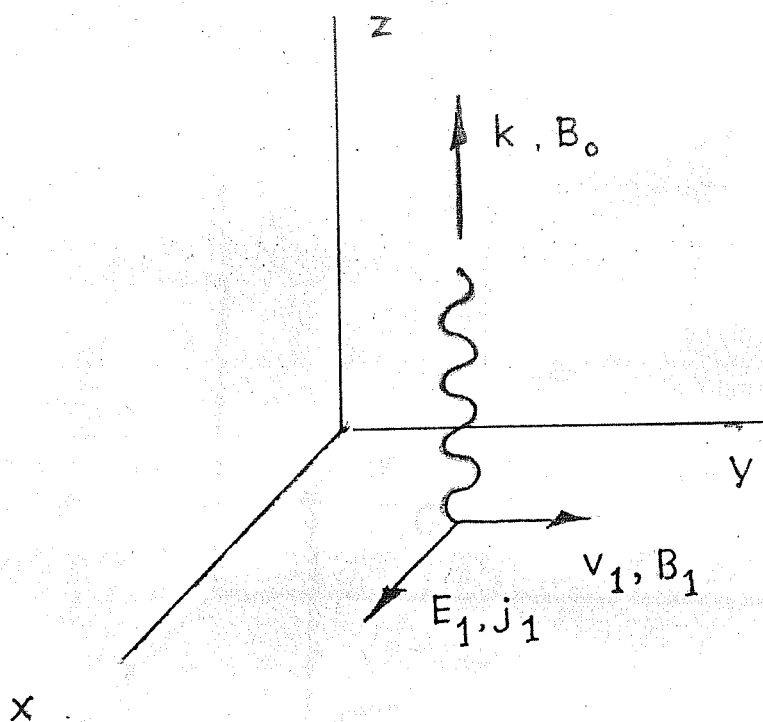
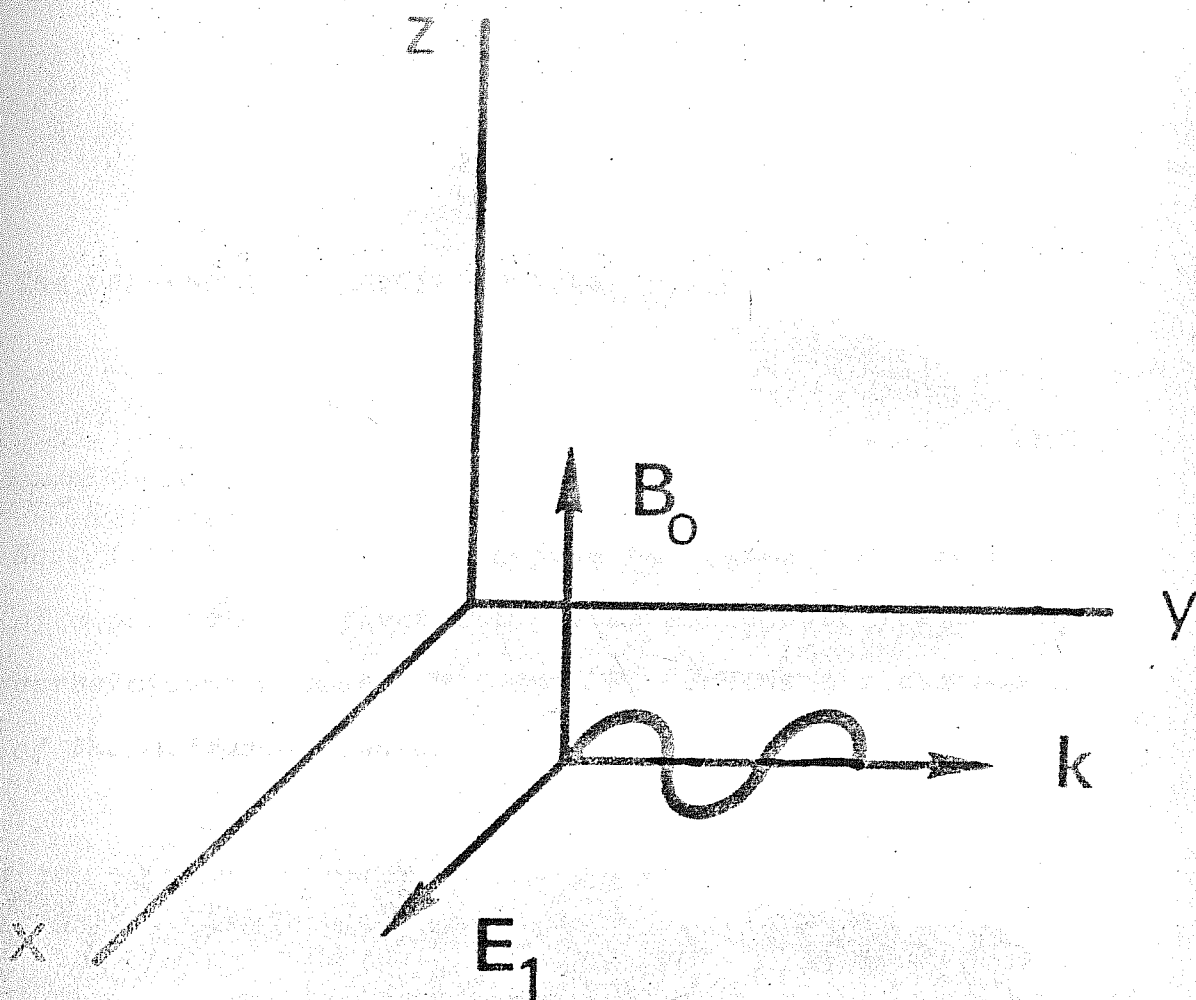


Fig. 3.1 Geometry of the Transverse Alfvén wave propagating along the external magnetic field.



*Fig. 3.2      Geometry of the magnetosonic wave.*

$$\dot{W}_Z = \frac{e \bar{E}_Z}{m} - \frac{\mu_m}{m} \frac{\partial B_{\parallel}}{\partial z}$$

(3.3.3)

The perpendicular drift from Eq. (3.3.2) is

$$\vec{W}_\perp \approx \vec{W}_E + \frac{m \vec{E}_\perp}{e B^2}$$

(3.3.4)

Eqs. (3.3.3) and (3.3.4) define the guiding centre motion of a particle in fluctuating electromagnetic fields. The correlations between  $W_\perp$  and  $W_Z$  define the components of the diffusion tensor.

$$D_{\parallel\parallel}(\nu) = \frac{1}{2} \sum_k \left[ \frac{e^2}{m^2} \langle |E_{k\parallel}|^2 \rangle + \frac{k_{\parallel}^2 \mu^2}{m^2} \langle |B_{k\parallel}|^2 \rangle \right] \bar{I} \quad (3.3.5)$$

$$D_{\perp\parallel}(\nu) = \sum_k \left[ \frac{e}{m B} \langle |E_{k\perp} E_{-k\parallel}| \rangle + \frac{k_{\parallel} \mu}{m B_0} \langle E_{k\perp} B_{-k\parallel} \rangle \right] \quad (3.3.6)$$

$$D_{\perp\perp}(\nu) = \frac{1}{B^2} \sum_k \langle |E_{k\perp}|^2 \rangle \bar{I} \quad (3.3.7)$$

where  $I$  is the perturbed orbit given by Eq.(3.1.6).

The perturbed orbit can be integrated as in Sec. 3.1 to obtain the diffusion in turbulent electromagnetic fields.

Unlike the electrostatic case,  $k_{\parallel}$  is very small. This makes velocity space diffusion much smaller in the case of electromagnetic turbulence than for a comparable level of electrostatic turbulence. Even though magnetic fluctuations do not contribute to spatial diffusion to this order of approximation, spatial diffusion is high because the transverse nature of  $E$  causes the  $E \times B$  drift to lie along  $k$ .

REFERENCES

- (1) Dupree, T.H. (1966) *Phys. Fluids* 9, 1773.  
 Dupree, T.H. (1967) *Phys. Fluids* 10, 1049.
  
- (2) Weinstock, J. (1968) *Phys. Fluids* 11, 1977.  
 Weinstock, J. (1969) *Phys. Fluids* 12, 1045.
  
- (3) Kolmogorov, A.N., "General Theory of Dynamical Systems and Classical Mechanics", in (1954 International Congress Math) translated in "Foundations of Mechanics", R. Abraham and J.E. Marsden, Benjamin (New York, 1978).  
  
 J. Moser, "Stable and Random Motions in Dynamical Systems" Study 77, *Annals of Mathematical Studies*, Princeton University Press (Princeton, 1973).
  
- (4) Watson, G.N., *A Treatise on the Theory of Bessel Functions*, Cambridge University Press, Great Britain, 1966.
  
- (5) Ichimaru, S. and M.N. Rosenbluth, *Phys. Fluids* 13, 2778 (1970); *Basic Principles of Plasma Physics*, W.A. Benjamin Inc., Massachusetts, 1973.
  
- (6) Matsuda, K. (1983) *Phys. Fluids* 26, 1508.
  
- (7) Schmidt, G., *Physics of High Temperature Plasmas*, Academic Press (1979).



## CHAPTER 4

### CALCULATION OF THE PERTURBED ORBIT

*The perturbed orbit integral for the guiding centre motion of a particle, defined by\**

$$I = \int_0^{\infty} dt \exp \left[ i(\omega - k_{\parallel} v_{\parallel})t - k_{\perp}^2 D_{\perp} t - k_{\perp} k_{\parallel} D_{\perp} t^2 - k_{\parallel}^2 D_{\parallel} t^3 \right]$$

(4.1)

---

\* A factor of 1/3 has been absorbed in the definition of

has been evaluated in Chapter 3 by truncating the expression for the orbit to retain only a single component of the diffusion tensor. This cannot be justified under the most general conditions. The components of  $D$  are non-linearly coupled through the perturbed orbit, and interesting effects could be lost by neglecting these coupling terms. Although the analytic integration of Eq.(4.1) is not possible if all the terms of  $D$  are retained, the integral can be expressed as a convolution (Sec. 4.1). Under certain limiting conditions, the convolution integral can be calculated to successive orders in an expansion parameter (Sec. 4.2).

Accurate numerical estimates of  $I$  are also difficult to obtain by the usual methods of quadrature because of the oscillating nature of the infinite time integration. By fitting the integrand to a Chebyshev series, a fast and accurate numerical code is developed to obtain  $I$  for an arbitrary set of diffusion coefficients (Sec. 4.3).

Since  $D$  and  $I$  are related self-consistently, there exists the possibility of setting up a numerical iterative scheme to obtain the diffusion coefficients. For an assumed spectral profile, the iterative scheme used to evaluate the diffusion satisfies both the criterion of stability, and of rapid convergence

to the self consistent values of  $D$ , starting from some initial estimate. (Sec. 4.4).

#### 4.1. THE PERTURBED ORBIT AS A CONVOLUTION INTEGRAL

The perturbed orbit can be written as the Fourier transform of  $f(t)g(t)$ , i.e.

$$\frac{I}{\sqrt{2\pi}} = \frac{1}{\sqrt{2\pi}} \int_{-\infty}^{\infty} \exp \left[ i(\omega - k_{\parallel} v_{\parallel})t \right] f(t) g(t) dt$$

where

$$f(t) = \exp \left[ -k_{\perp}^2 D_{\perp} t - k_{\parallel}^2 D_{\parallel} t^3 \right] h(t)$$

$$g(t) = \exp \left[ -k_{\perp} k_{\parallel} D_{\perp \parallel} t^2 \right]$$

and

$$h(t) = \begin{cases} 1 & t \geq 0 \\ 0 & t \leq 0 \end{cases}$$

(4.2)

This is expressed as the convolution

$$\frac{I}{\sqrt{2\pi}} = \frac{1}{\sqrt{2\pi}} F(\omega - k_{\parallel} v_{\parallel}) \otimes G(\omega - k_{\parallel} v_{\parallel})$$

(4.3)

where  $F$  and  $G$  are the Fourier transforms of  $f(t)$  and  $g(t)$ , namely,

$$F(\omega - k_{\parallel} v_{\parallel}) = \frac{1}{\sqrt{2\pi}} \int_0^{\infty} dt \exp \left[ i(\omega - k_{\parallel} v_{\parallel})t - k_{\perp}^2 D_{\perp} t - k_{\parallel}^2 D_{\parallel} t^3 \right] \quad (4.4)$$

$$\begin{aligned} G(\omega - k_{\parallel} v_{\parallel}) &= \frac{1}{\sqrt{2\pi}} \int_0^{\infty} dt \exp \left[ i(\omega - k_{\parallel} v_{\parallel})t - k_{\perp} k_{\parallel} D_{\perp\parallel} t^2 \right] \\ &= \frac{1}{\sqrt{2k_{\perp} k_{\parallel} D_{\perp\parallel}}} \exp \left[ - \frac{(\omega - k_{\parallel} v_{\parallel})^2}{4k_{\perp} k_{\parallel} D_{\perp\parallel}} \right] \end{aligned} \quad (4.5)$$

Since Eq.(4.1) is defined only for  $t \geq 0$ , the corresponding transform exists only for  $(\omega - k_{\parallel} v_{\parallel}) > 0$ . Physically this implies that the perturbed orbit is defined only for those particles that gain energy from the turbulent background.

The transform  $F$  (Eq.4.4) can be expressed in terms of the Lommel function  $S_{0, 1/3}(v)$  as

$$F(\omega - k_{\parallel} v_{\parallel}) = \frac{1}{\sqrt{2\pi}} \frac{1}{3\sqrt{3}} \left[ \frac{k_{\perp}^2 D_{\perp} - i(\omega - k_{\parallel} v_{\parallel})}{(k_{\parallel}^2 D_{\parallel})} \right]^{\frac{1}{2}} \int_{0, 1/3}^v (v) \quad (4.7)$$

where

$$V = 2 \left[ \frac{k_{\perp}^2 D_{\perp} - i(\omega - k_{\parallel} v_{\parallel})}{3(k_{\parallel}^2 D_{\parallel})^{1/3}} \right]^{3/2}$$

(4.8)

and

$$S_{0, 1/3}(V) = \frac{\bar{z}}{V} \int_0^{\infty} \exp \left[ -at^3 - zt \right] dt \quad (4.9)$$

with  $V = 2(z/3a)^{3/2}$  (Ref. 1, Pg. 76).

Combining Eqs. (4.3), (4.5) and (4.7) we obtain

$$I = \frac{1}{\sqrt{2}\pi} \frac{1}{(2k_{\perp} k_{\parallel} D_{\perp})^{1/2}} \int_{-\infty}^{\infty} \frac{du \times S_{0, 1/3}(X)}{\left[ k_{\perp}^2 D_{\perp} - i(\omega - k_{\parallel} v_{\parallel} - u) \right]} \exp \left[ -\frac{u^2}{4k_{\perp} k_{\parallel} D_{\perp}} \right] \quad (4.10)$$

where

$$X = 2 \left[ \frac{k_{\perp}^2 D_{\perp} - i(\omega - k_{\parallel} v_{\parallel} - u)}{3(k_{\parallel}^2 D_{\parallel})^{1/3}} \right]^{3/2}$$

or equivalently,

$$I = \frac{1}{\sqrt{2\pi}} \frac{1}{(2k_{\perp}k_{\parallel}D_{\perp\parallel})^{1/2}} \int_{-\infty}^{\infty} du \frac{y S_{0,1/2}(y)}{[k_{\perp}^2 D_{\perp} - iu]} \exp \left[ \frac{(\omega - k_{\parallel}V_{\parallel} - u)^2}{4k_{\perp}k_{\parallel}D_{\perp\parallel}} \right] \quad (4.11)$$

where

$$y = 2 \left[ \frac{k_{\perp}^2 D_{\perp} - iu}{3(k_{\parallel}^2 D_{\parallel})^{1/3}} \right]^{3/2}$$

#### 4.2. LIMITING VALUES OF THE PERTURBED ORBIT

The values of the Lommel function are tabulated or known in terms of other functions such as the Airy, Bessel and Anger functions. These expressions are listed in Appendix I, along with series and asymptotic expansions which are used in this section.

##### 4.2a. Strong Spatial Diffusion, $K_{\perp}^2 D \gg 3(k_{\parallel}^2 D_{\parallel})^{1/3}$

As discussed in Chapter 3, this condition is easily satisfied for ions. In the presence of strong spatial diffusion, we can use an asymptotic expansion for  $S_{0,1/3}(V)$ . Using equation (AI.8), for  $V \gg 1$ , we have



$$S_{0, 1/3}(v) = \frac{1}{v} \left[ 1 - \frac{8}{9v^2} + \dots \right]$$

Substituting in Eq.(4.10),

$$I \approx \frac{1}{\sqrt{2\pi}} \frac{1}{(2k_{\perp}k_{\parallel}\mathbb{D}_{\perp\parallel})^{1/2}} \int_{-\infty}^{\infty} du \exp\left[-\frac{u^2}{4k_{\perp}k_{\parallel}\mathbb{D}_{\perp\parallel}}\right] \\ \times \left[ \frac{1}{k_{\perp}^2 D_{\perp} - i(\omega - k_{\parallel}v_{\parallel} - u)} - \frac{6k_{\parallel}^2 \mathcal{D}_{\parallel}}{[k_{\perp}^2 D_{\perp} - i(\omega - k_{\parallel}v_{\parallel} - u)]^4} \right]$$

which gives

$$I = \frac{1}{i(4k_{\perp}k_{\parallel}\mathbb{D}_{\perp\parallel})^{1/2}} \mathbb{Z}(\xi) - \frac{k_{\parallel}^2 \mathcal{D}_{\parallel}}{(4k_{\perp}k_{\parallel}\mathbb{D}_{\perp\parallel})^2} \frac{d^3}{d\xi^3} \mathbb{Z}(\xi) \quad (4.12)$$

where

$$\xi = \frac{(\omega - k_{\parallel}v_{\parallel}) + ik_{\perp}^2 D_{\perp}}{(4k_{\perp}k_{\parallel}\mathbb{D}_{\perp\parallel})^{1/2}}$$

Recalling that the diffusion coefficients follow an ordering relation, Eq.(3.1.7), the condition  $k_{\perp}^2 D \gg (k_{\parallel}^2 \mathcal{D}_{\parallel})^{1/3}$  implies  $|\xi| \gg 1$ . Using the asymptotic expansion of the  $\mathbb{Z}$  function in Eq.(4.12), we have

$$I = \frac{1}{-L(\omega - k_{\parallel} v_{\parallel} + i k_{\perp}^2 D_{\perp})} \left[ 1 - \frac{6 k_{\parallel}^2 D_{\parallel}}{(\omega - k_{\parallel} v_{\parallel} + i k_{\perp}^2 D_{\perp})^3} \right]$$

(4.13)

The real part of the perturbed orbit contributes to particle diffusion, and the contribution is maximum for resonant particles with  $v_{\parallel} \approx \omega/k_{\parallel}$ . The imaginary part corresponds to reversible energy exchange between the particles and the waves and does not contribute to particle diffusion.

From Eq. (4.13), we infer that when spatial diffusion dominates, only resonance broadening appears in the lowest order of approximation. The velocity space diffusion  $\mathcal{L}_{\parallel}$ , responsible for changes in  $f_0(v)$ , occurs only in a higher order term. This provides some justification for neglecting changes in the distribution function in the stationary turbulent state achieved through spatial diffusion. Moreover, Eq. (4.13) provides a description for the behaviour of particles both near and far from resonance.  $I$  is approximately constant for all particles with velocities lying within the broadened resonance i.e. with  $(\omega - k_{\parallel} v_{\parallel}) \ll k_{\perp}^2 D_{\perp}$ . For sufficiently large  $D_{\perp}$ ,  $I$  becomes insensitive to the details of  $f_0(v)$  and is approximately constant for all the particles. In other words, the resonant character of  $I$  arising from  $(\omega - k_{\parallel} v_{\parallel})^{-1}$  is smeared out by strong spatial diffusion.

4.2b. Strong Velocity Space Diffusion,  $(k_{\parallel}^2 \lambda_D)^{1/3} \gg \frac{1}{3} k_{\perp}^2 D$

The electron is easily accelerated along  $B$  because of its light mass. Velocity space diffusion almost invariably dominates over spatial diffusion for electrons.

We examine first the orbit for particles close to resonance, satisfying  $|\omega - k_{\parallel} v_{\parallel}| \ll 3(k_{\parallel}^2 \lambda_D)^{1/3}$ . In Eq. (4.10), we use the small argument limit of  $S_0$ ,  $1/3(V)$  (Eq. (A1.9))

$$v \int_{0, 1/3} S_0(v) \sim \frac{\pi}{\sqrt{3}} \left[ \frac{2^{1/3}}{\Gamma(2/3)} - v^{2/3} - \frac{3v^{4/3}}{2^{1/3}\Gamma(1/3)} + \dots \right]$$

(4.14)

to obtain

$$I \sim \frac{\pi}{\sqrt{3}} \frac{2/3}{\Gamma(2/3)} \frac{1}{(k_{\parallel}^2 \lambda_D)^{1/3}} \left[ 1 - \frac{\Gamma(2/3)}{\Gamma(1/3)} \frac{k_{\perp}^2 D_1 - i(\omega - k_{\parallel} v_{\parallel})}{(k_{\parallel}^2 \lambda_D)^{1/3}} \right] \quad (4.15)$$

As seen from Eq. (4.15) the integral over the perturbed orbit in the presence of strong velocity space diffusion  $\mathcal{D}$  is quite distinct from the resonant response  $(\omega - k_{\parallel} v_{\parallel})^{-1}$ , or the broadened response  $(\omega - k_{\parallel} v_{\parallel} - i\eta)^{-1}$  obtained for spatial diffusion. The practice<sup>(2)</sup> of replacing the velocity space diffusion term in the orbit by a broadened resonance of the type  $(\omega - k_{\parallel} v_{\parallel} + i(k_{\parallel}^2 \mathcal{D}_{\parallel})^{1/3})^{-1}$  is therefore incorrect.

For non-resonant electrons satisfying  $(\omega - k_{\parallel} v_{\parallel}) \gg 3 (k_{\parallel}^2 \mathcal{D}_{\parallel})^{1/3}$ , we recover Eq. (4.13) showing that the form of  $I$  is the same for non-resonant particles regardless of whether spatial diffusion dominates over velocity space diffusion or vice versa.

To summarise, the results of this section are:

(i) for  $k_{\perp}^2 D_{\perp} \gg (k_{\parallel}^2 \mathcal{D}_{\parallel})^{1/3}$ , (e.g. for ions), for all  $v_{\parallel}$ ,

$$I \approx \frac{-1}{i(\omega - k_{\parallel} v_{\parallel} + i k_{\perp}^2 D_{\perp})} \left[ 1 - \frac{6 k_{\parallel}^2 \mathcal{D}_{\parallel}}{(\omega - k_{\parallel} v_{\parallel} + i k_{\perp}^2 D_{\perp})^3} \right] \quad (4.16a)$$

(ii) for  $(k_{\parallel}^2 \mathcal{D}_{\parallel})^{1/3} \gg k_{\perp}^2 D_{\perp}$ , (e.g. for electrons),  
if  $(\omega - k_{\parallel} v_{\parallel}) \gg 3 (k_{\parallel}^2 \mathcal{D}_{\parallel})^{1/3}$ ,

$$\bar{I} \approx - \frac{1}{(\omega - \frac{1}{2} v_{ii} + k_{\perp}^2 D_{\perp i})} \left[ 1 - \frac{\delta k_{\perp}^2 \mathcal{L}_{ii e}}{(\omega - k_{\perp} v_{ii} + i k_{\perp}^2 D_{\perp e})} \right] \quad (4.16b)$$

or, if,  $(\omega - k_{\perp} v_{ii}) \ll \frac{1}{3} (k_{\perp}^2 \mathcal{L}_{ii})^{1/3}$

$$\bar{I} \approx \frac{\bar{II}}{\sqrt{3}} \frac{2/3}{\Gamma(2/3)} \frac{1}{(k_{\perp}^2 \mathcal{L}_{ii})^{1/3}} \left[ 1 - \frac{\Gamma(2/3)}{\Gamma(1/3)} \frac{k_{\perp}^2 D_{\perp e} - i(\omega - k_{\perp} v_{ii})}{(k_{\perp}^2 \mathcal{L}_{ii})^{1/3}} \right] \quad (4.16c)$$

It is to be noted that  $\bar{II}_{ii}$  does not appear to this order of approximation.

The algebraic relations between the perturbed orbit  $I$ ,  $D_{\perp}$  and  $\mathcal{L}_{ii}$  can be written schematically for ions as

$$\begin{aligned} D_{\perp i} &= \propto \sum_k \bar{I}_i(k) \\ \bar{I}_i &= \frac{\beta}{\delta - D_{\perp i}} \left[ 1 - \frac{\delta \mathcal{L}_{ii i}}{(\delta - D_{\perp i})^2} \right] \\ D_{\perp i} &= \propto D_{\perp i} \end{aligned} \quad (4.17a)$$

and for the resonant electrons as

$$\mathcal{L}_{ii e} = \propto' \sum_k \bar{I}_e(k)$$

$$I_e = \frac{\beta'}{D_{ne}^{1/3}} \left[ 1 + \gamma' \left( \frac{D_{Le} - \epsilon}{D_{ne}} \right) \right]$$

$$D_{Le} = X' D_{ne}$$

(4.17b)

where  $\alpha$  etc. are parameters.

It is in principle possible to obtain self-consistent values of  $\tilde{D}$  by iterating Eq.(4.17) starting from some initial guess for  $D$ . It is also possible that there exist interesting regions in the parameter space which exhibit non-linear effects such as stochasticity. However, it is difficult to ensure that the limiting conditions under which the equations were obtained will be maintained in the course of the iteration process. An alternative approach is to obtain the perturbed orbit numerically, and, by an exact numerical iteration procedure, calculate the self-consistent values of  $D$ .

#### 4.3. NUMERICAL INTEGRATION OF THE PERTURBED ORBIT<sup>+</sup>

In this section we numerically integrate the perturbed orbit, Eq.(4.1), with initial estimates of the

---

<sup>+</sup> For the remainder of this chapter  $D_1 = \mathcal{D}_1$ ,  $D_2 = \mathcal{D}_{11}$  and  $D_3 = \mathcal{D}_1$ .



diffusion coefficients. This gives the nature of variation of  $I$  as a function of  $k$ ,  $v_{\perp}$  and  $\Theta (= k\hat{B})$ .

The infinite time integral is of the damped oscillatory type and is difficult to obtain accurately by the usual numerical integration procedures. We outline below a scheme for obtaining  $I$  to an accuracy of at least 6 significant figures.

The upper limit  $T$  of the integration is chosen such that for given values of  $k$ ,  $D$  and  $\Theta$ , the absolute value of the integrand is less than  $10^{-15}$  for all  $t > T$ . This in our case was  $T = 10^{-15} / \max [(k_{\perp}^2 D_1)^{1/3}, (k_{\perp} k_{\parallel} D_2)^{1/2}, k_{\perp}^2 D_3]$ . Within this range, the integrand is fitted to a Chebyshev polynomial<sup>(4)</sup> to an accuracy  $|f(x) - f^{\text{FIT}}(x)| < 10^{-8}$  everywhere. The choice of this orthogonal polynomial is governed by (i) the oscillatory nature of the integrand, and (ii) the minimax property of the Chebyshev polynomials. (When a continuous function  $f(x)$  in  $(a, b)$  is fitted to any orthogonal polynomial, then the maximum absolute error i.e.  $\max |f(x) - f^{\text{FIT}}(x)|$  for  $a \leq x \leq b$  is a minimum for the Chebyshev polynomial). Once the coefficients of the fit are known, the definite and indefinite time integrals are evaluated.

In order to check the numerical stability and accuracy of this method, we obtained numerical values for the

following special cases which are known analytically. The real and imaginary parts of  $I$  reduce to the following standard forms in the limits given below:

$$(i) \quad D_1 = D_3 = 0$$

$$\begin{aligned} \operatorname{Re}(I) &= \int_0^{\infty} \cos \omega t e^{-at^2} dt \\ &= \frac{\sqrt{\pi}}{2} a^{-1/2} e^{-\omega^2/4a} \end{aligned}$$

$$\begin{aligned} \operatorname{Im}(I) &= \int_0^{\infty} \sin \omega t e^{-at^2} dt \\ &= \frac{e^{-\omega^2/4a}}{a} \left[ a^{-1/2} \int_0^{\omega/2a} e^{t^2} dt \right] \end{aligned}$$

where the expression  $[ \dots ]$  is Dawson's integral.

$$(ii) \quad \theta = 90^\circ$$

$$\begin{aligned} \operatorname{Re}(I) &= \int_0^{\infty} e^{-at} dt \\ &= \frac{1}{a} \end{aligned}$$

$$\operatorname{Im}(I) = 0$$

In all cases our values compared with the exact values upto at least 6 significant figures.

The maximum number of terms in the expansion was 45. The variation of  $I$  with  $k$  and  $\theta$  for different  $V_{||}$  values are plotted in Figs. (4.1) and (4.2) respectively.

#### 4.4. SELF CONSISTENT VALUES OF THE DIFFUSION COEFFICIENT

The normalised<sup>+</sup> diffusion tensor is related self consistently to the orbit integral through the equations

$$\begin{pmatrix} D_1 \\ D_2 \\ D_3 \end{pmatrix}_j = 2 \left( \frac{m_i}{m_j} \right)^2 \int_0^\infty k^2 dk \int_0^{\pi/2} \sin \theta d\theta S(k, \theta) \begin{pmatrix} \cos^2 \theta \\ \cos \theta \sin \theta \\ \sin^2 \theta \end{pmatrix}_j \quad (4.4.1)$$

where

$$I = \int_0^\infty dt \exp \left[ i k \cos(\nu_p - \nu_{||}) t - k^2 \cos^2 \theta D_1 t^3 - k^2 \cos \theta \sin \theta D_2 t^2 - k^2 \sin^2 \theta D_3 t \right] \quad (4.4.2)$$

<sup>+</sup> The following normalisations have been used:

$$\omega_{pi} t = 1 ; \quad k \lambda_D = 1 ; \quad S(k, \theta) = \langle |\mathbf{E}|^2 \rangle / 8\pi n T_e V$$

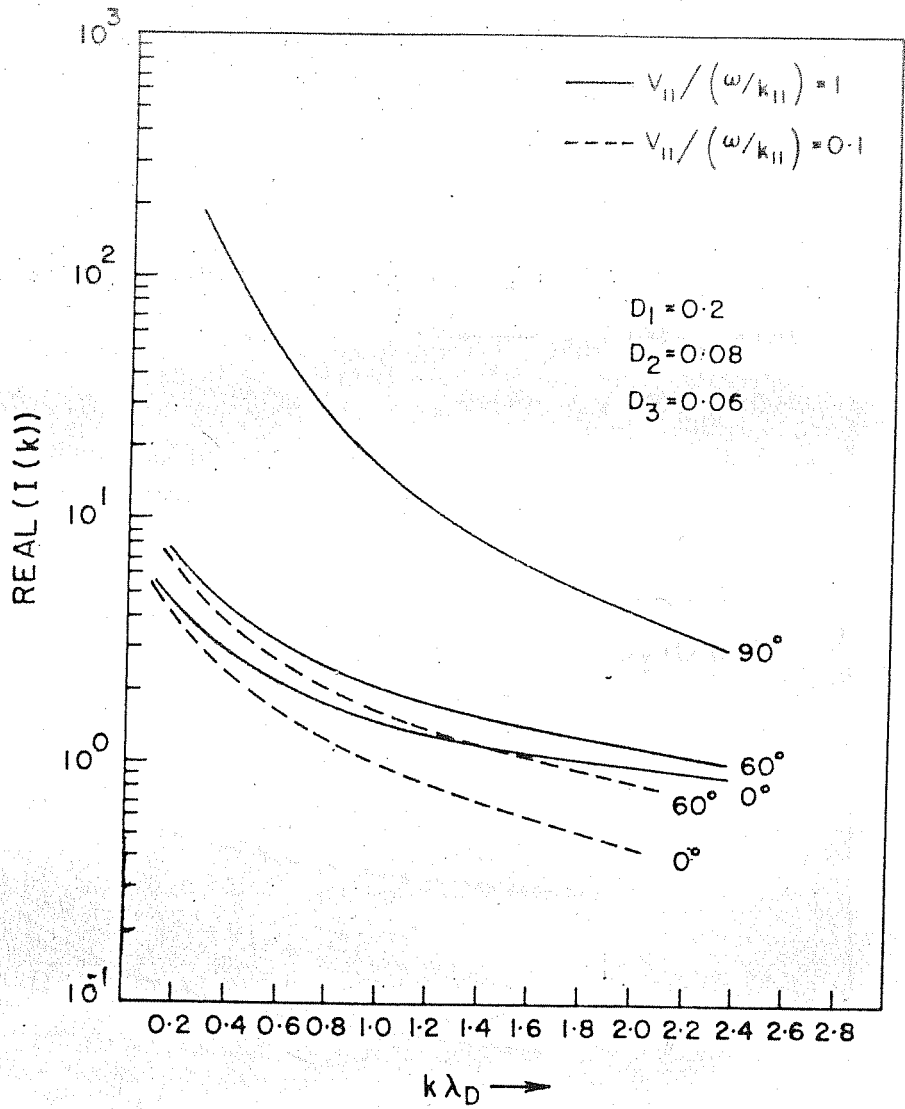


Fig. 4.1a

Real part of the Perturbed Orbit Integral  $I$  at different values of  $\theta$  for (i) a particle at resonance,  $V_{||} / (\omega/k_{||}) = 1$ , (ii) a particle far from resonance,  $V_{||} / (\omega/k_{||}) = 0.1$ . At  $\theta = 90^\circ$ ,  $\text{Re } I(k)$  coincides for both particles.

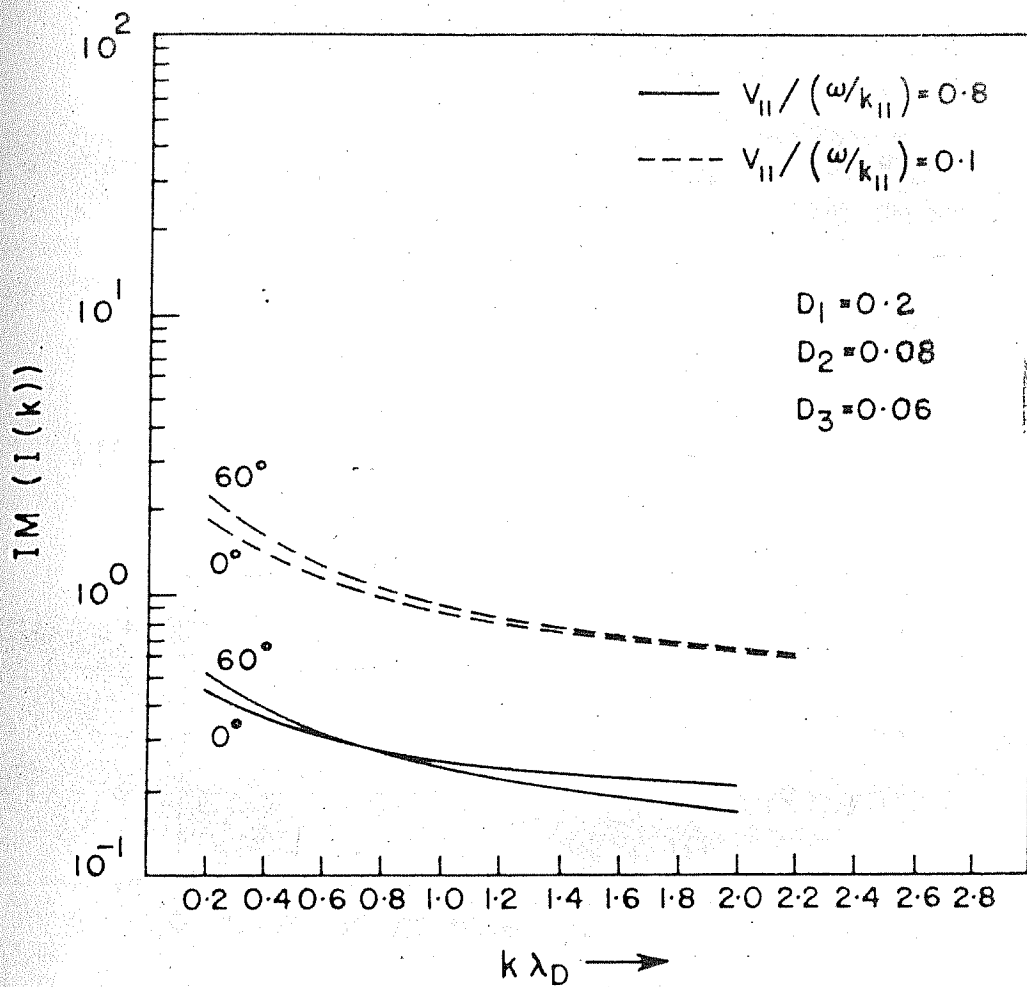


Fig. 4.1b

Imaginary part of  $I$  for (i) a particle at resonance,  $V_{||} / (\omega/k_{||}) = 0.8$ ,  
 (ii) a particle far from resonance,  $V_{||} / (\omega/k_{||}) = 0.1$ . At  $\theta = 90^\circ$ ,  
 $\text{Im } I(k) = 0$ .

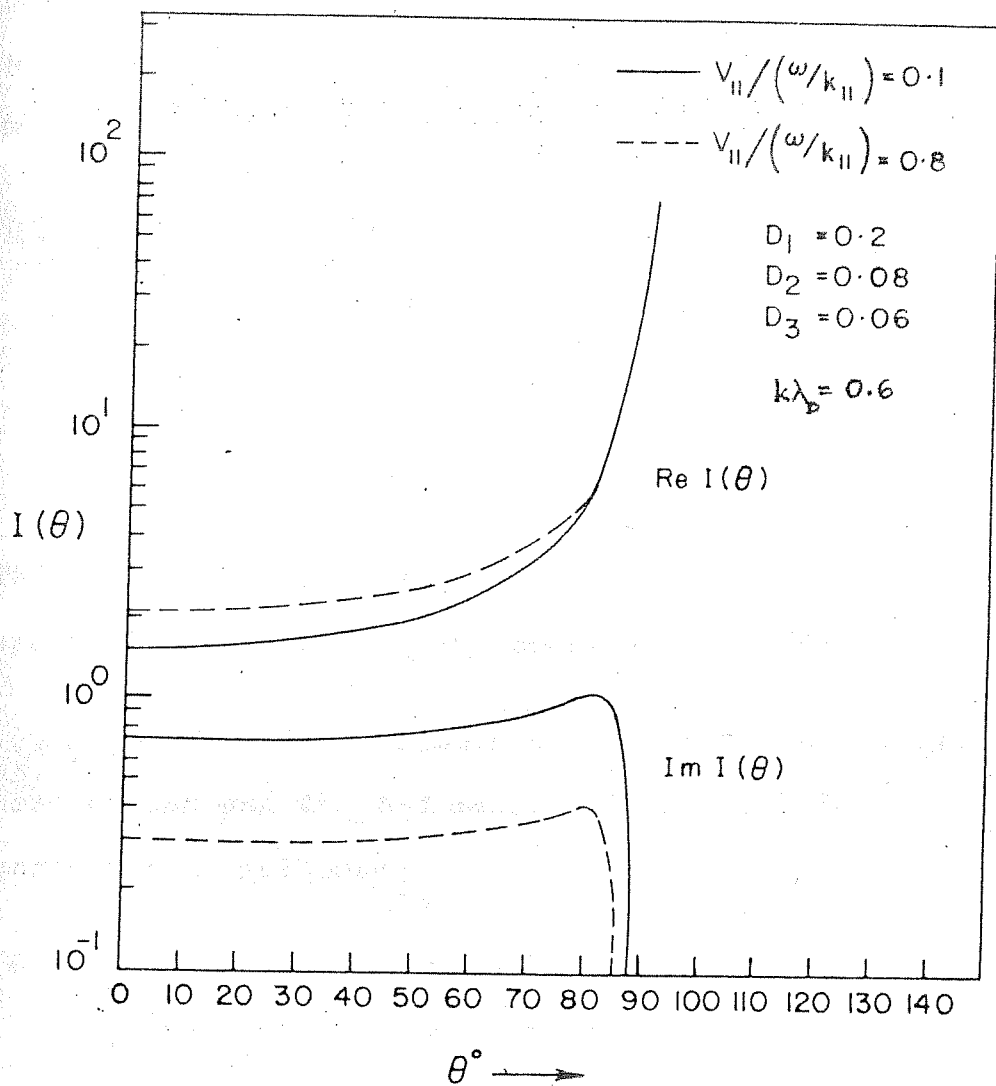


Fig. 4.2

The perturbed orbit integral  $I$  as a function of the wave propagation angle  $\theta$ .

and  $V_p$  is the wave phase velocity, and  $\omega_j$  the cyclotron frequency of the  $j^{\text{th}}$  species. For the fluctuation spectrum, we assumed the profile function at a turbulence level to be,

$$S(k, \theta) = \frac{\sum \exp \left[ - (k - k_0)^2 / (\Delta k_0)^2 \right] \cos \theta}{\int_0^\infty k^2 dk \int_0^{\pi/2} \sin \theta d\theta \exp \left[ - (k - k_0)^2 / (\Delta k_0)^2 \right] \cos \theta} \quad (4.4.3)$$

This profile is an idealized representation of the observed spectral behaviour of ion acoustic waves (Chapter 5).

Trial values of the diffusion coefficients were chosen and the 3-dimensional integral in Eq. (4.4.1) evaluated as follows:

- (i) the time integral was obtained by the procedure outlined in Sec. (4.3) to an accuracy of 1 in  $10^8$ .
- (ii) the angular integration over  $\theta$  with the three different  $\theta$  profiles was done using Simpson's Rule<sup>(3)</sup>. The step size taken was  $1^\circ$ , and consequently the error in the integral is also  $10^{-8}$ .
- (iii) the integration over  $K$  was done using the Gauss Laguerre 15 point quadrature formula<sup>(3)</sup>. Thus it is estimated that the 3-dimensional integral has been



evaluated to an accuracy of at least 6 significant figures.

- (iv) the self-consistent diffusion coefficients were obtained for ions from Eq. (4.4.1) for  $\Omega = 2$ ,  $\xi = 0.1, .01$  and the spectrum parameters  $k_0 = 0.5$  and  $\Delta K_0 = 0.25$ , by an iterative scheme. Reasonable initial trial values for  $D_i$ 's were taken, and the iteration terminated when successive values for each of the  $D$ 's converged to 3 significant figures. In general 3-4 iterations were required for convergence. The procedure was also tested for a poor initial guess of the  $D$ 's. The convergence in this case was slower, but the converged values were in excellent agreement with those obtained from a judicious choice of the initial  $D$ 's.

In Fig. (4.3) and (4.4) we show the convergence of the  $D$ 's as a function of the iteration number for a good initial guess and a poor initial estimate of  $D$ , for  $\xi = 0.1$  and  $V_{||} = 0.5(\omega/k_{||})$

The values of  $D$  as a function of  $V_{||}$  are shown in Fig. (4.5) at  $\xi = 0.1$  and  $\xi = 0.01$ . The convergence for  $V_{||} = 0.1$  at  $\xi = 0.01$  was not obtained.

It is evident from Fig. (4.5) that  $D$  falls sharply as we move away from the resonance at  $V_{||} = V_P$

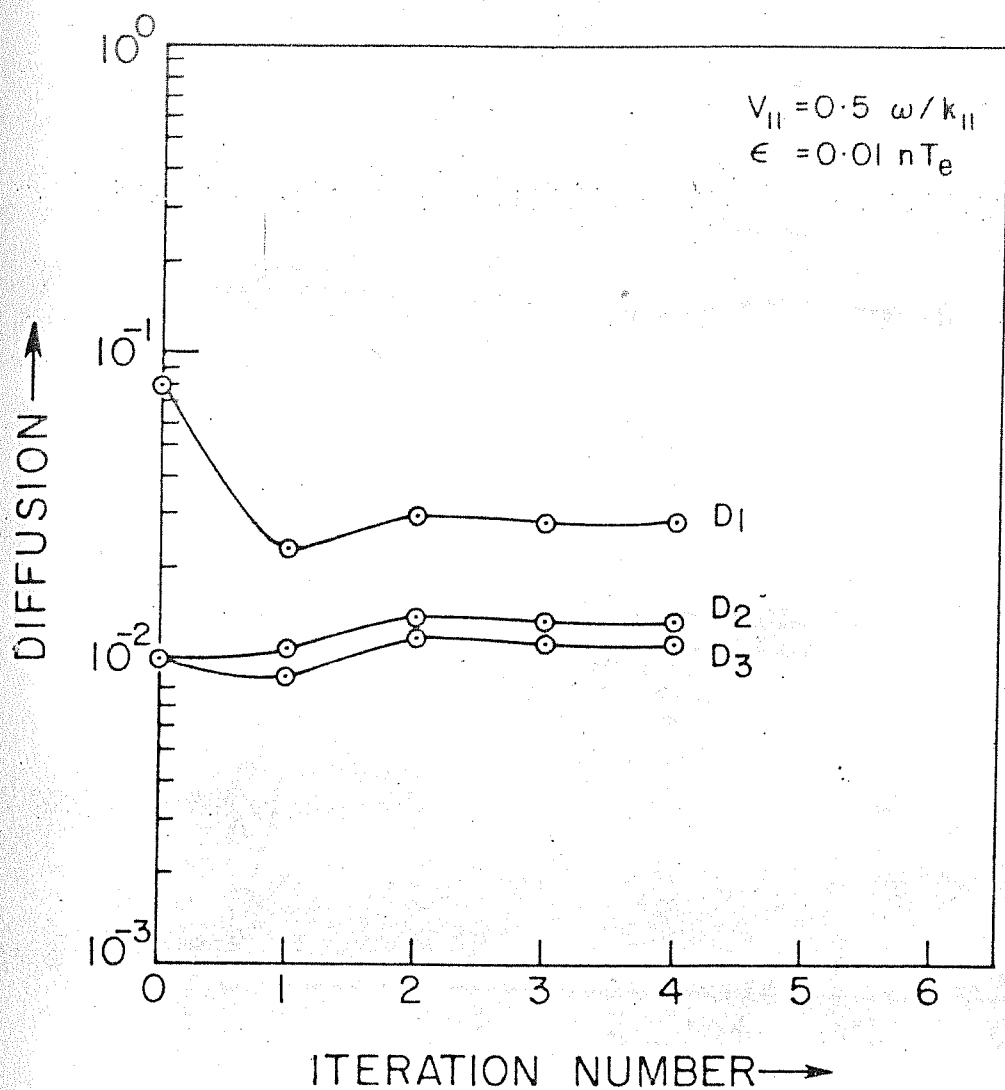


Fig. 4.3

Convergence of the diffusion coefficient in the iterative scheme for the calculation of  $D$ , for a reasonable initial value of  $D$ .

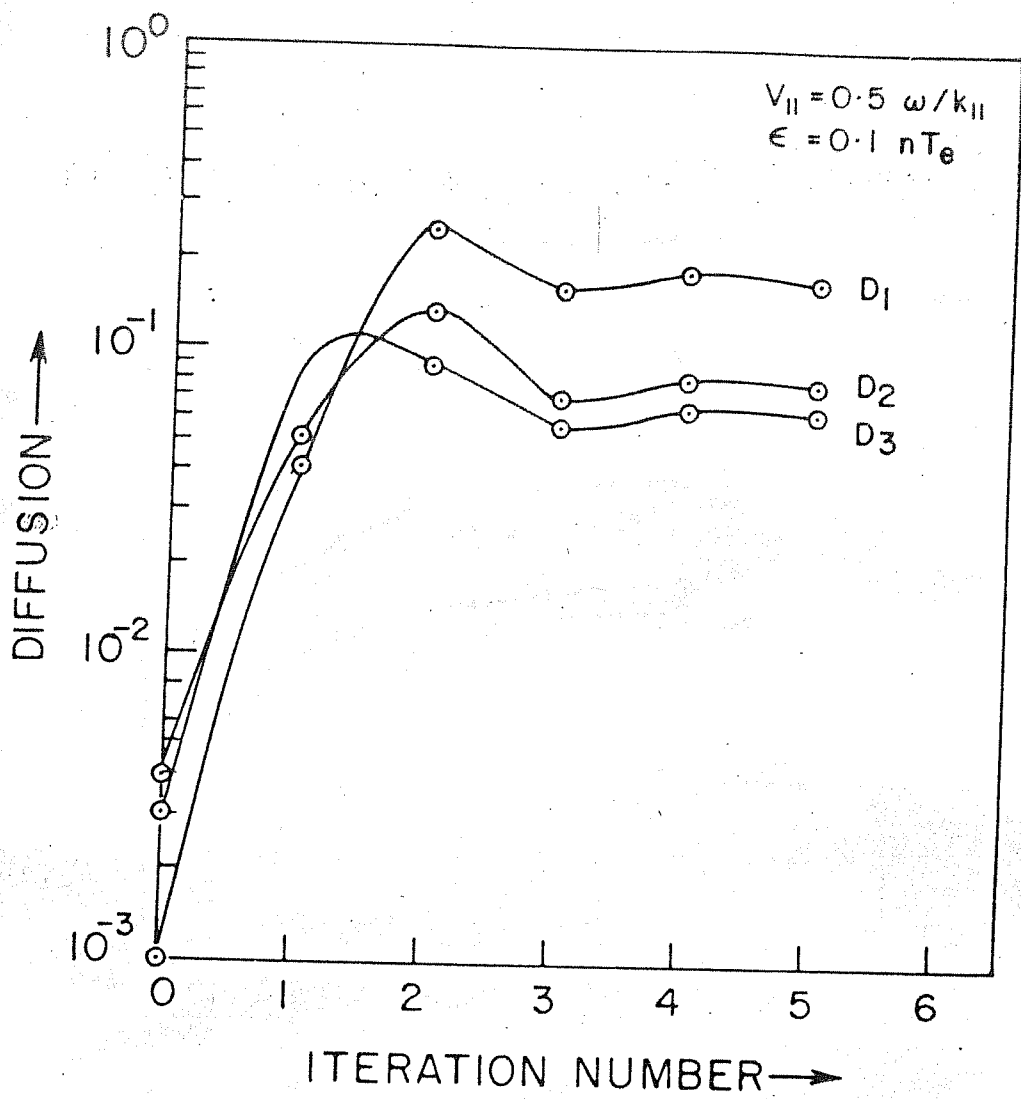


Fig. 4.4

Convergence of  $D$  to its self-consistent value, for a poor initial value of  $D$ .

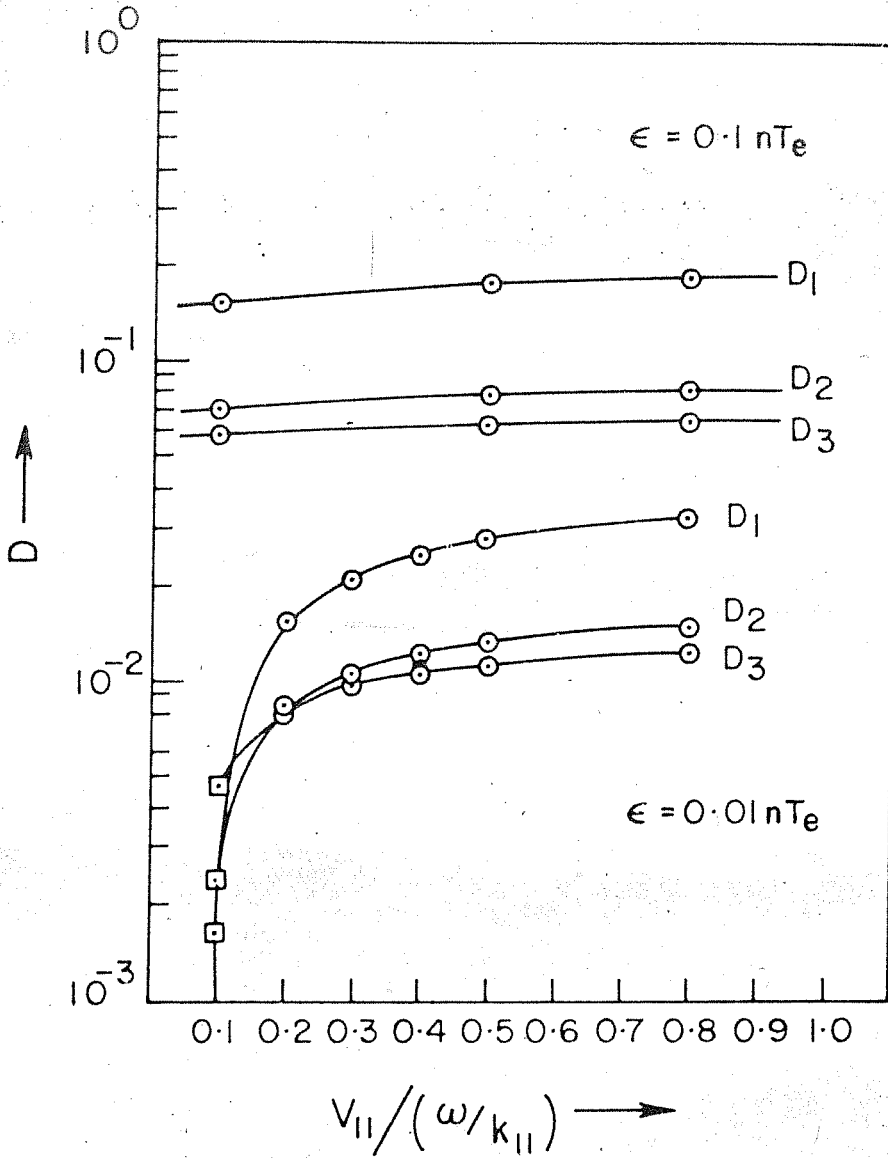


Fig. 4.5

Converged values of  $D_1$ ,  $D_2$  and  $D_3$  as a function of the particle velocity  $V_{||}$ , at  $\mathcal{E} = 0.01 nT_e$  and  $0.1 nT_e$ . The velocity dependence at  $\mathcal{E} = 0.01 nT_e$  is smeared out by resonance broadening at  $\mathcal{E} = 0.1 nT_e$ . ( $\square$  - value not converged).

for low turbulent energy  $\mathcal{E} = 0.01$ . This is no longer true at  $\mathcal{E} = 0.1$  where  $D$  is relatively flat over a wide range of  $V_{11}$ . This feature has an extremely important consequence, namely, that it enables us to calculate the fluctuation spectrum analytically in the limit of high turbulent energy.

REFERENCES

- (1) W. Magnus, F. Oberhettinger and R.P. Soni, *Formulas and Theorems for the Special Functions of Mathematical Physics*, Springer-Verlag, New York (1966).
- (2) A. Hasegawa, *Plasma Instabilities and Nonlinear Effects*, Springer-Verlag (1975), Sec. 4.2, Pg. 154-160.
- (3) M. Abramowitz and I. Stegun, *Handbook of Mathematical Functions*, Dover Publications, New York (1972).
- (4) L. Fox, and I.B. Parker (1968) "Chebyshev Polynomials in Numerical Analysis", Oxford University Press: Oxford, Pg. 58-59.

## CHAPTER 5

### NONLINEAR DISPERSION RELATION

According to the linear response theory, the plasma response to the field  $E$  is governed by the linear relation

$$\vec{D} = \vec{\epsilon} \cdot E$$

where  $\vec{\epsilon}$  is the linear dielectric function. In the presence of stronger fields, the response may contain quadratic or higher order terms, e.g.

$$D_i = \epsilon_{ij} E_j + \chi_{ijk} E_j E_k + \dots$$



This type of non-linearity in the dielectric response of the plasma will not be discussed here. The collective plasma response is assumed to remain within the bounds of the linear response theory. Only the non-linearity in the single particle response to the turbulent background, and its effect on the dielectric properties will be considered.

The entire behaviour of the turbulent plasma, the normal modes it supports, and the degree of screening due to polarization are determined by the dielectric function in the turbulent state. In the usual linear theory, the dielectric function is obtained by considering the collective motion of the particles in the average or macroscopic fields, while neglecting the effect of fluctuations. Turbulent or suprathermal fluctuations nonlinearly perturb the particle orbits. The dielectric function in the turbulent state is therefore obtained from the collective response of the particles moving along perturbed orbits. This is the nonlinear dielectric function,  $\epsilon_{NL}$  as defined in the context of the Perturbed Orbit Theory.

In this Chapter, we indicate how the non-linear dispersion relation is obtained in the guiding centre approximation (  $\omega \ll \Omega_i$  ) (Sec. 5.1), and obtain  $\epsilon_{NL}$  for turbulent ion acoustic waves in a magnetic field. The dispersion relation is then solved to obtain the nonlinear frequency and growth rate in the turbulent state (Sec. 5.2).

As seen in Chapter 3, higher frequency ( $\omega > \Omega_i$ ) turbulence results in velocity space diffusion. We examine the effect of velocity space diffusion on the dielectric function (Sec. 5.3). The dispersion relation for ion-cyclotron waves is obtained and solved in the presence of an average spatial diffusion (Sec. 5.4).

### 5.1. DIELECTRIC FUNCTION IN A TURBULENT PLASMA

Consider an electron moving in an electric field  $E_0 \exp i(k \cdot r - \omega t)$ . In the frame moving with the electron, the acceleration of the electron at  $r_0$  is

$$\ddot{\delta r} = \frac{e}{m} \vec{E}_0 e^{i\omega' t} \exp \left[ i k \cdot (\vec{r}_0 + \vec{\delta r}) \right] \quad (5.1.1)$$

where  $\omega' = \omega - k \cdot V$  is the Doppler shifted frequency seen by the electron moving with velocity  $V$ . In the linear theory, the perturbation of the position of the electron due to the electric field is neglected, so that

$$\ddot{\delta r} \approx \frac{e}{m} \vec{E}_0 \exp \left[ i (k \cdot r_0 - \omega' t) \right] \quad (5.1.2)$$

In the frame moving with the unperturbed electron, we integrate along the unperturbed trajectory to obtain

$$\vec{r} = -\frac{e}{m} \frac{\vec{E}_0}{\omega'} \exp \left[ i(\vec{k} \cdot \vec{r}_0 - \omega' t) \right]$$

In the laboratory frame,

$$\vec{r} = -\frac{e}{m} \frac{\vec{E}}{(\omega - \vec{k} \cdot \vec{v})^2} \quad (5.1.3)$$

where  $\vec{E} = \vec{E}_0 \exp i(\vec{k} \cdot \vec{r}_0 - \omega t)$ . The dipole moment produced by the electron displacement is

$$\vec{p} = e \vec{r} = -\frac{e^2 \vec{E}}{m(\omega - \vec{k} \cdot \vec{v})^2}$$

The dielectric polarization  $\vec{P}$  is

$$\vec{P} = -\frac{e^2 n \vec{E}}{m} \int \frac{f_0(v) d^3 v}{(\omega - \vec{k} \cdot \vec{v})^2}$$

and the induction or displacement vector  $\vec{D}$  is

$$\vec{D} = \left( 1 - \frac{4\pi e^2}{m} \int \frac{f_0 d^3 v}{(\omega - \vec{k} \cdot \vec{v})^2} \right) \vec{E}$$

In a plasma with several species, the dielectric function is therefore

$$\underline{\underline{\epsilon}} = 1 + \sum_j \frac{\omega_{pj}^2}{k^2} \int \frac{\vec{k} \cdot \frac{\partial f_0}{\partial \vec{v}} d^3v}{(\omega - \vec{k} \cdot \vec{v})}$$

This is easily generalised in the presence of a magnetic field (if finite gyroradius effects are neglected) to

$$\underline{\underline{\epsilon}} = 1 + \sum_j \frac{\omega_{pj}^2}{k^2} \int \frac{k_{||} \frac{\partial f_{0j}}{\partial v_{||}} dv_{||}}{(\omega - k_{||} v_{||})} \quad (5.1.4)$$

In a turbulent plasma, the particles diffuse away from the unperturbed orbits. Replacing the unknown true orbit by the statistically averaged guiding centre orbit in Eq. (5.1.2), we have

$$\begin{aligned} \vec{r} &= \frac{e}{m} \vec{E}_{k, \omega} \left\langle \exp \left[ i(\vec{k} \cdot \vec{r} - \omega t) \right] \right\rangle \\ &= \frac{e}{m} \vec{E}_{k, \omega} \exp \left[ i(k_{||} v_{||} - \omega)t + k_{\perp}^2 D_{\perp} t \right. \\ &\quad \left. + k_{\perp} k_{||} D_{||} t^2 + k_{||}^2 D_{||} t^3 \right] \quad (5.1.5) \end{aligned}$$

where the perturbed orbit is defined from  $-\infty$  to  $t$ .

The double time integration of Eq. (5.1.5), required to obtain the displacement  $\vec{D}$ , is not easy to

perform. For simplicity we assume  $\Delta_{||}$  and  $D_{||}$  are small. The particle displacement in the presence of spatial diffusion only is

$$\vec{r} = \frac{e}{m} \frac{\vec{E}_{k\omega}}{[(\omega - k_{||}v_{||}) + i k_{\perp}^2 D_{\perp}]^2}$$

and the polarization is

$$\vec{P} = \frac{en_0}{m} \vec{E}_{k\omega} \int \frac{f_0(v) dv}{[(\omega - k_{||}v_{||}) + i k_{\perp}^2 D_{\perp}]^2} \quad (5.1.6)$$

where  $f_0(v)$  is the equilibrium distribution function in the turbulent state.

The nonlinear dielectric function is then

$$\epsilon_{NL} = 1 + \sum_j \frac{\omega_{pj}^2}{k^2} \int dv_{||} \frac{k_{||} \frac{\partial f_0}{\partial v_{||}}}{[(\omega - k_{||}v_{||}) + i k_{\perp}^2 D_{\perp}]} \quad (5.1.7)$$

The non-linear dielectric function in Eq. (5.1.7) may be obtained by simply replacing  $\omega$  by  $\omega + i k_{\perp}^2 D_{\perp}$  in the resonance term of the linear dielectric function (Eq. 5.1.4). This is Catto's <sup>(1)</sup> prescription for obtaining

$\epsilon_{NL}$ , which is valid only if velocity space diffusion can be neglected. The dielectric function in the presence of only velocity space diffusion is discussed in Sec. (5.3).

## 5.2. ION-ACOUSTIC WAVES IN A MAGNETIC FIELD

In a magnetic field  $B$ , the ion acoustic mode is split into the fast mode with  $\omega > \Omega_i$ , and the slow mode with  $\omega < \Omega_i$ . We consider here the slow mode in a thermal plasma with  $V_{Te} \gg C_s > V_{Ti}$ , (where  $C_s$  is the ion acoustic speed  $(T_e/m_i)^{1/2}$ ). The waves are excited by an electron drift along  $B$ . The velocity distribution function is

$$f_e(v) = \sum_j \frac{1}{(\sqrt{\pi} V_{Tj})^{3/2}} \exp \left[ -\frac{(V_{\parallel} - V_{0j})^2 + V_{\perp}^2}{2V_{Tj}^2} \right] \quad (5.2.1)$$

where  $V_{0e} = V_0$  and  $V_{0i} = 0$ .

The linear dielectric function in a magnetic field is<sup>(2)</sup>

$$\epsilon(k, \omega) = \sum_j \frac{\omega_{pj}^2}{k^2} \sum_{n=-\infty}^{\infty} \int d\vec{v} \frac{J_n^2 \left( \frac{k_{\perp} V_{\perp}}{\Omega_j} \right)}{k_{\parallel} v_{\parallel} - (\omega - n\Omega_j)} \times \frac{k_{\parallel} \frac{\partial f_{0j}}{\partial v_{\parallel}} + \frac{n\Omega_j}{V_{\perp}} \frac{\partial f_0}{\partial v_{\perp}}}{k_{\parallel} v_{\parallel} - (\omega - n\Omega_j)} \quad (5.2.2)$$

Substituting for  $f_{0j}(V)$  from Eq. (5.2.1) and integrating over  $V$ , we get,

$$\begin{aligned} \epsilon(k, \omega) = & 1 + \sum_j \frac{\omega_{pj}^2}{k^2 v_{Tj}^2} \sum_{n=-\infty}^{\infty} e^{-\lambda_j} I_n(\lambda_j) \\ & \times \left[ 1 + \left( \frac{\omega - k_{\parallel} v_{0j}}{\sqrt{2} k_{\parallel} v_{Tj}} \right) \right] \left( \frac{\omega - n \Omega_j - k_{\parallel} v_{0j}}{\sqrt{2} k_{\parallel} v_{Tj}} \right) \end{aligned} \quad (5.2.3)$$

where  $\lambda_j = K_{\perp}^2 \frac{D_j^2}{j^2}$ .

For low frequency waves, only the  $n = 0 \pm 1$  terms are retained. Assuming  $K_{\perp} \frac{D_j}{j} \ll 1$ , and that electron gyroradius effects are negligible, we expand the  $Z$  function in the appropriate limits for electrons and ions to obtain

$$\begin{aligned} \text{Re } \epsilon_L(k, \omega) = & 1 + \frac{1}{k^2 \lambda_{De}^2} - \frac{\omega_{pe}^2 \cos^2 \theta}{\omega^2} \left( 1 - k_{\perp}^2 \frac{D_e^2}{j^2} \right) \\ & - \frac{\omega_{pi}^2 \sin^2 \theta}{\omega^2 - \Omega_i^2} \end{aligned} \quad (5.2.4)$$



$$\text{Im } \epsilon_L(k, \omega) = \left(\frac{\pi}{2}\right)^{1/2} \left[ \frac{(\omega - k_{\parallel} v_{D_e})}{k_{\parallel} v_{T_e}} \frac{1}{k^2 \lambda_{D_e}^2} + \frac{\omega}{k_{\parallel} v_{T_i}} \frac{1}{k^2 \lambda_{D_i}^2} e^{-\left(\frac{\omega^2}{k_{\parallel}^2 v_{T_i}^2}\right)} \right] \quad (5.2.5)$$

From Eq. (5.2.4), the slow and fast acoustic waves and the first harmonic of the ion cyclotron wave are obtained in different frequency regimes:

(i)  $\omega \ll \Omega_i$ , slow acoustic wave

$$\text{Re } \epsilon(k, \omega) = \left( \frac{1 + k^2 \lambda_D^2 + k_{\perp}^2 \rho_s^2}{k^2 \lambda_D^2} \right) \left[ 1 - \frac{k_{\parallel}^2 \bar{c}_s^2}{\omega^2} \right]$$

$$\bar{c}_s = c_s / (1 + k^2 \lambda_D^2 + k_{\perp}^2 \rho_s^2)^{1/2} < c_s$$

(5.2.6)

Dispersion relation:  $\omega^2 = k_{\parallel}^2 \bar{c}_s^2$

(ii)  $\omega \gg \Omega_i$ , fast acoustic wave

$$\text{Re } \epsilon(k, \omega) = \left( \frac{1 + k^2 \lambda_{De}^2}{k^2 \lambda_{De}^2} \right) \left[ 1 - \frac{k_{\perp}^2 \tilde{c}_s^2}{\omega^2} \right]$$

$$\tilde{c}_s = c_s / (1 + k^2 \lambda_D^2)^{1/2}$$

(5.2.7)

Dispersion relation:  $\omega^2 = k^2 \tilde{c}_s^2$

(iii)  $\omega \sim \Omega_i$ , ion cyclotron wave

$$\text{Re } \epsilon(\omega, k) = \left( \frac{1 + k^2 \lambda_D^2}{k^2 \lambda_D^2} \right) \left[ 1 - \frac{k_{\perp}^2 \bar{c}_s^2}{\omega^2 - \Omega_i^2} \right]$$

(5.2.8)

Dispersion relation:  $\omega^2 = \Omega_i^2 + k_{\perp}^2 \bar{c}_s^2$

The slow acoustic wave is treated in this section and the ion-cyclotron wave in Sec. (5.3).

From the solution of the equations  $\text{Re } \epsilon(\omega, k) = 0$  and  $\gamma = -\text{Im } \epsilon / (\partial \text{Re } \epsilon / \partial \omega)_{\omega = \omega_L}$  the linear frequency and growth rate of the slow acoustic wave are obtained.

$$\omega_L = \pm k_{\parallel} \bar{c}_s$$

$$\gamma_L = \left( \frac{\pi}{8} \right)^{1/2} \frac{k_{\parallel} \bar{c}_s}{(1 + k^2 \lambda_D^2 + k_{\perp}^2 \bar{c}_s^2)} \left[ \mu^{1/2} \left( \frac{k_{\parallel} v_0 - \omega_L}{k_{\parallel} \bar{c}_s} \right) - \bar{c}^{3/2} \frac{\omega_L}{k_{\parallel} \bar{c}_s} \exp \left( -\frac{\omega_L^2 \bar{c}}{k_{\parallel}^2 \bar{c}_s^2} \right) \right] \quad (5.2.9)$$

where  $\mu = \frac{m_e}{m_i}$ ,  $\bar{c} = T_i/T_e$ . The mode is driven unstable when  $\gamma_L$  becomes positive.

We now perform an identical linear stability analysis of the turbulent state, where the effect of the turbulence is included through the perturbed orbits of the particles. The non-linear dielectric function is

$$\epsilon_{NL}(\omega, k) = \left[ 1 + \sum_j \frac{\omega_{pj}^2}{k^2 v_{Tj}^2} \sum_{n=-\infty}^{\infty} e^{-\lambda_j} I_n(\lambda_j) \right] \times$$

$$\left[ 1 + \frac{\omega - k_{\parallel} v_{0j}}{\sqrt{2} k_{\parallel} v_{Tj}} \right] \left( \frac{\omega - n \Omega_j - k_{\parallel} v_{0j} + i k_{\perp}^2 D_j}{\sqrt{2} k_{\parallel} v_{Tj}} \right) \quad (5.2.10)$$

As discussed in Chapter 3, Sec. (3.1a), the level of turbulent energy required for the spatial diffusion of the bulk of electron distribution is very high. At turbulent energies  $\sim 0.1 nT_e$ , the diffusion of electrons can be neglected. Even if turbulent diffusion of electrons is high, this does not affect the low frequency dispersion relation since the integration along the electron orbits only contributes to  $\epsilon$  the term  $1 + 1/k^2 \lambda_D^2$  which is independent of orbit diffusion.

Retaining only ion diffusion,  $\epsilon_{NL}$  for the nonlinear slow acoustic wave is obtained in the limit

$$\omega \ll \Omega_i,$$

$$\begin{aligned}
\epsilon_{\text{NL}}(\omega, k) = A & \left[ 1 + \frac{i\eta}{\omega + i\eta} \frac{\bar{c}_s^2}{V_{Te}^2} \right. \\
& \left. + \left( \frac{1}{(\omega + i\eta)^2} + \frac{i\eta}{(\omega + i\eta)^3} \right) k_{\parallel}^2 \bar{c}_s^2 \right] \\
& + i \left( \frac{\pi}{2} \right)^{1/2} \left[ \left( \frac{\omega - k_{\parallel} v_{Te}}{k_{\parallel} v_{Te}} \right) \frac{1}{k^2 \lambda_{De}^2} \right. \\
& \left. + \frac{\omega}{k_{\parallel} v_{Te}} \frac{\omega_i}{k \lambda_{Di}^2} \exp \left\{ - \left( \frac{\omega^2 - \eta^2}{2 k^2 v_{Te}^2} \right) \right\} \right]
\end{aligned}
\tag{5.2.11}$$

where

$$A = (1 + k^2 \lambda_{De}^2 + K_{\perp}^2 \int_s^{\infty} \frac{1}{s^2}) / k^2 \lambda_{De}^2$$

$$\eta = k^2 \lambda_{Di}^2$$

and  $\sigma$  occurs in the expansion of  $Z(X + iy)$  and has the values

$$\sigma = \begin{cases} 0 & y > 1/X \\ 1 & \text{for } |y| < 1/X \\ 2 & -y > 1/X \end{cases}$$

If  $\omega = \omega_{NL} + i\gamma'_{NL}$  is the solution of  $\epsilon_{NL} = 0$ , and if  $\eta, \gamma'_{NL} \ll \omega_{NL}$ , the real and imaginary parts of  $\epsilon_{NL}$  are,

$$\text{Re } \epsilon_{NL} \approx A \left[ 1 - \frac{k_{\parallel}^2 \bar{c}_s^2}{\omega_{NL}^2} + \frac{\eta(\eta + \gamma'_{NL})}{\omega_{NL}^2} \frac{\bar{c}_s^2}{v_{Te}^2} \right] \quad (5.2.12)$$

$$\text{Im } \epsilon_{NL} = A \frac{2k_{\parallel}^2 \bar{c}_s^2}{\omega_{NL}^3} \left[ \gamma'_{NL} + \frac{3}{2} \eta \left( 1 + \frac{\omega_{NL}^2}{3k_{\parallel}^2 v_{Te}^2} \right) - \gamma'_L \right] \quad (5.2.13)$$

where  $\gamma'_L$  is the linear growth rate altered by the diffusion, and is given by

$$\gamma'_L = -\frac{1}{A} \left( \frac{\pi}{2} \right)^{1/2} \left[ \left( \frac{\omega - k_{\parallel} v_0}{k_{\parallel} v_{Te}} \right) \cdot \frac{1}{k^2 \lambda_D^2} + \frac{\omega_{NL}}{k_{\parallel} v_{Te}} \frac{1}{k^2 \lambda_D^2} \exp \left\{ - \left( \frac{\omega_{NL} - \eta}{2k_{\parallel}^2 v_{Te}^2} \right)^2 \right\} \right] \frac{\omega_{NL}}{2k_{\parallel}^2 \bar{c}_s^2} \quad (5.2.14)$$

Setting  $\epsilon_{NL}$  to zero, the nonlinear frequency  $\omega_{NL}$  and growth rate  $\gamma'_{NL}$  are obtained.

$$\omega_{NL} = k_{||} \bar{c}_s \left[ 1 - \frac{\gamma \left( \eta + \gamma'_{NL} \right)}{k_{||}^2 V_{Ti}^2} \right]^{1/2}$$

(5.2.15)

$$\gamma'_{NL} = \gamma'_L - \frac{3}{2} \gamma \left( 1 + \frac{\omega_{NL}^2}{3 k_{||}^2 V_{Ti}^2} \right)$$

(5.2.16)

Eqs. (5.2.15) and (5.2.16) are coupled. If  $\gamma'_{NL} \ll \gamma_L$ , then  $\omega_{NL} \approx k_{||} \bar{c}_s \left[ 1 - \gamma^2 / k_{||}^2 V_{Ti}^2 \right]^{1/2}$ . The frequency is lowered as a result of scattering off the particles. For ion resonance broadening to be effective the ion temperature must be sufficiently high so that at least some ions fall within the resonance width  $\gamma_L$ . Moreover, for physically meaningful results,  $\gamma_L$  must not exceed  $k_{||} V_{Ti}$ . If  $\gamma_L$  becomes so large that all the ions are included in the broadened resonance, a further increase in cannot produce any physical effect.

The growth rate  $\gamma'_{NL}$  refers to a perturbation about the turbulent state. If  $\gamma'_{NL}$  is negative, perturbations about this state will decay to give another realization of the same turbulent state. We see from Eq. (5.2.16) that the ion diffusion  $\gamma_L$  has a stabilizing effect on the turbulent state. The effect is enhanced by

the factor  $\omega_{NL}^2 / 3k_{||}^2 v_{Ti}^2$ . It would appear that the condition for stationarity is  $\phi'_{NL} = 0$ . However, the self-consistent nature of the relations between the level of fluctuations and the diffusion requires that  $\text{Im } \omega$  lie sufficiently far below the real axis in the  $\omega$ -plane to ensure stationarity. This point will be discussed in greater detail in Chapter 6, where we calculate the fluctuation spectrum.

### 5.3. EFFECT OF VELOCITY SPACE DIFFUSION

As seen in Sec. (3.2), particles diffuse in velocity space in the presence of higher frequency ( $\omega \gtrsim \Omega_i$ ) turbulence. In this section, we examine the effect of velocity space diffusion on the dielectric function.

The perturbed orbit is,

$$e^{i\omega t} \langle e^{ik \cdot \Delta R} \rangle = \sum_{n=-\infty}^{\infty} J_n^2 \left( \frac{k_{\perp} v_i}{\Omega_j} \right)$$

$$e^{i(\omega - k_{||} v_{||} - n \Omega_j)t - \vec{k} \cdot \vec{x} \cdot \vec{k}}$$

(5.3.1)

The dielectric function in terms of the perturbed orbit may be written as



$$\epsilon_{NL}(k, \omega) = 1 - \sum_j i \frac{\omega_{pj}^2}{k^2} \int_0^\infty dt \sum_{n=-\infty}^{\infty} \int d\vec{v}$$

$$\left[ J_n^2 \left( \frac{k_\perp v_\perp}{\Omega_j} \right) \left( k_\parallel \frac{\partial f_{0j}}{\partial v_\parallel} + \frac{n \Omega_j}{v_\perp} \frac{\partial f_0}{\partial v_\perp} \right) \right]$$

$$\exp \left[ i(\omega - k_\parallel v_\parallel - n \Omega_j)t - \vec{k} \cdot \vec{b} \cdot \vec{k} t^3 \right] \quad (5.3.2)$$

### 5.3.a. Ion Diffusion

Let us consider the change in  $\epsilon$  due to ion diffusion. With  $f_{0i}(v) = (2\pi V_{Ti})^{-3/2} \exp(-v^2/2V_{Ti}^2)$ , the integral over  $v_\perp$  gives

$$\epsilon_{NL}^{ion}(k, \omega) = - \frac{i \omega_{pi}^2}{k^2 V_{Ti}^2} \sum_{n=-\infty}^{\infty} e^{-\lambda_i} J_n(\lambda_i) \times$$

$$\int dv_\parallel [-k_\parallel v_\parallel - n \Omega_i] f_0(v_\parallel) \times$$

$$\int dt \exp \left[ i(\omega - k_\parallel v_\parallel - n \Omega_i)t - \vec{k} \cdot \vec{b} \cdot \vec{k} t^3 \right] \quad (5.3.3)$$

where  $\lambda_i = k_\perp^2 \frac{v_{Ti}^2}{\Omega_i^2}$ .

The time integral gives the Lommel function<sup>(3)</sup>

$$\int e^{i(\omega - k_{\parallel} v_{\parallel} - n\Omega_i)t - \bar{k} \cdot \bar{D} \cdot \bar{k} t^3} dt$$

$$= \frac{i}{\omega - k_{\parallel} v_{\parallel} - n\Omega_i} \bar{z} S_{0, 1/3}(\bar{z}) \quad (5.3.4)$$

where  $\bar{z} = 2 \left( \frac{\omega - k_{\parallel} v_{\parallel} - n\Omega_i}{3i (k \cdot \chi_i k)^{1/2}} \right)^{3/2}$  (5.3.5)

Therefore,

$$\epsilon_{NL}^{ion}(k, \omega) = \frac{1}{k^2 \lambda_{Di}^2} \sum_{n=-\infty}^{\infty} e^{-\lambda_i} \bar{I}_n(\lambda_i)$$

$$\int dv_{\parallel} f_0(v_{\parallel}) \left[ 1 - \frac{\omega}{\omega - k_{\parallel} v_{\parallel} - n\Omega_i} \right] \bar{z} S_{0, 1/3}(\bar{z})$$

(5.3.6)

Far from resonance  $|z| \gg 1$ , (Eq. (A1.8))

$$\bar{z} S_{0, 1/3}(\bar{z}) \approx \left[ 1 - \frac{8}{9 \bar{z}^2} \right]$$

$$\epsilon_{NL}^{-ion}(k, \omega) = \frac{1}{k^2 \lambda_{Di}^2} \sum_{n=-\infty}^{\infty} e^{-\lambda_i} I_n(\lambda_i)$$

$$\int dv_{||} f_0(v_{||}) \left[ 1 - \frac{\omega}{\omega - k_{||} v_{||} - n\Omega} \right] \left[ 1 - \frac{Q(k, \lambda, k)}{i(\omega - k_{||} v_{||} - n\Omega)^3} \right]$$

(5.3.7)

To lowest order in  $\lambda$ , the linear dielectric function is recovered from Eq. (5.3.7). It may be noted that the velocity diffusion term does not contribute to a resonance broadening  $\omega + i\gamma$ . This result is particularly important in view of the fact that the velocity diffusion term  $k \cdot \lambda \cdot k \cdot t^3$  in the orbit is sometimes<sup>(4)</sup> approximated by  $(k \cdot \lambda \cdot k)^{1/3} t$  which gives rise to a resonance broadening  $\omega + i(k \cdot \lambda \cdot k)^{1/3}$ .

Another important conclusion from this is that while spatial diffusion can lead to a stationary turbulent state, velocity space diffusion does not lead to a similar effect. On a longer time scale, velocity diffusion can alter the unstable particle velocity distribution, which may quench the turbulence.

### 5.3.b. Electron Diffusion

For the resonant electron response, we replace the perturbed orbit integral in Eq. (5.3.2) by Eqn. (4.16c) with  $k_{\perp}^2 D_{\perp} = 0$ . Neglecting all electron gyro-effects, we obtain, approximately, the electron contribution to  $\epsilon_{NL}$

$$\begin{aligned} \epsilon_{NL}^{electron}(k, \omega) = & \left( \frac{\pi}{3} \right)^{1/3} \frac{2/3}{\Gamma(2/3)} \frac{1}{k^2 \lambda_D^2} \frac{k_{\parallel} V_T}{(k_{\parallel}^2 D_{\parallel})^{1/3}} \\ & \times \left[ 1 - \frac{\Gamma(2/3)}{\Gamma(1/3)} \frac{(\omega - k_{\parallel} V_0)}{(k_{\parallel}^2 D_{\parallel})^{1/3}} \right] \quad (5.3.8) \end{aligned}$$

where  $V_0$  is the drift speed along  $B$  of the Maxwellian electron distribution.

The linear growth rate is modified by the turbulent diffusion of electrons in velocity space.

### 5.4. NON-LINEAR ION CYCLOTRON DISPERSION RELATION

As seen in Sec. (5.3), pure velocity space diffusion does not lead to a stationary turbulent state. A quasi-stationary state for turbulent fluctuations at  $\omega \sim \Omega_i$  may be obtained through the average spatial diffusion  $D$ , described in Sec. 3.2.c.

In terms of  $D$ , the non-linear dielectric function is

$$\begin{aligned} \epsilon_{NL}(\omega, k) = & 1 + \sum_j \frac{\omega_{pj}^2}{k^2 v_{Tj}^2} \sum_{n=-\infty}^{\infty} e^{-\lambda_j} I_n(\lambda_j) \\ & \times \left[ 1 + Z \left( \frac{\omega + i k_{\perp}^2 D_j - n \Omega_j - k_{\parallel} v_{0j}}{\sqrt{2} k_{\parallel} v_{Tj}} \right) \right] \end{aligned} \quad (5.4.1)$$

The  $n = 0$  mode gives rise to the ion-acoustic waves considered in Sec.(5.2). When  $\omega \sim \Omega_i$ , the  $n = 1$  mode dominates over the others. The dielectric function in the presence of the first harmonic of the ion-cyclotron wave is

$$\epsilon_{NL}^{ic} = \left( 1 + \frac{1}{k^2 \lambda_D^2} \right) \left[ 1 - k_{\perp}^2 \frac{D^2}{\Omega_i^2} \left\{ \frac{\Omega_i^2 - i\eta(\omega + i\eta)}{(\omega + i\eta)^2 - \Omega_i^2} \right\} \right] \quad (5.4.2)$$

where  $\eta = i k_{\perp}^2 D \ll \omega$ .

The solution of this equation gives the nonlinear frequency  $\omega_{NL}$  and growth rate  $\gamma_{NL}$  of ion-cyclotron waves.

The non-linear frequency is

$$\omega_{NL}^2 = (\Omega_i^2 + \eta^2) \left( 1 + k_{\perp}^2 \frac{c_s^2}{J_s^2} \right)$$

(5.4.3)

where  $c_s = \frac{(T_e/m_i)^{1/2}}{1 + k^2 D^2}$ ,  $\bar{J}_s = \frac{\bar{c}_s}{\Omega_i}$

The nonlinear growth rate is

$$\gamma_{NL} = \gamma_L' - \eta \frac{\omega_{NL}^2}{(\omega_{NL}^2 - (\Omega_i^2 + \eta^2))} \quad (5.4.4)$$

where

$$\gamma_L' = - \frac{\text{Im } \epsilon_L}{\frac{\partial \text{Re } \epsilon_{NL}}{\partial (\lambda)}} \bigg|_{(\lambda) = (\lambda)_{NL}}$$

is the linear growth rate modified by the nonlinear frequency shift.

REFERENCES

- (1) Catto, P.J. (1978) *Phys. Fluids* 21, 147.
- (2) See, for example, Hasegawa, A., (1975) *Plasma Instabilities and Nonlinear Effects*, Springer-Verlag, New York.
- (3) Magnus, W., F. Oberhettinger and R.P. Soni, (1966), *Formulas and Theorems for the Special Functions of Mathematical Physics*, Springer-Verlag, New York.
- (4) Hasegawa, A., (1975), *Plasma Instabilities and Non-linear Effects*, Springer-Verlag, N.Y., Pg. 159, Eq.(4.50).

## CHAPTER 6

### SPECTRUM OF TURBULENT ION ACOUSTIC WAVES

The Perturbed Orbit Theory of Dupree and Weinstock<sup>(1)</sup> has been discussed in Chapters 3-5, and based on it, test particle diffusion rates and the dielectric function in a turbulent plasma have been obtained. The test particle diffusion cannot be physically observed in the absence of gradients. It is necessary that physically observable parameters of the turbulent plasma be calculated, and compared with observations. One of the important measurable features of the turbulent state is the fluctuation spectrum. However, as pointed out by Cook and Taylor<sup>(2)</sup>, the equilibrium fluctuation spectrum in the stationary, turbulent plasma had not been obtained in the initial



Dupree-Weinstock theory, which was in this sense incomplete. The fluctuation spectrum was formally obtained by Cook and Taylor using a superposition principle of dressed particles. In their formulation, the spectrum is an implicit function of the diffusion, and cannot be explicitly calculated in general.

From our numerical study of the behaviour of  $D$  (Chapter 4, Fig. 4.5), we have seen that at high levels of turbulence,  $D$  is almost constant for particles within a wide range of velocities. In this limit, we find that the spectrum can be explicitly calculated from the knowledge of the non-linear dielectric function obtained from the Perturbed Orbit Theory. Using the superposition principle, we calculate the spectrum of ion acoustic waves excited by an electron drift along  $B_0$ .

In the next section we review the earlier theoretical work on the ion-acoustic spectrum (Sec. 6.1). We then describe the superposition principle and its extension to turbulent plasmas (Sec. 6.2). In Sec. 6.3, we obtain the ion-acoustic spectrum analytically in  $(k, \Theta)$  space. The spectrum is numerically evaluated and compared with earlier theoretical spectra, laboratory measurements and simulations.

### 6.1. ION ACOUSTIC SPECTRUM

The earliest theoretical calculations<sup>(3)</sup> of the ion-acoustic turbulence spectrum suffered from certain drawbacks, such as a divergence at low  $k$ . This could be rectified by the addition of ion-neutral collisions<sup>(4)</sup>. These were essentially quasilinear calculations applicable to weak turbulence. The inclusion of higher order perturbations to the particle motion, in a renormalized quasilinear theory, removed the low- $k$  divergence in collisionless plasma. The renormalized quasilinear theory of ion-acoustic turbulence has been dealt with in detail by Horton and Choi<sup>(5)</sup>, who have obtained the spectrum by a mode simulation technique, and have also reviewed the literature on spectral observations and computer simulation results. All these calculations belong to a class of initial value problems, where the time evolution is studied by taking explicitly into account the feedback action of the oscillations on the single particle distribution functions, while the wave-wave interaction is treated perturbatively.

A second class of problems arises if connection to an external energy source is maintained. Under such conditions the system can go to a new equilibrium or stationary state where large fluctuating fields co-exist with linearly unstable distribution functions and enhanced levels of diffusion. It is this class of problems that we shall consider here.

Stationary ion-acoustic spectra have been obtained by Ichimaru<sup>(6)</sup> in the absence of a magnetic field. Another calculation by Sleeper<sup>(7)</sup> et al determines the angular extent of the spectrum in the  $\vec{k}$  plane.

## 6.2. SUPERPOSITION PRINCIPLE OF DRESSED PARTICLES<sup>(2)</sup>

As is well known, the field of a charge in a thermal plasma is screened out at distances larger than the Debye length. The degree of screening, arising from the collective response of all the particles, depends on the plasma dielectric function. It is simulated by assigning a dressing to each charge in the plasma. The superposition of the fields of the dressed particles gives rise to the correct screened field at a given point. All further interactions between the dressed particles are neglected, which now move as free particles in the plasma.

In a quiescent plasma, the fluctuation spectrum obtained from a superposition of dressed fields is

$$\left\langle \frac{|E_k|^2}{V} \right\rangle = \sum_j \left( \frac{4\pi}{k^2} n e^2 \right) \int d\omega \left( \frac{f_0(v) d\vec{v}}{|\epsilon(\omega, k)|^2} \delta(\omega - \vec{k} \cdot \vec{v}) \right) \quad (6.1)$$

where  $\epsilon(\omega - k \cdot V)$  arises from the integration over the free propagator  $e^{i(\omega - k \cdot V)t}$  of the dressed particles. The spectrum diverges at the onset of instability signalled by  $\epsilon \rightarrow 0$ .

As seen in Chapters 3-5, the turbulent growth of fluctuations in a linearly unstable plasma supporting a wide spectrum of frequencies causes the particles to diffuse about their unperturbed trajectories. The diffusion can lead to the stabilization of further growth of the fluctuations, and to the formation of a stationary state. The dressing of the particles in the stationary state will be determined by the stable nonlinear dielectric function  $\epsilon_{NL}$ . By a superposition principle analogous to that employed for a quiescent plasma, the spectrum in the turbulent plasma can be written as

$$\frac{\langle |E_k|^2 \rangle}{V} = \sum_j \frac{(4\pi)^2 n e^2}{k^2} \int d\omega \int \frac{f_{0j}(V)}{|\epsilon_{NL}(\omega, k)|^2} \delta(\omega - \bar{k} \cdot \bar{V}) \quad (6.2)$$

where  $f_0(V)$  is the equilibrium distribution function in the turbulent plasma.

### 6.3. CALCULATION OF THE SPECTRUM

Although, the spectrum can be formally obtained using the superposition principle described above,

the explicit calculation of the turbulence spectrum is difficult for several reasons.

Firstly, the self-consistent nature of the formulation relating several unknowns e.g.  $f_0$ ,  $D$ ,  $\epsilon$ , and  $\langle |\mathbf{E}|^2 \rangle / V$  requires that some approximate estimates for some of them must be made before the others can be calculated analytically. Numerically, the error introduced by this could be removed by employing an iteration process to obtain the correct self-consistent values of the unknowns. It is assumed that such an iteration process would converge.

Secondly,  $\epsilon_{NL}$  is a function of the diffusion  $D$ , which depends on the particle velocity  $V$ . This makes it difficult to perform the velocity integral in Eq.(6.2). However, as seen in Chapter 4 (Fig. 4.5), at high levels of turbulence ( $\epsilon \sim 0.1 n T_e$ ),  $D$  is relatively constant over a wide range of  $V$ . The velocity integral can then be performed to obtain the spectrum explicitly. The dielectric function  $\epsilon_{NL}$  in the presence of turbulent slow acoustic waves has been calculated using Perturbed Orbit Theory (Chapter 5, Sec. 2).

$$\begin{aligned} \frac{1}{|\epsilon_{NL}(k, \omega)|^2} &= \frac{1}{A^2} \left[ 1 - \frac{\omega_{NL}}{(\omega_r + i\omega_i)^2} \right]^{-1} \left[ c.c. \right]^{-1} \\ &= \frac{1}{A^2} \left[ 1 + 2 \text{Re} \left[ N \left\{ \frac{1}{(\omega_r - \omega_c)} - \frac{1}{\omega_r + \omega_c} \right\} \right] \right] \quad (6.3) \end{aligned}$$

where  $\omega_0 = \omega_{NL} - i\gamma'_{NL}$  is the solution of the nonlinear dispersion relation,

$$N = \frac{\omega_0^2 (\omega_0^2 + 2\gamma_{NL}^2) + \gamma_{NL}^4}{-2i\omega_0 \gamma'_{NL}} \quad (6.3a)$$

and  $A = (1 + k^2 \lambda_D^2 + k_\perp^2 \rho_s^2) / k^2 \lambda_D^2$ . Substituting for  $\epsilon_{NL}$  in Eq.(6.2), and assuming that the particle distribution in stationary equilibrium with the turbulent plasma is Maxwellian with an electron drift along  $B$ , we obtain the ion contribution to the spectrum, to be

$$\begin{aligned} \frac{(4\pi)^2 n_i e^2}{k^2} \int \frac{dv_{||}}{\sqrt{2\pi} v_{Ti}} \frac{e^{-v_{||}^2 / 2 v_{Ti}^2}}{|\epsilon_{NL}(k_{||} v_{||}, k)|^2} \\ = 1 + 4 \text{Re} \left[ \left( \frac{N}{\sqrt{2} k_{||} v_{Ti}} \right) \right] \left( \frac{\omega_0}{\sqrt{2} k_{||} v_{Ti}} \right) \quad (6.4) \end{aligned}$$

The contribution from the drifting electron is

$$\begin{aligned}
 & \frac{(4\pi)^2 n_e e^2}{k^2} \int_{-\infty}^{\infty} \frac{dv_{||}}{\sqrt{2\pi} v_{Te}} \frac{e^{-\frac{(v_{||}-v_0)^2}{2v_{Te}^2}}}{|E_{NL}(k_{||}v_{||}, k)|^2} \\
 &= 1 + 2 \operatorname{Re} \left\{ \left( \frac{N}{\sqrt{2} k_{||} v_{Te}} \right) \sum_{+,-} \int \left( \frac{\omega_0 \pm k_{||} v_0}{\sqrt{2} k_{||} v_{Te}} \right) \right\}
 \end{aligned}
 \tag{6.5}$$

The total fluctuation spectrum is

$$\begin{aligned}
 \frac{\langle |E_k|^2 \rangle}{V} &= \frac{(4\pi)^2 n_e e^2}{k^2} \cdot \frac{1}{A^2} \sum_j \left\{ 1 + \right. \\
 & \quad \left. 2 \operatorname{Re} \left[ \left( \frac{N}{\sqrt{2} k_{||} v_{Te}} \right) \sum_{+,-} \int \left( \frac{\omega_0 \pm k_{||} v_0}{\sqrt{2} k_{||} v_{Te}} \right) \right] \right\}
 \end{aligned}
 \tag{6.6}$$

When normalised to the electron thermal energy, the spectrum is

$$S(k, \theta) = \frac{\langle |E_k|^2 \rangle}{8\pi T_e V}$$

$$= \frac{k^2 \lambda_D^2}{(1 + k^2 \lambda_D^2 + k_\perp^2 \lambda_s^2)^2} \sum_j \left[ 1 + 2 \operatorname{Re} \frac{N}{\sqrt{2} k_\parallel v_{Tj}} \sum_{+,-} \mp \left( \frac{\omega \pm k_\parallel v_{Tj}}{\sqrt{2} k_\parallel v_{Tj}} \right) \right] \quad (6.7)$$

For a quiescent plasma without an electron drift or magnetic field, we recover the thermal acoustic fluctuation spectrum from Eq. (6.7),

$$\frac{\langle |E_k|^2 \rangle}{V} = 4\pi T_e \frac{k^2 \lambda_D^2}{(1 + k^2 \lambda_D^2)^2} \quad (6.8)$$

In Eq. (6.7), as  $\gamma'_{NL}$  tends to zero, i.e. the pole of  $\zeta_{NL}$  approaches the real axis from below, the spectrum diverges, which indicates that the state can no longer be stationary. This situation is the exact non-linear analogue of the onset of instability in the linear regime described by Cook and Taylor.  $\gamma'_{NL}$  gives the growth rate of perturbations about the turbulent state, and if  $\gamma'_{NL} = 0$ , all perturbations remain indefinitely in that state instead of decaying away. It is important to note, therefore, that  $\gamma'_{NL} = 0$  does not give a condition for stationarity. For the state to be stationary,  $\operatorname{Im} \zeta$  must



be sufficiently far below the real axis to ensure that perturbations about the turbulent state decay back to the same state faster than a certain rate, which must be determined from the self-consistent solution of the equations relating the spectrum and the diffusion coefficient.

#### 6.4. NUMERICAL RESULTS

The spectrum  $S(\vec{k})$  is computed for a typical set of ion acoustic wave parameters, viz.,  $T_e/T_i = 10$ ,  $V_o/C_s = 100$ ,  $\Omega_i/\omega_{pi} = 2$ , and turbulence level  $\xi/nTe \sim 0.1$ . The diffusion coefficient  $D/C_s \lambda$  is taken to be 0.035. The spectrum obtained, (Fig.6.1), peaks at  $k \lambda_D \sim 0.4$  at  $\Theta = 0^\circ$ . For larger angles, the peak value falls, while the peak shifts to lower values of  $k$ .  $S(k, \Theta)$  follows a power law in  $k$ , ( $S \sim k^{-\alpha}$ ) with the same index  $\alpha = 3.54 \pm 0.03$  for all  $\Theta$  (Fig.6.2). The classical Kolmogorov exponent for a 3 dimensional spectrum is  $-11/3$ . If the fractal dimension  $D_F$  of the turbulence is taken into account, the Kolmogorov exponent is replaced by  $11/3 + B$ , where  $B = (3-D_F)/3$  (Mandelbrot<sup>(8)</sup>, 1977). From this we infer that the fractal dimension in our model is  $D_F = 3.38$ .

The angular spectrum

$$S(\Theta) = 2\pi \int k^2 dk S(k, \Theta) \quad (6.9)$$

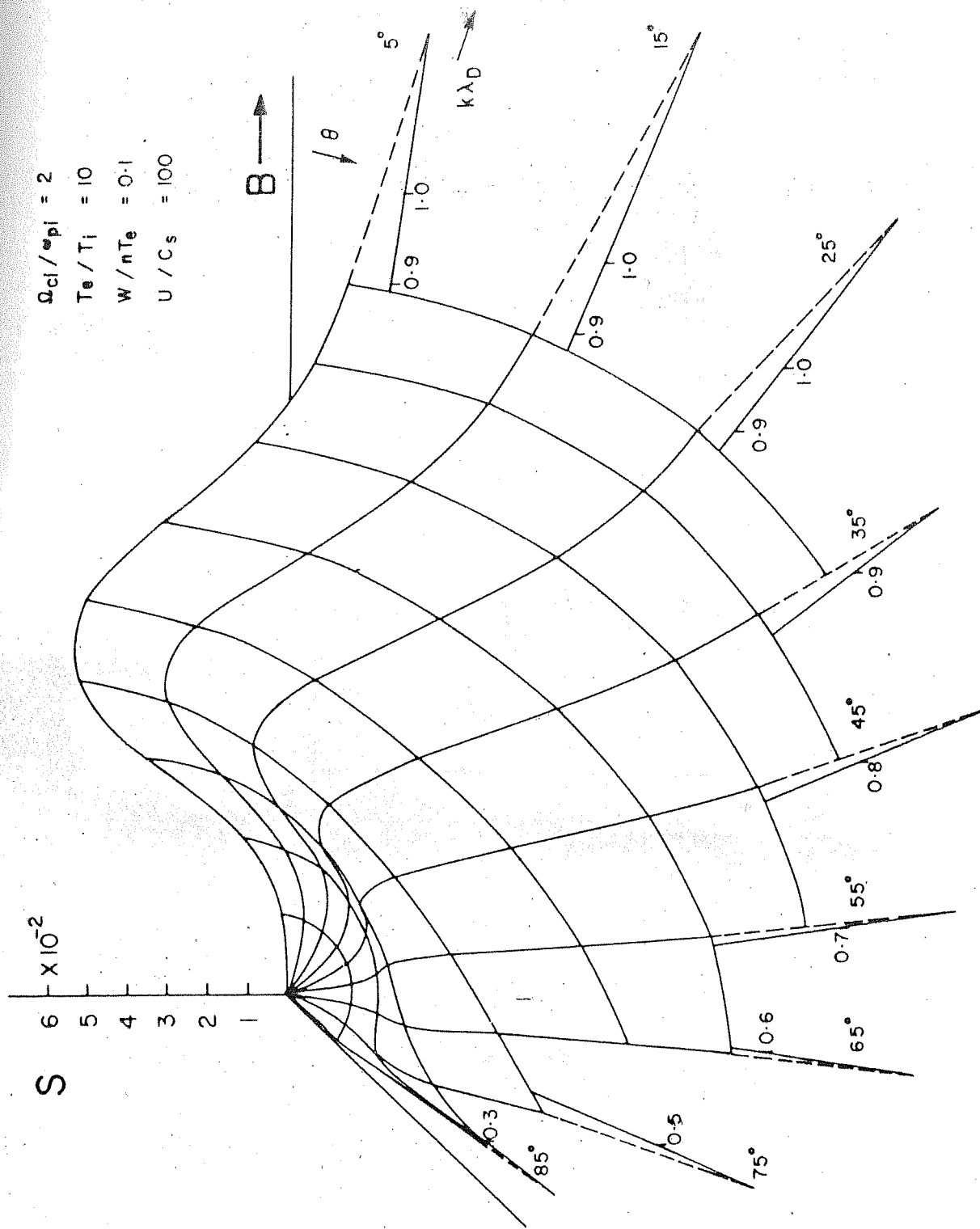


Fig. 6.1 Wave number spectrum  $S(k, \theta)$  of current driven ion acoustic turbulence calculated using the Superposition Principle of Dressed Particles and the Perturbed Orbit Theory.

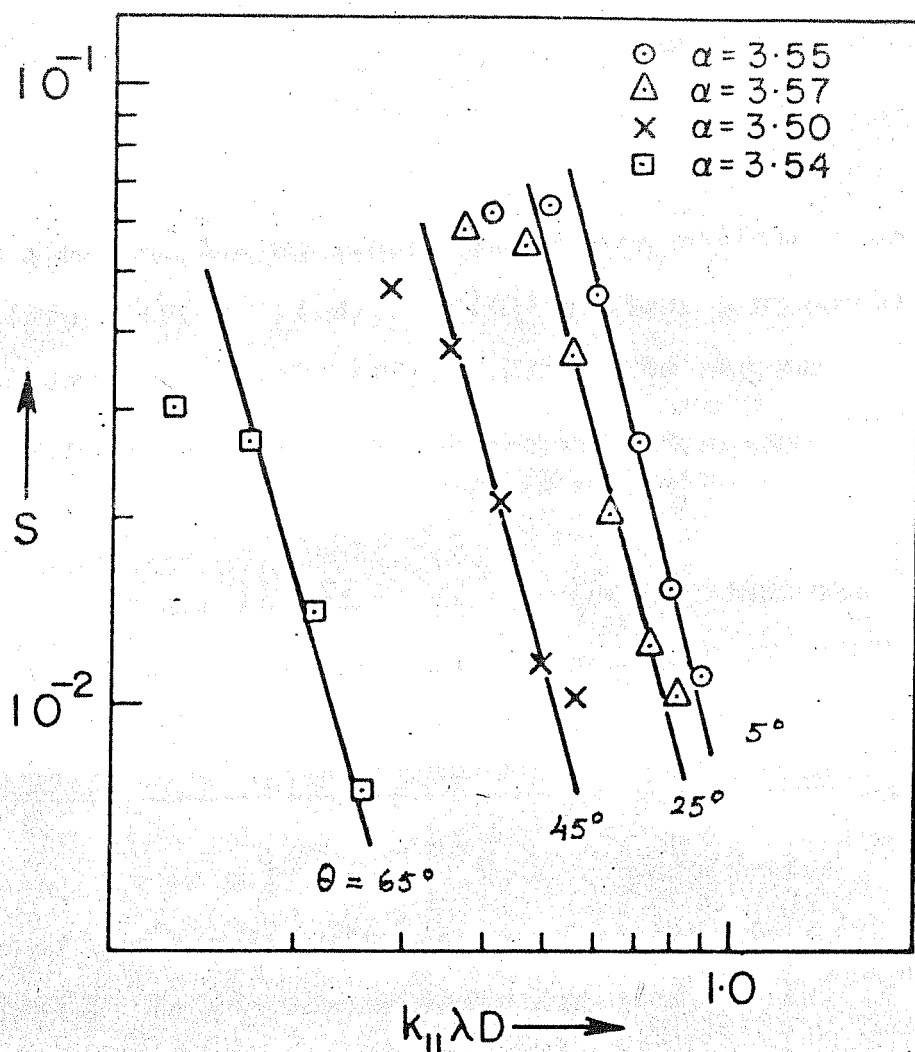


Fig. 6.2

Power law dependence  $S(k, \theta) \sim k_{||}^{-\alpha}$  for several values of  $\theta$ . The average value of  $\alpha = 3.54 \pm 0.03$ .

and the frequency spectrum,

$$S(\omega) = 2\pi \int k^2 dk \int \sin\theta d\theta S(k, \theta) \delta(\omega - f(\vec{k})) \quad (6.10)$$

where  $\omega = f(\vec{k})$  is the nonlinear dispersion relation, are evaluated (Figs. (6.3), (6.4)).  $S(\omega)$  follows a power law in  $\omega$  with exponent  $-2.62$ . (Fig.(6.5)). The angular intensity falls to half its peak value between  $\theta = 40-45^\circ$  (Fig.6.3).

It may be noted, in particular, that the spectra go smoothly to zero at low  $k$  and  $\omega$ .

## 6.5. COMPARISON WITH OBSERVED SPECTRA AND SIMULATIONS

It is difficult to make a quantitative comparison of our results with observed spectra in a magnetic field. In most experiments and simulations<sup>(9-11)</sup>, turbulence levels are lower and the ions are unmagnetized ( $\omega_{pi} \gg \Omega_i$ ), in contrast to our assumption  $\Omega_i = 2 \omega_{pi}$ . In addition, some of the features observed may be due to cyclotron modes  $n \geq 1$ , which we have not considered here. The anomalous  $\vec{k}$  spectrum, dominated by waves propagating at oblique angles to  $B$ , appears to be one such feature. We shall discuss this in Chapter 7.

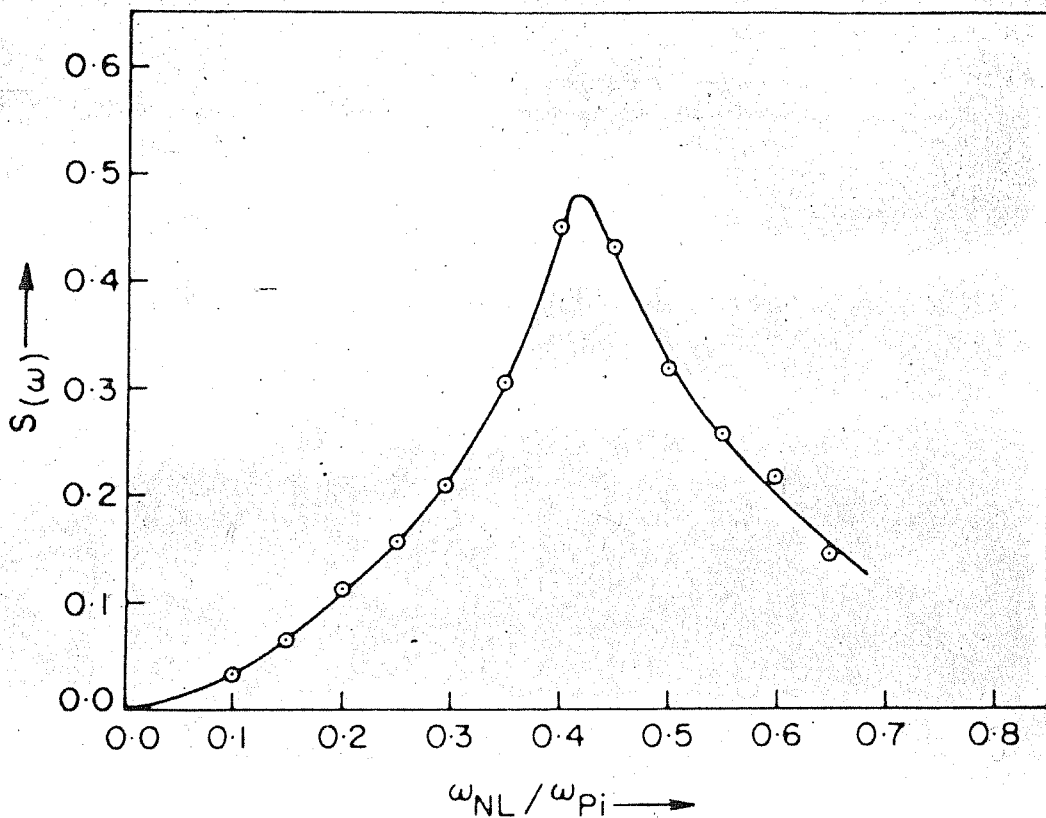
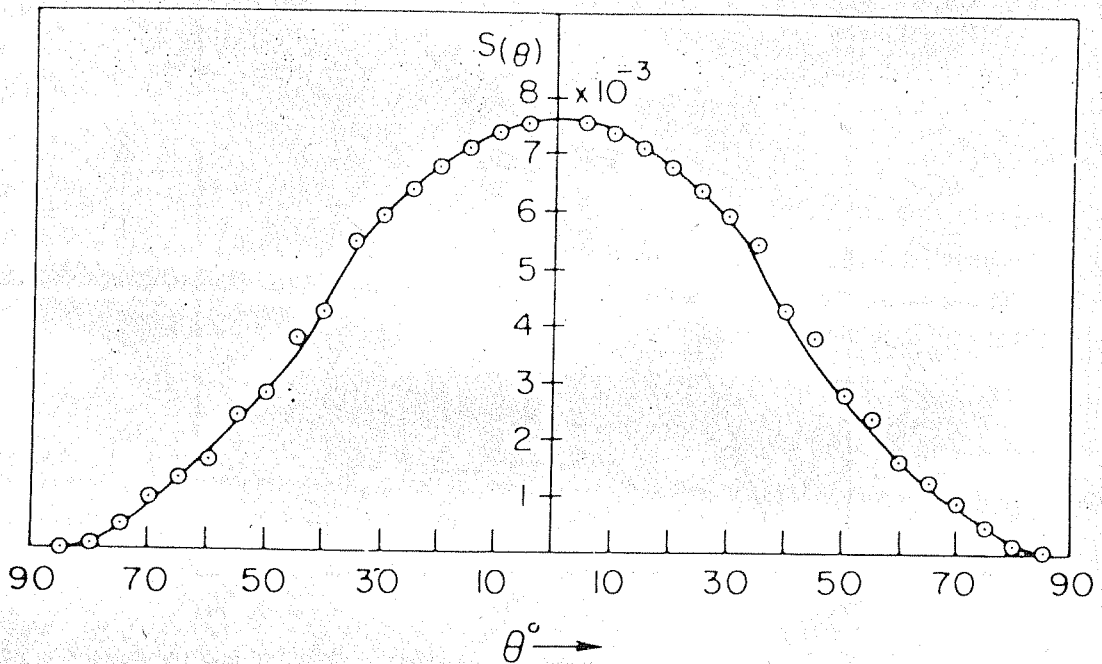


Fig. 6.3. Frequency spectrum of current driven ion acoustic turbulence calculated using the Superposition Principle of Dressed Particles and Perturbed Orbit Theory.



*Fig. 6.4 Angular spectrum of current driven ion acoustic turbulence calculated using the Superposition Principle of Dressed Particles and Perturbed Orbit Theory.*

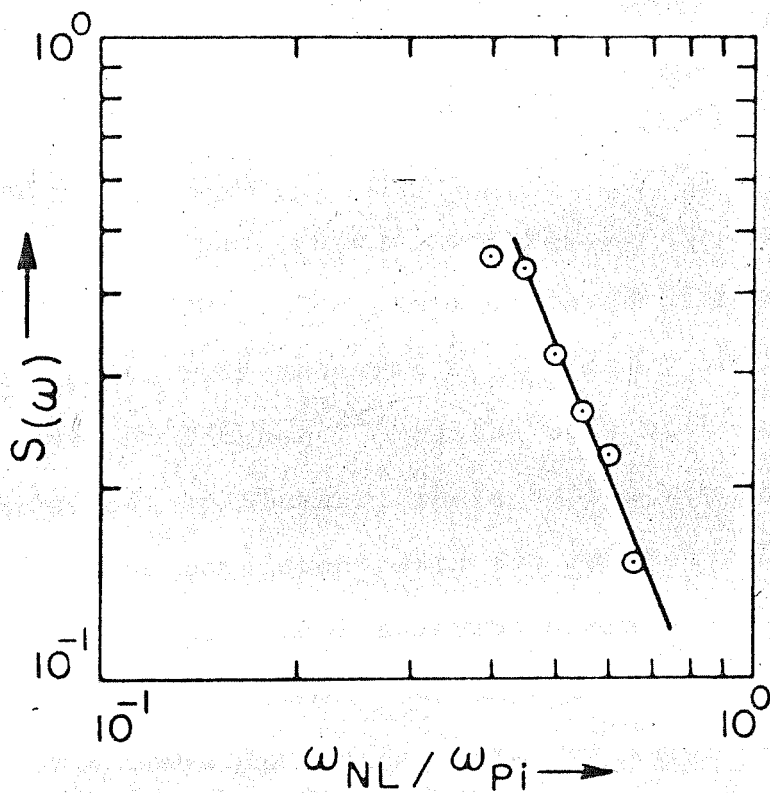


Fig. 6.5 Power law dependence of the frequency spectrum (Fig. 6.3) ( $S(\omega) \sim \omega^{-\alpha}$ ) with index  $\alpha = 2.61$ .

Since the slow acoustic wave is essentially similar to the ion acoustic wave in an unmagnetized plasma (except for a change in velocity and increased dispersion), it is appropriate to compare our results with ion sound turbulence measurements in an unmagnetised plasma<sup>(12-17)</sup>.

Some typical measured spectra are shown in Figs. 6.6 to 6.10. The shape of the 3-dimensional  $k$  spectrum (Fig. 6.6) measured by  $\text{CO}_2$  laser scattering experiments of Slusher<sup>(14)</sup> agrees well with ours (Fig. 6.1). As pointed out by Slusher, the spectrum obtained by him appeared to be consistent with ion resonance broadening, but theoretical spectra in 3-dimensions were not available for comparison at that time. The angular spread  $\Delta\theta$  in  $S$  is  $\sim 30^\circ$ . The power law index of the measured  $k$  spectra<sup>(13)</sup> is  $-4.8 \pm 0.5$ , which is high compared to our index (Fig. 6.2).

The shape of the measured frequency spectra (e.g. Figs. 6.7, 6.8), are consistent with our theoretical spectrum (Fig. 6.3). However, the spectrum measured by Gurnett (Fig. 6.8) does not appear to have a power law structure. The index of the power law in  $S(\omega)$  measured in various experiments, ranges between  $-1.7$  to  $-2.8$  which compares well with our value of  $-2.6$  (Fig. 6.5).

The angular spectrum obtained by us (Fig. 6.4) has the same form as the measured spectra (Figs. 6.9, 6.10).



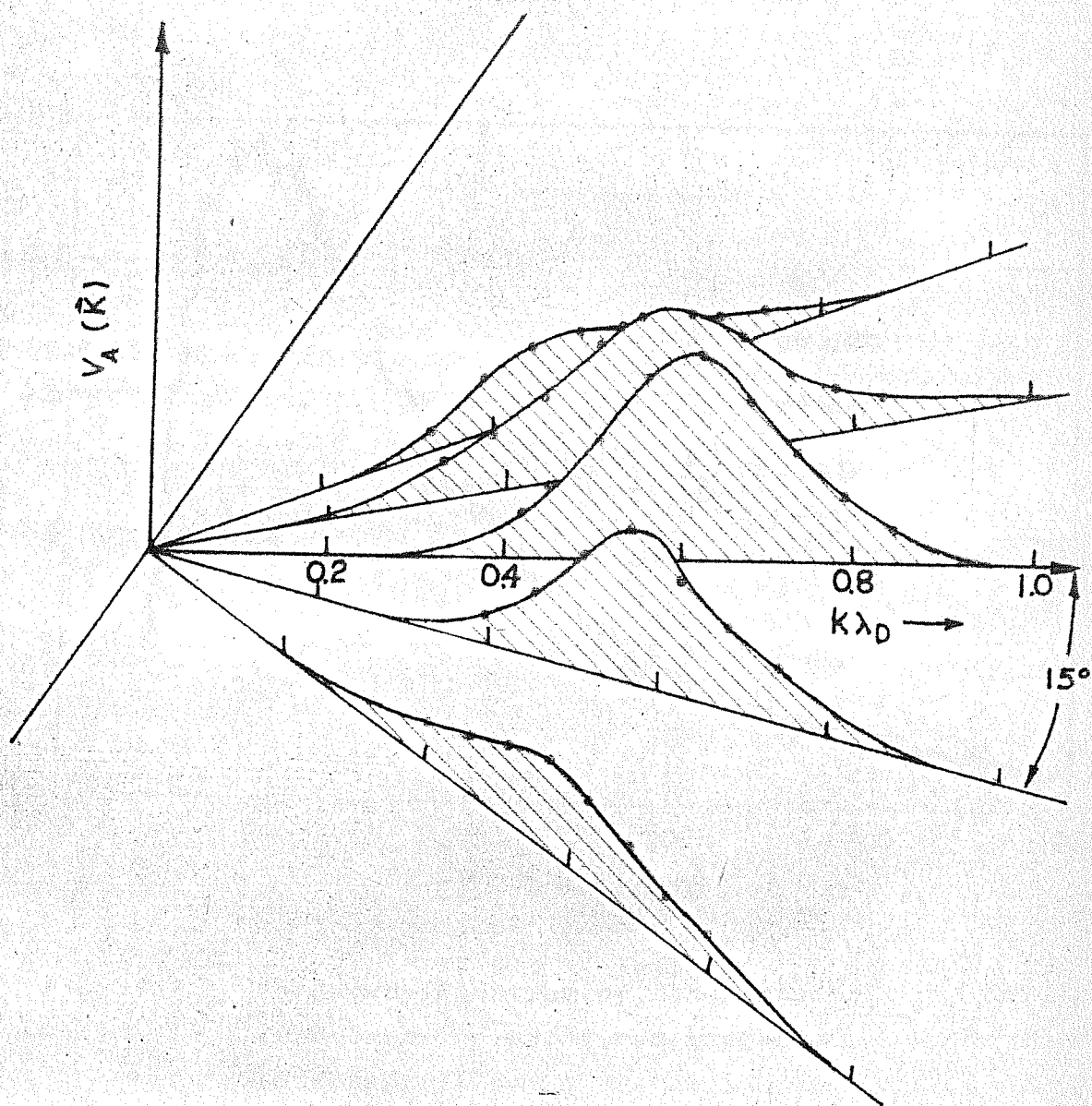


Fig. 6.6

Wave number spectrum of ion-acoustic turbulence measured by  $\text{CO}_2$  laser scattering (Slusher et al.; 1980).

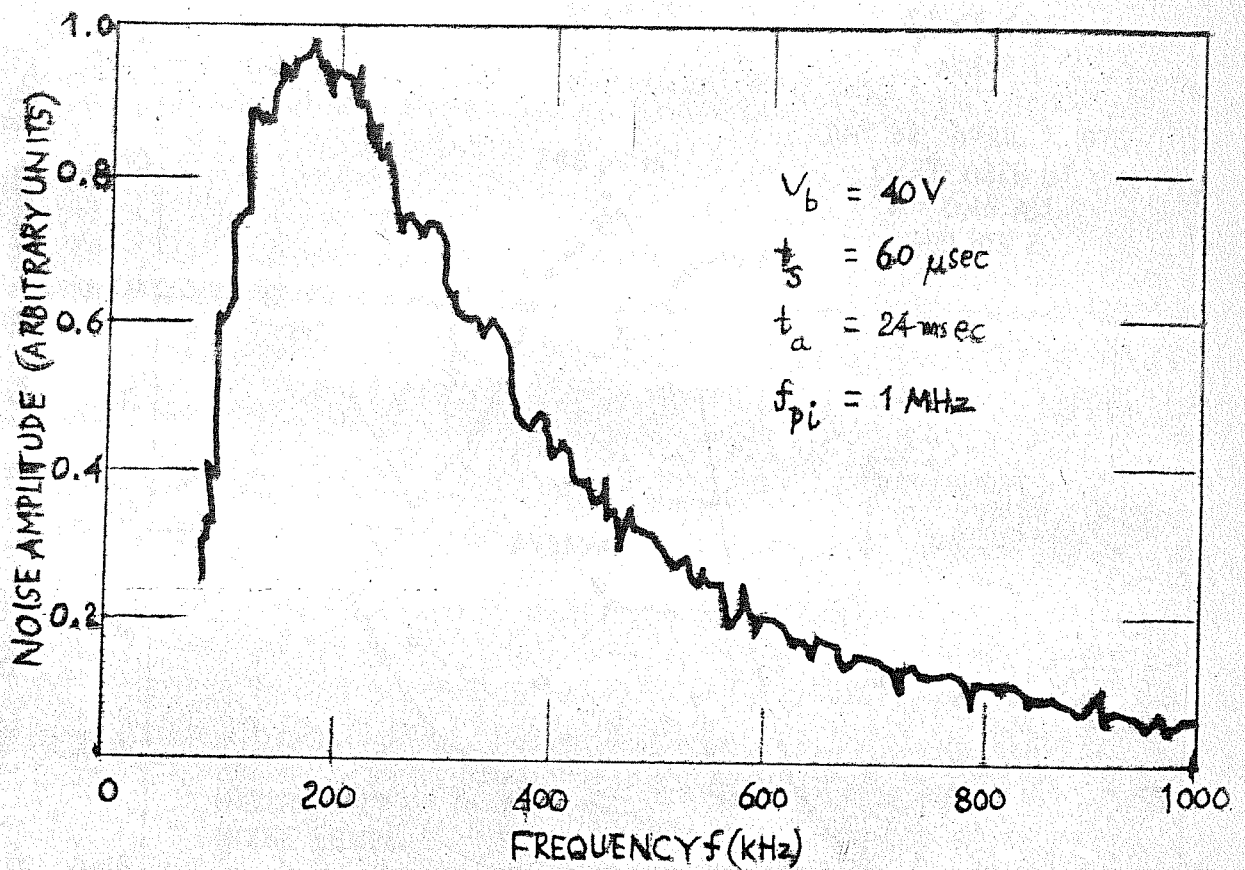


Fig. 6.7 Frequency Spectrum of Ion Acoustic Turbulence by probe measurements (Stenzel; 1978)

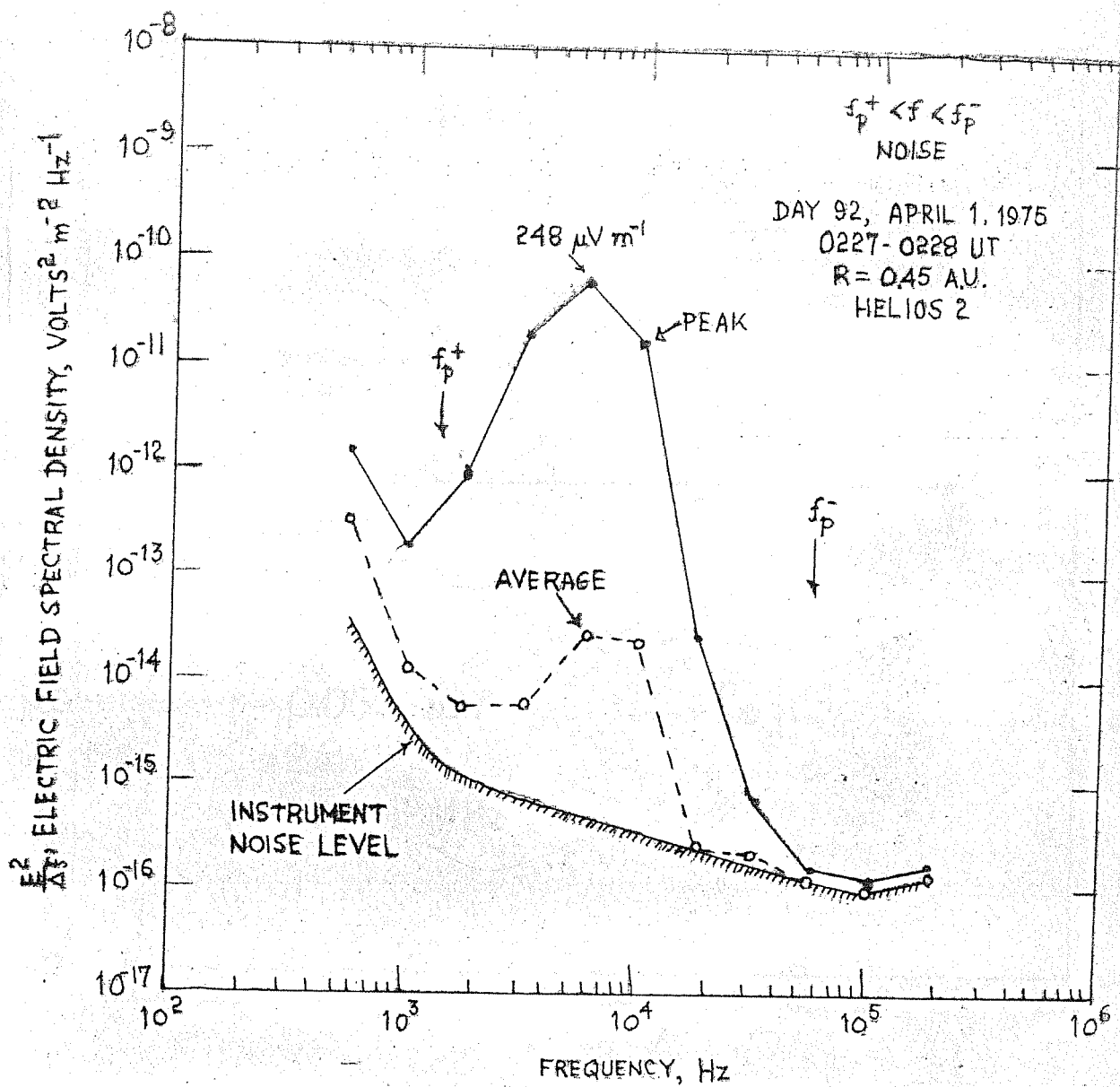


Fig. 6.8 Frequency spectrum of Ion Sound Turbulence measured in the Solar Wind (Gurnett and Frank; 1978)

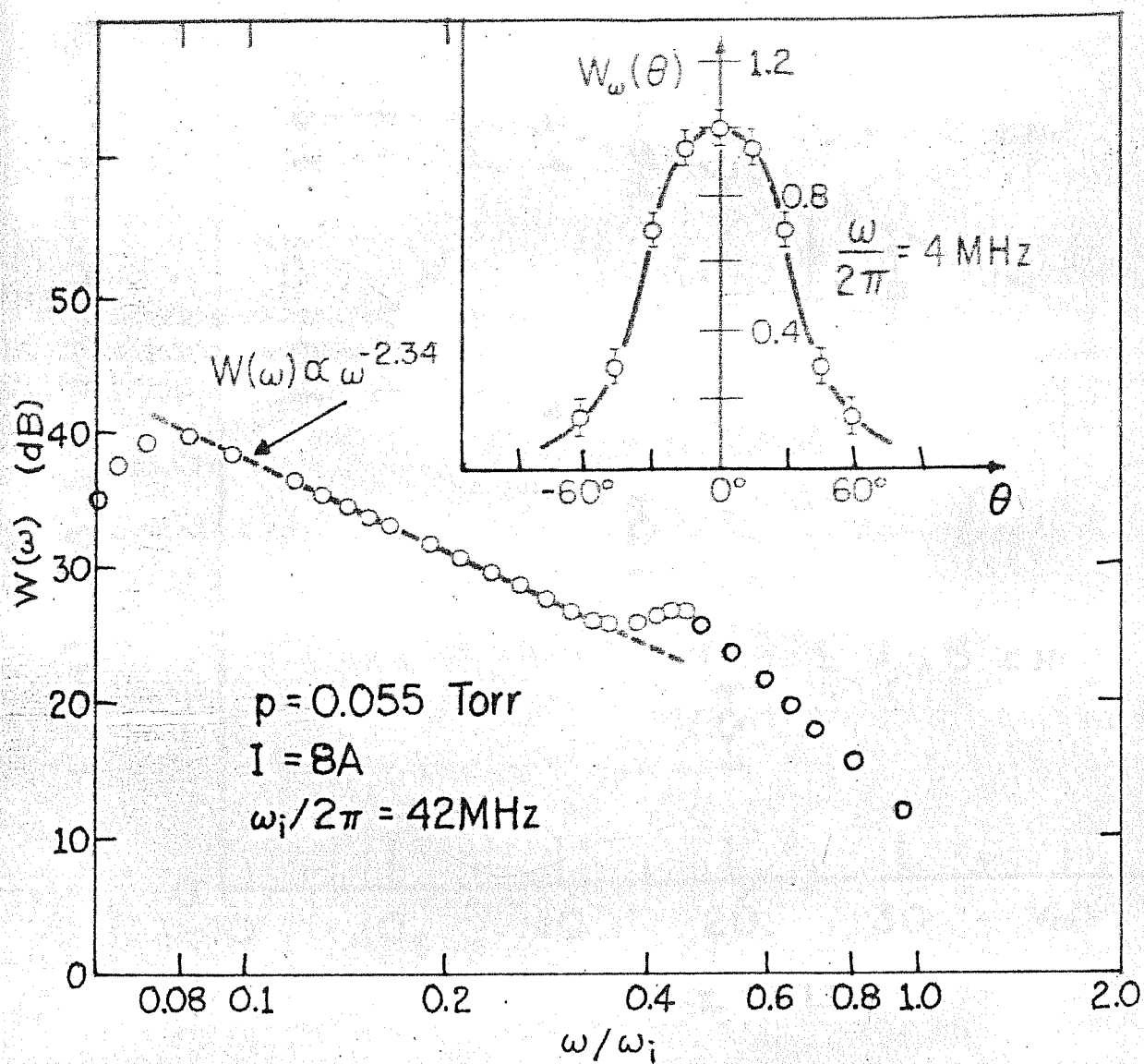


Fig. 6.9 Frequency spectrum and angular spectrum  
 (Yamada and Raether; 1974)

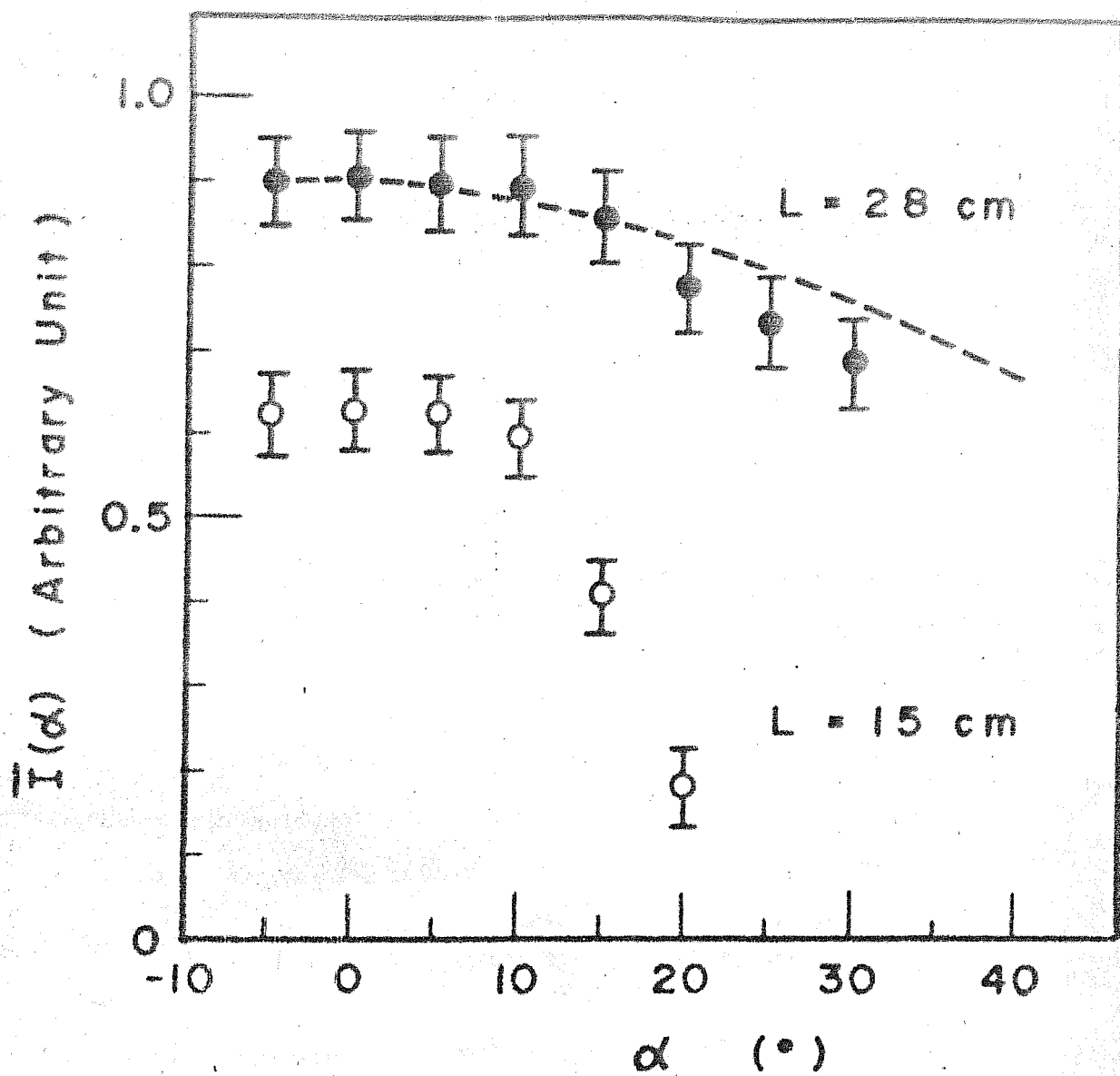


Fig. 6.10 Angular spectrum obtained by microwave scattering (Mase and Tsukishima; 1975)

The energy is peaked along the direction of the electron drift. This also agrees with the short time behaviour of  $S(\vec{k})$  obtained by computer simulation (Fig. 6.11). In Fig. 6.11, the peak of the spectrum shifts away from  $\vec{k} = 0$  after a longer time interval. This is an anomalous feature which we shall discuss in Chapter 7.

## 6.6. COMPARISON WITH THEORETICAL SPECTRA

The early theoretical ion acoustic spectra<sup>(3,11)</sup> exhibited a pure power law dependence without the cut off at low  $k$  or low  $\omega$ , which was found in all measured spectra. This feature is similar to the divergence in the Coulomb cross-section when polarization effects are not included. A self-consistent cut off is present in the spectrum calculated from renormalized turbulence theory<sup>(5)</sup>. (Fig. 6.13). Since the dressed particle picture induces polarization effects, this feature is built into our spectrum. The stationary spectrum  $S(k)$  that we have calculated compares well with the spectrum obtained by Horton and Choi<sup>(5)</sup> (Fig. 6.14) using a mode simulation technique.

The shape of the angular spectrum calculated on the basis of the Perturbed Orbit Theory by Sleeper et al<sup>(7)</sup> (Fig. 6.12) is consistent with ours.

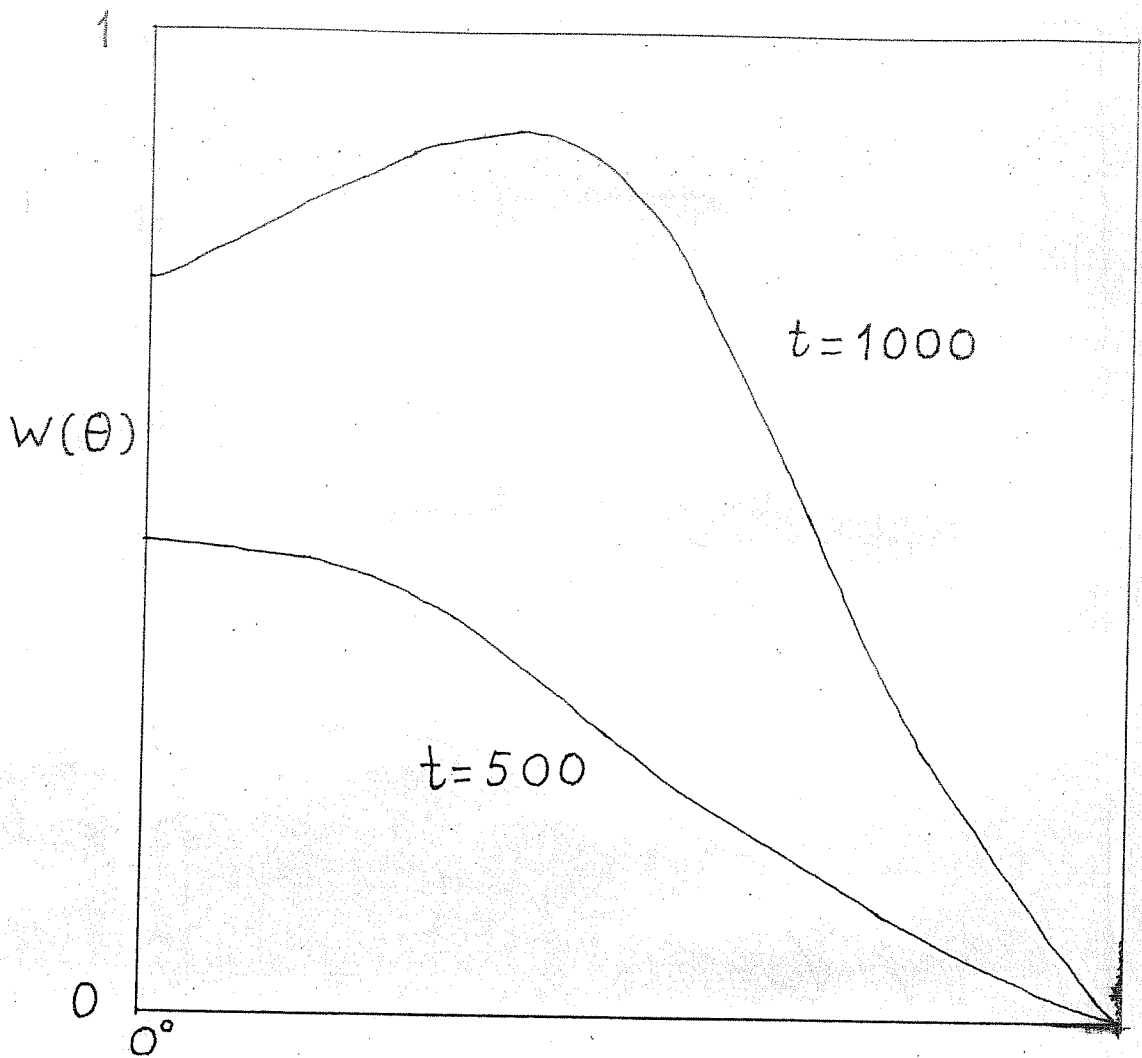


Fig. 6.11. Angular spectrum obtained from a computer simulation of ion acoustic turbulence in a magnetic field (Biskamp and Chodura; 1971)

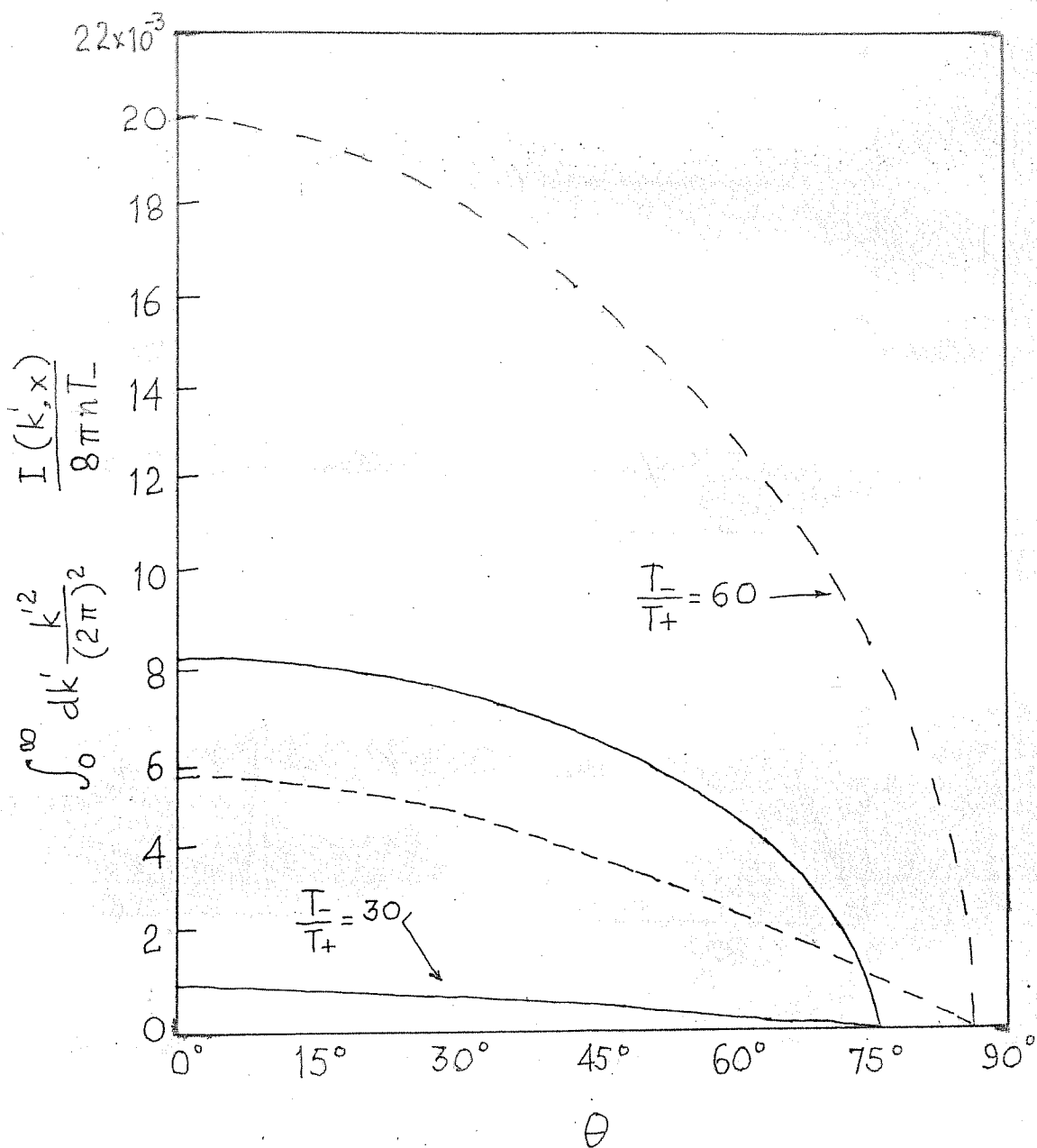


Fig. 6.12 Theoretical angular spectrum obtained from Perturbed Orbit Theory (Sleeper et al; 1973)



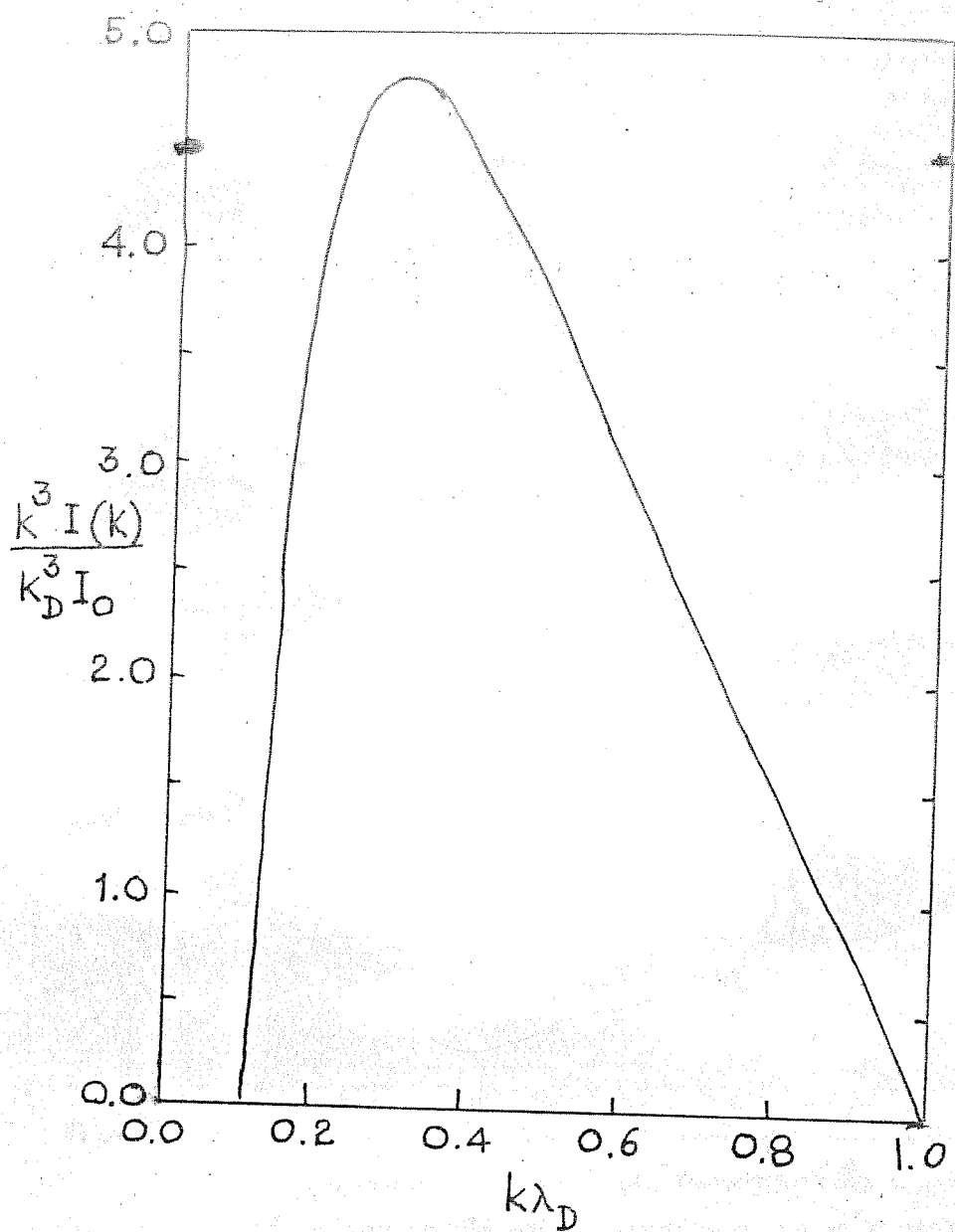


Fig. 6.13 Theoretical spectrum  $S(k)$  obtained from Renormalised Quasilinear theory (Horton and Choi; 1979)

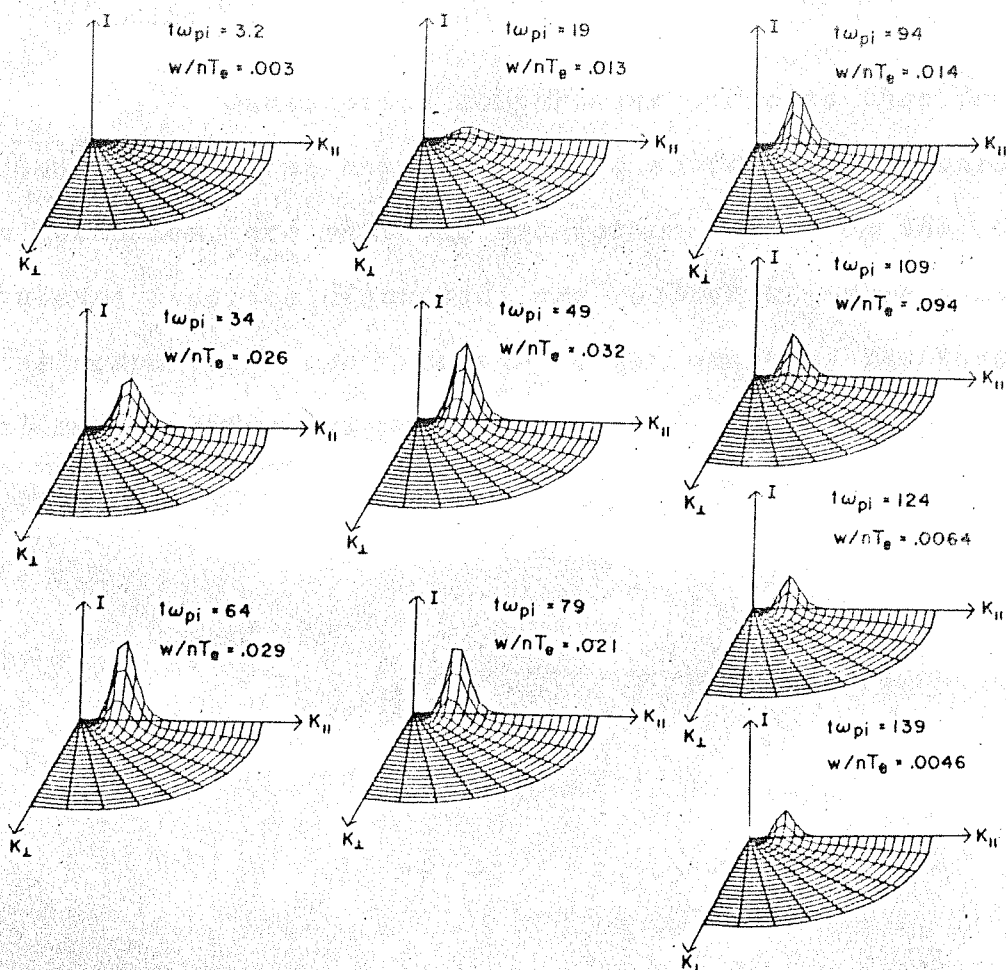


Fig. 6.14 Time evolution of the ion acoustic spectrum based on Renormalised Quasi-linear Theory obtained from a mode simulation technique (Horton and Choi; 1979).

## 6.7. CONCLUSIONS

*Qualitative comparisons indicate that ion resonance broadening appears to be a satisfactory saturation mechanism, and that the predictions based on the turbulence theories discussed, are realistic. More quantitative comparisons are necessary after matching the theoretical and experimental parameters.*

REFERENCES

- (1) Dupree T.H. (1966) *Phys. Fluids* 9, 1773  
 Dupree T.H. (1967) *Phys. Fluids* 10, 1049  
 Weinstock J. (1968) *Phys. Fluids* 11, 1977  
 Weinstock J. (1969) *Phys. Fluids* 12, 1045
- (2) Cook, I. and J.B. Taylor (1973) *J. Plasma Phys.* 9, 131.
- (3) Kadomtsev, B.B. (1965) *Plasma Turbulence*, Academic Press, London.
- (4) Galeev, A.A. and R.S. Sagdeev (1973) in *Nonlinear Plasma Theory*, *Revs. of Plasma Phys.* Vol. 7, ed. M.A. Leontovich.
- (5) Horton, W. and Duk-in-Choi (1979) *Phys. Repts.* 49, 273.
- (6) Ichimaru, S. and T. Nakamo (1968), *Phys. Rev.* 165, 231.
- (7) Sleeper, A.M., J. Weinstock, and B. Bezzerides, (1973) *Phys. Fluids* 16, 1508; (1972) *Phys. Rev. Letts.* 29, 343.
- (8) Mandelbrot, B.B. (1977) *FRACTALS*, pg. 161, W.H. Freeman and Co., San Francisco.
- (9) Gekelman, W. and R.L. Stenzel (1978) *Phys. Fluids*, 21, 2014.

- (10) Biskamp, D. and R. Chodura (1971) *Phys. Rev. Letts.* 27, 1553.
- (11) Ishihara, O. and A. Hirose (1983) *Phys. Rev. Letts.* 51, 1783.
- (12) Yamada, M. and M. Raether (1974), *Phys. Rev. Letts.* 32, 99.
- (13) Mase, A. and T. Tsukishima (1975), *Phys. Fluids* 18, 464.
- (14) Slusher, R.E., C.M. Surko, D.R. Moler and M. Porkolab (1976) *Phys. Rev. Letts.* 36, 674; (1980) *Phys. Fluids* 23, 472.
- (15) Ilic, D.B. (1977) *Phys. Fluids* 20, 1717.
- (16) Stenzel, R.L. (1978) *Phys. Fluids* 21, 99.
- (17) Kawai, Y., Ch. Hollenstein and M. Guyot (1978) *Phys. Fluids* 21, 970.
- (18) Nishikawa, K. and C.S. Wu, *Phys. Rev. Letts.* 23, 1020.

## CHAPTER 7

### FLUCTUATION SPECTRUM OF HIGHER FREQUENCY ELECTROSTATIC AND ELECTROMAGNETIC TURBULENCE

By an extension of the superposition principle<sup>(1)</sup> introduced in Chapter 6, it is possible to obtain analytically the spectrum of higher frequency turbulent electrostatic and electromagnetic fluctuations, in a magnetic field.

#### 7.1. ELECTROSTATIC FLUCTUATIONS

The unperturbed helical orbit of a particle in an external magnetic field, when averaged over the perpendicular velocity, is

$$\begin{aligned}
 & e^{i(\omega t - k \cdot \Delta R)} \\
 &= \sum_{n=-\infty}^{\infty} J_n^2(k_{\perp} \rho_j) \exp [i(\omega - k_{\parallel} v_{ij} - n\Omega_j)t]
 \end{aligned}
 \tag{7.1.1}$$

Eqn. (7.1.1) also represents the trajectories of uncorrelated dressed particles moving in a turbulent plasma.

By a superposition of the fields of the dressed particles, the electric field fluctuation spectrum in the turbulent plasma is obtained as,

$$\frac{\langle |E_k|^2 \rangle}{V} = \frac{(4\pi)^2 e^2 n}{k^2} \sum_j \int d v_{\parallel} f_{0j}(v_{\parallel}) \sum_{n=-\infty}^{\infty} J_n^2(k_{\perp} \rho_j) \delta(\omega - k_{\parallel} v_{ij} - n\Omega_j)
 \tag{7.1.2}$$

where  $\epsilon_{NL}$  is the nonlinear dielectric function that determines the dressing on the particles.

The  $n = 0$  term of Eq. (7.1.2) gives the ion-acoustic spectrum calculated in Chapter 6.

$\epsilon_{NL}$  contains all the cyclotron harmonics.

The spectrum for each  $n$  can be obtained approximately by replacing  $\epsilon_{NL}$  by  $\epsilon_{NL}^{(n)}$  where only the terms corresponding to the  $n^{\text{th}}$  cyclotron harmonic are retained. The  $n = 0$  term gives the ion-acoustic spectrum.

The spectrum for the first harmonic of the ion-cyclotron wave is

$$\frac{\langle |E_k|^2 \rangle}{V} = \frac{(4\pi)^2 n e^2}{k^2} \sum_j J_1^2(k_{\perp} \rho_{ji}) \int \frac{dv_{\parallel} f_{oj}(v_{\parallel})}{|\epsilon_{NL}^{(1)}(\omega, k)|^2} \delta(\omega - k_{\parallel} v_{\parallel} - n \Omega_j)$$

(7.1.3)

where  $\epsilon_{NL}^{(1)}$  is the dielectric function for the first harmonic of the ion-cyclotron wave calculated earlier (Eq. (5.4.2)),

$$\epsilon_{NL}^{(1)}(\omega, k) = \left(1 + \frac{1}{k^2 \lambda_D^2}\right) \left[ 1 - k_{\perp}^2 \bar{\rho}^2 \times \left\{ \frac{\Omega_i^2 - i\eta(\omega + i\eta)}{(\omega + i\eta)^2 - \Omega_i^2} \right\} \right] + \text{Im} \epsilon_L$$



$$\approx \left(1 + \frac{1}{k^2 \lambda_D^2}\right) \left[ \frac{(\omega + i\delta - \omega_0)(\omega + i\delta + \omega_0)}{(\omega + i\delta)^2 - \Omega_i^2} \right] \quad (7.1.4)$$

where

$$\delta = \eta \left(1 + \frac{1}{2} k_{\perp}^2 \bar{J}_s^2\right) - \gamma_L' \quad ; \quad \omega_0^2 = (\Omega_i^2 + \eta^2) (1 + k_{\perp}^2 \bar{J}_s^2)$$

Substituting for  $\Xi_{NL}(1)$  from Eq. (7.1.4) in Eq. (7.1.3), and performing the velocity integration under the assumption that the diffusion is independent of velocity (see Fig. (4.5)), we obtain the spectrum of current driven ion-cyclotron turbulence. Assuming that the particle distribution in equilibrium with the turbulent fluctuations is

$$f_o(v) = \sum_j \frac{1}{(2\pi v_{Tj})^{3/2}} \exp \left[ - \frac{v_{\perp}^2 + (v_{\parallel} - v_{oj})^2}{2v_{Tj}^2} \right] \quad (7.1.5)$$

with  $v_{oe} = v_o$  and  $v_{oi} = 0$ , the spectrum is

$$\frac{\langle |E_k|^2 \rangle}{V} = \frac{(4\pi)^2 n e^2}{k^2} \frac{k^2 \lambda_D^2}{(1 + k^2 \lambda_D^2)} \times$$

$$\sum_j J_1^2(k_{\perp}^2 J_j) \left[ 1 + \frac{2}{\sqrt{2} k_{\parallel} v_{Tj}} \operatorname{Re} N \sum_{+,-} \left[ \frac{\omega_0 \pm k_{\parallel} v_{Tj} + i\delta}{\sqrt{2} k_{\parallel} v_{Tj}} \right] \right]$$

(7.1.6)

where

$$N = \frac{[(\omega_0 + i\delta)^2 - \Omega_i^2 - \delta^2]^2}{8i\omega_0\delta(\omega_0 + i\delta)}$$

$$\omega_0^2 = (-\Omega_i^2 + \eta^2)(1 + k_{\perp}^2 \bar{J}_s^2)$$

$$\delta = \eta \left( 1 + \frac{1}{2} k_{\perp}^2 \bar{J}_s^2 \right) - \gamma_L'$$

(7.1.7)

and

$$\gamma_L' = - \operatorname{Im} \epsilon_L \left/ \frac{\partial \operatorname{Re} \epsilon_{NL}}{\partial \omega} \right|_{\omega = \omega_0}$$

as defined earlier.

Let us examine the features of the ion-cyclotron spectrum Eq. (7.1.6). Since  $k_{\perp} \frac{D}{j_e}$  is usually very small, the electron contribution to the spectrum, governed by  $J_1^2(k_{\perp} \frac{D}{j_e})$ , is small.

There is no energy in the fluctuation spectrum along the magnetic field, for which  $k = k_{\parallel}$ . The contribution to the fluctuation spectrum comes from waves propagating at an angle to  $B$ .

Typically, in turbulence driven by an electron drift along the magnetic field, several  $n$  modes will be excited. Initially, if the particle velocities are low, only the  $n = 0$  ion-acoustic mode is excited. At this point, the energy is maximum along  $B$ , as shown by the spectrum we have calculated (Fig. 6.1). As particles are drawn out into the tail by velocity space diffusion, they can begin to excite the  $n = 1$  mode, which contributes in directions away from  $B$ . If the ion temperature increases by turbulent heating, the contribution from the ion-cyclotron wave increases and at  $k_{\perp} \frac{D}{j_i} \sim 2$ , it begins to dominate over the  $n = 0$  mode.

Our formulation for obtaining stationary spectra cannot describe the time evolution pictured above. However, computer simulations<sup>(2,3)</sup> of current driven ion-acoustic turbulence clearly show this behaviour (Figs. (7.1) and (7.2)).

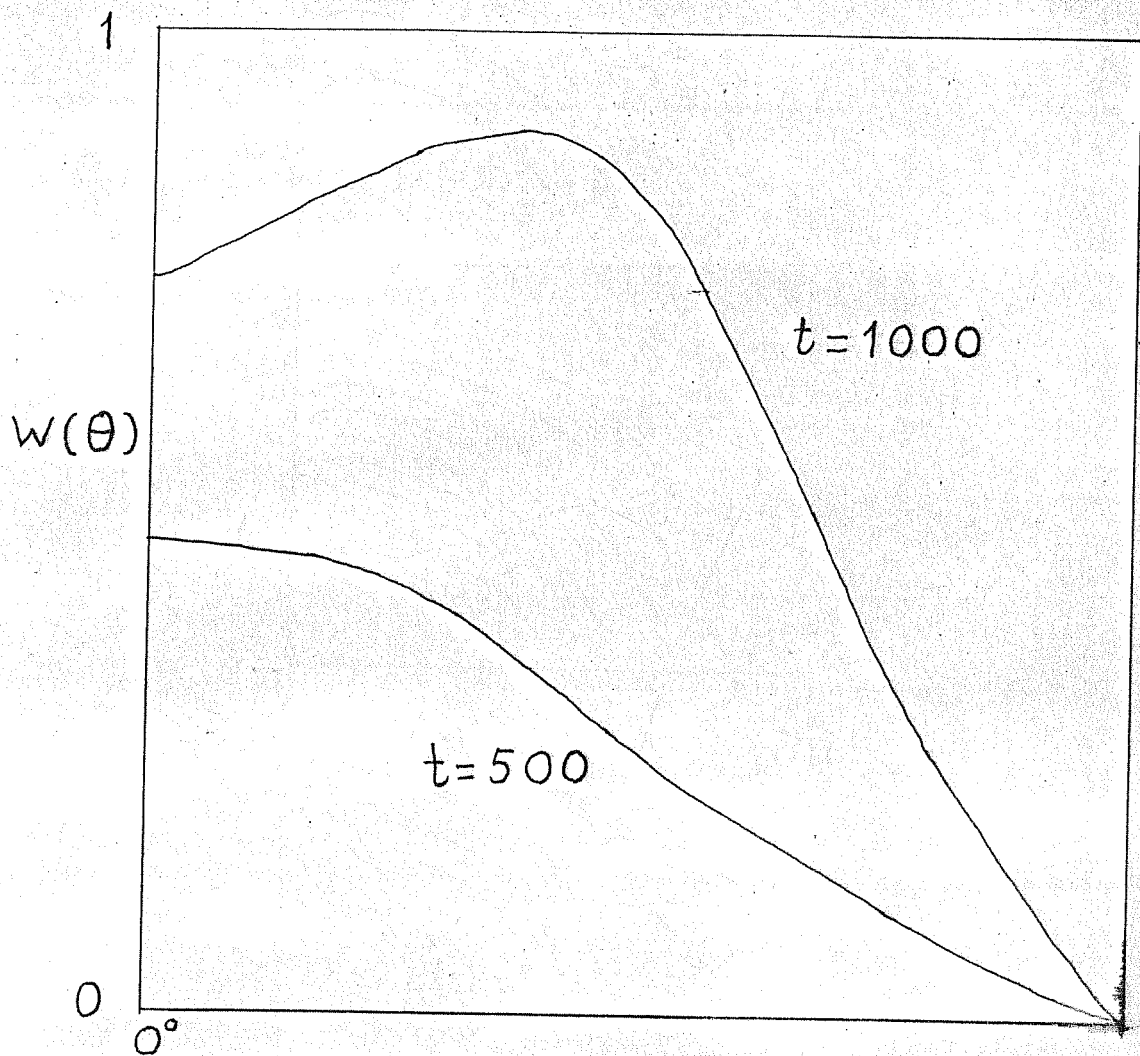


Fig. 7.1. Angular spectrum obtained from a computer simulation of ion acoustic turbulence in a magnetic field (Biskamp and Chodura; 1971)

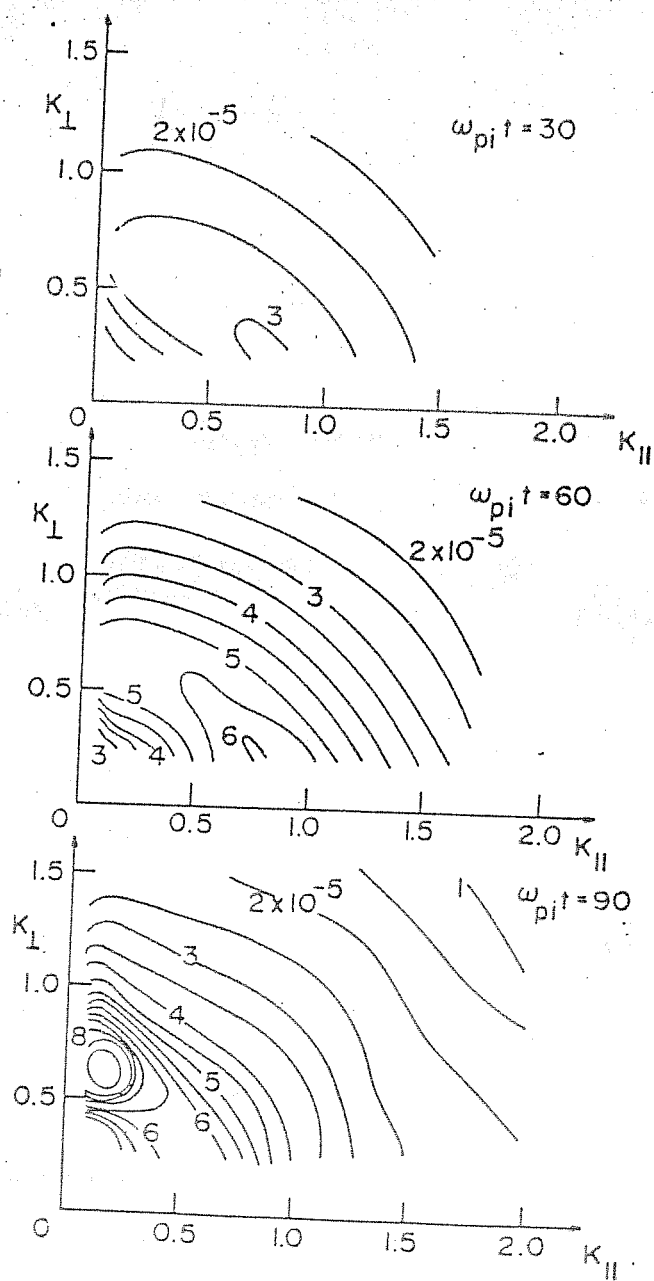


Fig. 7.2 Contour plots of the  $k$  spectrum of electric field energy density of ion acoustic waves in a magnetic field (Ishihara and Hirose; 1983)

The peaking of the spectrum at an angle away from  $B$ , referred to as the anomalous feature of the  $k$  spectrum, has been experimentally observed by Gekelman and Stenzel<sup>(4)</sup>, and noted by Ishihara and Hirose<sup>(3)</sup> in their simulation of the multidimensional quasilinear evolution of the ion-acoustic instability in a magnetic field. In Reference 3, the singular  $\delta$  function in the quasilinear diffusion coefficient is approximated by

$$\frac{\eta}{(\omega - k_{\parallel} v_{\parallel})^2 + \eta^2}$$

which is identical in form to the nonlinearly broadened diffusion (Eq.(3.1.8)). We expect, therefore, that our analytical results can be compared to their simulation results.

Ishihara and Hirose also mention that there is no theoretical explanation for the anomalous  $k$  spectrum, which is not predicted by linear theory. The explanation they offer is in terms of the angular dependence of the high energy ion tail that is produced during the simulation. It would appear that the anomalous  $k$  spectrum can be easily explained by the generation of ion-cyclotron turbulence as our calculations show. Numerical estimates of the spectrum are needed for quantitative comparison with the observations and simulations.

## 7.2. SPECTRUM OF ELECTROMAGNETIC FLUCTUATIONS

In this section we briefly sketch how to obtain the low frequency electromagnetic field fluctuation spectrum in a stationary turbulent state. The spectrum is obtained by a superposition of dressed currents, dynamically screened by the dielectric function. The electric field  $E$  in a plasma due to a current density  $J$  is given by<sup>(5)</sup>

$$\vec{E}_{k\omega} = \frac{4\pi}{i\omega} \vec{Z}(k, \omega) \cdot \vec{J}(k, \omega) \quad (7.2.1)$$

where  $\vec{Z}$  is the inverse of the dispersion tensor  $\vec{\Delta}$ , defined by

$$\vec{Z} \cdot \vec{\Delta} = \vec{I}$$

and

$$\vec{\Delta} = \vec{\epsilon} - \frac{c^2 k^2}{\omega^2} \vec{I}_T \quad (7.2.2)$$

Using the superposition principle, the fluctuation spectrum is

$$\langle E E^*(k, \omega) \rangle = \frac{(4\pi)^2}{\omega^2} Z(k, \omega) \cdot \langle J J^*(k, \omega) \rangle^{(0)} \cdot Z^\dagger(k, \omega)$$

(7.2.3)

where  $\langle J J^*(k, \omega) \rangle^{(0)}$  is the ensemble average of the uncorrelated current fluctuations. The electromagnetic spectrum in an isotropic medium can be written in a simplified form,

$$\langle E E^*(k, \omega) \rangle = \sum_j \frac{(4\pi)^2 N e^2}{k^2} \int d\vec{v} f_{0j}(v) \delta(\omega - \vec{k} \cdot \vec{v})$$

$$\times \left\{ \frac{\vec{I}_L}{|\epsilon_L(k, \omega)|^2} + \frac{1}{2} \frac{|\vec{k} \times \vec{v}|^2}{\omega^2} \frac{\vec{I}_T}{|\epsilon_T(k, \omega) - \frac{k^2 c^2}{\omega^2}|^2} \right\}$$

In the presence of a magnetic field, this simplification is not possible.

Let us consider low frequency hydromagnetic turbulence.



The dressed current correlations are evaluated along the unperturbed guiding centre orbits (Sec. 3.3). The nonlinear dielectric tensor  $\bar{\epsilon}_{NL}$  for hydromagnetic waves is obtained from Perturbed Orbit Theory by replacing  $\omega$  by  $\omega + i\eta$  in  $\bar{\epsilon}_L$ , and taking the low frequency limit  $\omega \rightarrow 0$  and  $c^2 \gg v_A^2$ .  $Z$  is then obtained from Eq.(7.2.2).

The electromagnetic fluctuation spectrum can then be calculated from Eq.(7.2.3).

REFERENCES

- 1           Cook, I. and Taylor, J.B. (1973) *J. Plasma Phys.* 9, 131.
- 2           Biskamp, D. and R. Chodura (1971) *Phys. Rev. Letts.* 27, 1553.
- 3           Ishihara, I. and A. Hirose (1983), *Phys. Rev. Letts.* 51, 1783.
- 4           Gekelman, W. and R.L. Stenzel (1978) *Phys. Fluids* 21, 2014.
- 5           Ichimaru, S. (1973) *Basic Principles of Plasma Physics*, W.A. Benjamin Inc., Reading, Mass., USA.

## SUMMARY AND CONCLUSIONS

In this thesis we have considered low frequency waves that are excited by a beam or current along an external magnetic field in a plasma. The study is conducted along two lines contained in Parts I and II of the thesis.

The aim in Part I is to explain certain observed phenomena in space, in terms of the linear theory of plasma waves. In particular, our study of high speed streams in the solar wind shows that magnetosonic waves generated by the fast stream can account for the enhanced interplanetary scintillation observed at the same time. The instability condition is violated with the advance of the stream, which confines this effect to the leading edges of the stream. The existence of stable double ion streams in the solar wind is also explained on this basis (Chapter I).

In Chapter 2, we have considered the role of substorm particles in the generation of micropulsations. Linear stability analysis indicates that a low velocity stream, acting in conjunction with the thermal anisotropy in the magnetospheric plasma, can trigger an instability. This low frequency wave modulates the geomagnetic field, leading to micropulsations.

While the linear theory is well established for infinitesimal fields, and verified through extensive experimentation, the same cannot be said of the nonlinear theories describing finite fluctuations and plasma turbulence. One of our aims in Part II of the thesis, which is concerned with wave particle effects in turbulent plasmas, has been to critically examine the existing nonlinear theories and define and extend their region of applicability.

In Chapter 3, we have considered the diffusion of particles in the turbulent fields using Perturbed Orbit Theory. While the effects arising from spatial diffusion of particles in the turbulent fields had been well documented earlier, the nature of the velocity space diffusion had not been carefully examined. The guiding centre diffusion coefficients have been obtained analytically by neglecting the coupling between the components of the diffusion tensor in phase space. It is seen that the level of turbulent energy required for ion diffusion is lower than that the level required for the high temperature electrons.

The perturbation of helical orbits in a magnetic field has been considered in Sec. 3.2. We have obtained nonlinear diffusion coefficients which reduce to the Fokker-Planck diffusion coefficients in a magnetic

field when orbit perturbation effects are neglected. The guiding centre diffusion of particles in low frequency electromagnetic fields have been obtained in Sec. 3.3. The results of Secs. 3.2 and 3.3 are new to the best of our knowledge, and show that the nonlinear scaling of  $\bar{D}$  is different from the quasilinear scaling.

The complete orbit integral has been evaluated in Chapter 4 by an accurate numerical routine. We have also obtained the self-consistent values of the diffusion coefficient by a rapidly convergent iterative scheme. We have found that the resonant nature of the diffusion coefficient at low turbulence levels gets smeared out at high turbulent energy, making  $\bar{D}$  almost independent of  $V$ . The above scheme is only partially self-consistent since the fluctuation spectrum is introduced as a parameter, and remains constant during the iteration. The fully self-consistent numerical solution would require not only the evaluation of the spectrum, but also the evolution of the particle distribution functions during the iteration process.

The effects of turbulent fluctuations on the dielectric response of the plasma has been considered in Chapter 5. While spatial diffusion gives rise to the well known resonance broadening and consequent stabilization,

it is found that velocity space diffusion does not lead to the same effect. Velocity space diffusion can quench the turbulence, but not give rise to a stationary turbulent state. By a linear stability analysis of the stationary turbulent state, arising from spatial diffusion, the non-linear dispersion relation for ion-acoustic and ion-cyclotron waves have been obtained, and solved for the non-linear frequency and growth rate.

Our next aim in this part was to calculate explicitly some observable parameters of the turbulent state, and compare them with experiment. This provides a check for the existing theories. Although turbulence has been observed for some time, explicit theoretical calculations of observables has been lacking. This may have been due to the self-consistent nature of the statistical theories which makes explicit calculations difficult. By synthesising the Perturbed Orbit Theory and an equivalent description in terms of the Superposition of Dressed Particles, we have explicitly calculated the fluctuation spectrum of Ion-Acoustic Waves. The comparison of our spectrum with observed ion-acoustic spectra and simulations, both in wave number and frequency, is very encouraging, leading one to suppose that the statistical theories provide a reliable framework for the study of turbulent plasma.

The spectrum of ion-cyclotron waves has been obtained in Chapter 7. We find that the form of the spectrum offers a simple explanation for the anomalous  $\vec{k}$  spectrum observed in simulations and experiments on current driven ion-acoustic turbulence in a magnetic field. The extension of the formalism to low frequency electromagnetic fluctuations is briefly outlined.

Further refinement is possible along these lines by including the effects of mode coupling, the change in the particle distribution functions, and obtaining the time evolution of the spectrum.

The diffusion coefficients obtained can be used to calculate the transport properties in a turbulent plasma, which have important practical applications in the areas of plasma heating and confinement. Much further work lies in this direction once the plasma turbulence theories can be made tractable and as easily used as the linear theory.

# APPENDIX I : Properties of the Lommel Function

1. The Lommel function  $S_{0, 1/3}(V)$  is defined by

$$\int_0^\infty e^{-a^3 t^3 - zt} dt = \bar{z}^{-1} V S_{0, 1/3}(V) \quad (AI.1)$$

where  $V = 2 \left( \bar{z}/3a \right)^{3/2}$

(Magnus et al., Pg. 76).

2.  $S_{0, 1/3}(V)$  can be expressed in terms of the Anger functions  $\mathbb{J}_{\pm 1/3}(V)$  and Bessel functions  $J_{\pm 1/3}(V)$  as

$$S_{0, 1/3}(V) = \frac{\pi}{2} \frac{1}{\sin \pi/3} \left[ \mathbb{J}_{1/3}(V) - \mathbb{J}_{-1/3}(V) - J_{1/3}(V) + J_{-1/3}(V) \right] \quad (AI.2)$$

(Magnus et al., Pg. 112)

3. For large values of the argument and

$$-\pi < \arg V < \pi$$



$$\bar{J}_\nu(v) = \bar{J}_\nu(v) + \frac{1}{\pi v} \sin(\pi \nu) \times$$

$$\left[ \sum_{m=0}^{M-1} (-1)^m 2^{2m} \frac{\Gamma\left(m+\frac{1}{2}+\frac{\nu}{2}\right)}{\Gamma\left(\frac{1}{2}+\frac{\nu}{2}\right)} \frac{\Gamma\left(m+\frac{1}{2}-\frac{\nu}{2}\right)}{\Gamma\left(\frac{1}{2}-\frac{\nu}{2}\right)} v^{-2m} \right.$$

$$+ O(v^{-2M})$$

$$+ \nu \sum_{m=0}^{M-1} (-1)^m 2^{2m} \frac{\Gamma\left(m+1+\frac{\nu}{2}\right)}{\Gamma\left(1+\frac{\nu}{2}\right)} \frac{\Gamma\left(m+1-\frac{\nu}{2}\right)}{\Gamma\left(1-\frac{\nu}{2}\right)} v^{-2m-1}$$

$$+ O(|v|^{-2M-1}) \Big] \quad (\text{AI. 3})$$

(Magnus et al., Pg. 118).

4.

For small values of the argument,

$$\begin{aligned} \bar{J}_\nu(v) = & \cos \frac{\pi \nu}{2} \sum_{m=0}^{\infty} (-1)^m \left(\frac{v}{2}\right)^{2m} \left[ \frac{\Gamma\left(m+1+\frac{\nu}{2}\right) \Gamma\left(m+1-\frac{\nu}{2}\right)}{\Gamma\left(\frac{1}{2}+\frac{\nu}{2}\right) \Gamma\left(\frac{1}{2}-\frac{\nu}{2}\right)} \right]^{-1} \\ & + \sin \frac{\pi \nu}{2} \sum_{m=0}^{\infty} (-1)^m \left(\frac{v}{2}\right)^{2m+1} \left[ \frac{\Gamma\left(m+\frac{3}{2}+\frac{\nu}{2}\right) \Gamma\left(m+\frac{3}{2}-\frac{\nu}{2}\right)}{\Gamma\left(\frac{3}{2}+\frac{\nu}{2}\right) \Gamma\left(\frac{3}{2}-\frac{\nu}{2}\right)} \right]^{-1} \end{aligned}$$

(AI. 4a)

$$\begin{aligned} \bar{J}_{-\nu}(v) &= \cos \frac{\pi \nu}{2} \sum_{m=0}^{\infty} (-1)^m \left(\frac{v}{2}\right)^{2m} \left[ \Gamma\left(m+1-\frac{\nu}{2}\right) \Gamma\left(m+1+\frac{\nu}{2}\right) \right]^{-1} \\ &\quad - \sin \frac{\pi \nu}{2} \sum_{m=0}^{\infty} (-1)^m \left(\frac{v}{2}\right)^{2m+1} \left[ \Gamma\left(m+\frac{3}{2}-\frac{\nu}{2}\right) \Gamma\left(m+\frac{3}{2}+\frac{\nu}{2}\right) \right]^{-1} \end{aligned}$$

(AI. 4b)

(Magnus et al., Pg. 117).

Therefore,

$$\begin{aligned} \bar{J}_{1/3} - \bar{J}_{-1/3} &= 2 \sin \pi/6 \times \\ &\quad \sum_{m=0}^{\infty} (-1)^m \left(\frac{v}{2}\right)^{2m+1} \left[ \Gamma\left(m+\frac{3}{2}+\frac{1}{6}\right) \Gamma\left(m+\frac{3}{2}-\frac{1}{6}\right) \right]^{-1} \\ &\approx \frac{(v/2)}{\Gamma(5/3) \Gamma(4/3)} \end{aligned}$$

(AI. 5)

5. Limiting values of the Bessel function  $J$  for small arguments,

$$\bar{J}_{\nu}(v) \sim (v/2)^{\nu} / \Gamma(1+\nu) \quad (\nu \neq -1, -2, -3)$$

$$\bar{J}_{-\nu}(v) \sim (v/2)^{-\nu} / \Gamma(1-\nu)$$

(AI. 6)

(Abramowitz, Pg. 360).

$$\bar{J}_{1/3}(v) - \bar{J}_{-1/3}(v) \sim \frac{1}{\Gamma(4/3)} (v/2)^{1/3} - \frac{1}{\Gamma(2/3)} (v/2)^{-1/3} \quad (\text{AI. 7})$$

6. From Eq. (AI.3), for large values of  $V$ ,

$$\bar{J}_{1/3}(v) - \bar{J}_{1/3}(v) = \frac{1}{\pi v} \sin \frac{\pi}{3} \left\{ 1 + \frac{1}{3v} - \frac{8}{9v^2} + \dots \right\}$$

$$\bar{J}_{-1/3}(v) - \bar{J}_{-1/3}(v) = \frac{-1}{\pi v} \sin \frac{\pi}{3} \left\{ 1 - \frac{1}{3v} - \frac{8}{9v^2} + \dots \right\}$$

Substituting in Eq. (AI.2), the asymptotic value of  $S_{0,1/3}(V)$  for large  $V$  is

$$S_{0,1/3}(v) = \frac{1}{v} \left\{ 1 - \frac{8}{9v^2} \right\} \quad (\text{AI. 8})$$

7. For small  $V$ , substituting Eqs. (AI.5) and (AI.7) in (AI.2),

$$S_{0,1/3}(V) \approx \frac{\pi}{V^3} \left[ \frac{(V/2)}{\Gamma(5/3)\Gamma(4/3)} - \frac{(V/2)^{1/3}}{\Gamma(4/3)} + \frac{(V/2)^{-1/3}}{\Gamma(2/3)} \right]$$

or

$$V S_{0,1/3}(V) \approx \frac{2\pi}{V^3} \left[ \frac{(V/2)^{2/3}}{\Gamma(2/3)} - \frac{(V/2)^{4/3}}{\Gamma(4/3)} + \frac{(V/2)^4}{\Gamma(5/3)\Gamma(4/3)} + \dots \right] \quad (\text{AI.9})$$

## REFERENCES

Abramowitz, M. and I.A. Stegun, (1964) *Handbook of Mathematical Functions*, Dover, N.Y.

Magnus, W., F. Oberhettinger and R.P. Soni (1966) *Formulas and Theorems for the Special Functions of Mathematical Physics*, Springer-Verlag, N.Y.